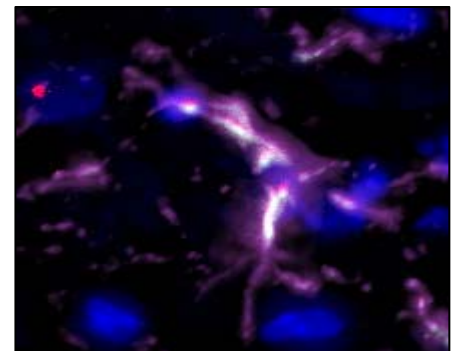
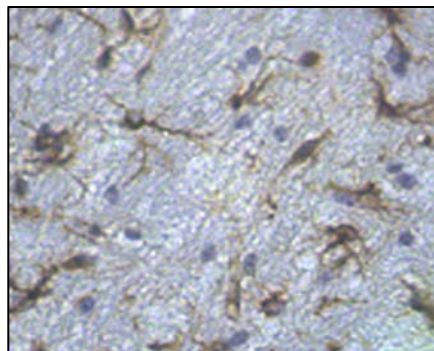
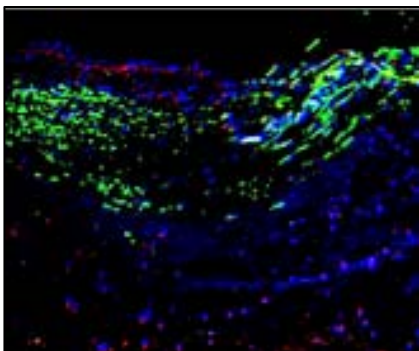


Colorado State University
**College of Veterinary Medicine
and Biomedical Sciences**
10TH ANNUAL CVMS RESEARCH DAY
SCIENTIFIC PROCEEDINGS
The Hilton Hotel
February 21st 2009



CVMBS Research Day February 21, 2009

<u>Schedule Of Events</u>		<u>Room</u>
11:30-12:00	Poster set up	Salon II, III
12:00	Opening remarks – Dr. James Graham	Salon I
12:05	Pfizer Research Award Winner–Dr. Elaine Carnevale "Effect of maternal age on assisted reproductive technologies in the mare"	Salon I
12:45	Break	
1:00-5:15	Oral Presentation I: Basic Sciences	Salon I
1:00-5:15	Oral Presentation II: Basic Sciences	Salon V
1:00-5:15	Oral Presentation III: Clinical Sciences	Salon IV
1:00-3:00	Poster Session I (Odd Numbered Posters)	Salon II, III
3:15-5:00	Poster Session II (Even Numbered Posters)	Salon II, III
5:15-6:30	Social Hour, Remove Posters	Salon II, III
6:00	Awards	Salon I

Oral Presentation: - Please limit to a 12 minute talk with 1-3 minutes for questions and changeover. Oral presentations will be in Salons I IV & V.

Poster Presentation: - Hang your posters on Feb. 21 from 11:30-12:00 in the Salons II & III. Individuals presenting the poster must be in attendance to discuss their materials with judges as listed above.

PFIZER RESEARCH AWARD WINNER

CVMBBS Research Day

Dr. Elaine Carnevale

Effect of maternal age on assisted reproductive technologies in the mare

Salon I
The Hilton Hotel
Fort Collins, CO

Dr. Carnevale obtained her DVM from Colorado State University in 1985. She continued her education in equine reproductive physiology, with a MS from Colorado State University in 1988 and a PhD from University of Wisconsin in 1994. Dr. Carnevale has worked in private practices and taught at Southern Illinois University. She is currently an Assistant Professor in the Department of Biomedical Sciences. Her appointment includes teaching, research and clinical work at CSU's Equine Reproduction Laboratory. Dr. Carnevale's clinical program focuses on the use of new assisted reproductive technologies, such as oocyte transfer and intracytoplasmic sperm injection for subfertile mares and stallions. Research interests are focused on assisted reproductive techniques and the effect of maternal aging on reproduction.

Oral Presentations

SESSION 1: BASIC SCIENCE

1:00-5:15 PM

Salon I

1:00	Bevins	Pathogen seroprevalence among bobcat (<i>Lynx rufus</i>) and puma (<i>Puma concolor</i>) populations in the western United States	MIP
1:15	Bosco-Lauth	Pre-existing immunity to related flaviviruses protects against infection by Japanese encephalitis virus in hamsters	MIP
1:30	Chaskey	The Effects of Short RNAs and the Recruitment of Decay Enzymes on Sindbis Viral RNA Stability	MIP
1:45	Chung	Attenuation of TRPC6 expression specifically reduced the diacylglycerol-mediated increase in intracellular calcium in human myometrial cells	BMS
2:00	Cullingford	Comparison of dose and injection frequency using porcine FSH and recombinant FSH for superovulating mares	BMS
2:15	Fromme	Molecular Regulation of the Developing Trophoblast	BMS
2:30	Gonzales	Sustainable TRPM4 Channel Activity in Freshly-Isolated Cerebral Artery Smooth Muscle Cells	BMS
2:45	Linke	Potential alternative to the avian influenza vaccine: Assessment of shRNA plasmids targeting viral and avian proteins	CS
3:00		BREAK	
3:15	Guth	Systemic Depletion of Tumor-Associated Macrophages and Myeloid Suppressor Cells by Liposomal Clodronate Controls the Growth of Established Tumors	CS
3:30	Guttormsen	Disruption of Tcfap2c in Primordial Germ Cells using Blimp1-Cre Prevents Germ Cell Production	BMS
3:45	Haley	Ultrasensitive Detection of PrPCWD in CWD-exposed, Conventional Test Negative Deer	MIP
4:00	Kurt	Trans-species amplification of CWD and correlation with 170N of substrate PrP	MIP
4:15	Lacerda	Differential protein expression between normal and myxomatous canine mitral valves	CS
4:30	Lee	Identification of novel targets of the RNA binding protein, CUGBP1	MIP
4:45	Lehman	Chronic feline immunodeficiency virus infection alters bone marrow-derived myeloid dendritic cell function	MIP

Oral Presentations

SESSION 2: BASIC & CLINICAL SCIENCE

1:00-5:15 PM

Salon V

1:00	Munk	Are Salmon Farms in British Columbia Currently Managed for Sustainability?	MIP
1:15	Wilsterman	Efficacy of nitazoxanide as an antiviral agent for the treatment of EHV-1 infection	CS
1:30	Pecoraro	Receptor Binding Affinity of Recent Canine Influenza A Viruses	MIP
1:45	Pfaff	Biomarkers of metastasis and resistance to chemotherapy in canine osteosarcoma	CS
2:00	Propst	Genetic Deletion of the purM Gene from Burkholderia pseudomallei Renders the Strain Completely Avirulent	MIP
2:15	Quintana	Toll-like receptor and antimicrobial peptide expression in the equine respiratory tract	MIP
2:30	Seelig	Pathogenesis of Chronic Wasting Disease in Transgenic Mice	MIP
2:45	Slota	Characterization of Upland Gamebird Facilities in the United States	ERHS
3:00		Break	
3:15	Sokoloski	Mosquito RNA-Binding Proteins Modulate Deadenylation of Alphavirus RNAs	MIP
3:30	Sottnik	Activation of innate immunity links bone infection and inhibition of osteosarcoma growth	CS
3:45	Torley	MicroRNA's in Ovine Reproduction	BMS
4:00	Walling	Associations of Intracystic Biochemicals and Markers of Inflammation with Breast Cancer Risk in Women with Benign Cystic Breast Disease – a Prospective Study	ERHS
4:15	Zhang	CUG-BP1 RNA binding protein binds to TNF mRNA and regulates its stability	MIP
4:30	Zimmerman	The effects of joint geometry on fracture in Thoroughbred racehorses	CS
4:45	Wittenburg	Sodium valproate to enhance doxorubicin sensitivity: Phase I evaluation	CS
			CS

Oral Presentations

SESSION 3: CLINICAL SCIENCE

1:00-5:15 PM

Salon IV

1:00	Bradley	Use of SmartPill technology to assess effects of Iberogast and ondansetron on gastrointestinal motility	CS
1:15	Burton	Effects of Daily Low-Dose Cyclophosphamide on Regulatory T-cells in Dogs with Cancer	CS
1:30	Miller	Detection of infectious agents and anti-erythrocyte antibodies in cats with anemia	CS
1:45	Cabano	Mechanical Comparison of Two Suture Materials for Extra-Capsular Stifle Stabilization	CS
2:00	Catbagan	Comparison of the efficacy of an oral transmucosal buprenorphine and sustained release subcutaneous buprenorphine in cats post surgical ovariohysterectomy	CS
2:15	Eucher	Prevalence of Bartonella and haemoplasma DNA in samples from non-owned free-roaming cats admitted to animal shelters in Colorado and Florida	CS
2:30	Tuohy	Clinical experience with stereotactic radiosurgery for extremity osteosarcoma	CS
2:45	Gleyzolle	Correction of Acute Functional Mitral Regurgitation: Development of a Dynamic Epicardial Device	CS
3:00		BREAK	
3:15	Kennedy	Evaluation of Interlaboratory Variance in Paired Serum Bile Acid Assays	CS
3:30	Butler	Cigarette smoking and mammographic density: The Study of Women's Health Across the Nation (SWAN)	ERHS
3:45	Marcus	Flow Cytometric Prognostic Factors in Canine B Cell Lymphoma	MIP
4:00	Neary	The Effects of a Predominantly Onion Diet on Pregnant Does	CS
4:15	Robinson	Comparison of temperature readings from a percutaneous thermal sensing microchip with temperature readings from a digital rectal thermometer in equids.	CS
4:30	Scruggs	Serotonin Transporter Expression Is Locally Down-regulated In Canine Degenerative Mitral Valves	CS
4:45	Steneroden	Prevalence of environmental Salmonella in Colorado animal shelters	CS

Poster Presentations

Session 1 - Odd Numbered Posters 1:00- 3:00 PM
Session 2 - Even Numbered Posters 3:15- 5:00PM

BASIC SCIENCES			
#1	Aria	Solid-phase tissue electrophoresis enhances sodium dodecyl sulfate-based decellularization of xenogeneic bioscaffolds	CS
#2	Ashley	ISG15 is a molecular sentinel that functions to assist mothers in coping with environmental stressors imposed on pregnancy	BMS
#3	Bradbury	Topical imidacloprid and moxidectin prevents flea transmission of Bartonella henselae in cats	CS
#4	Carsten	Resveratrol and muscadine grape extract reduce radiation-induced bone marrow PU.1 gene loss and chromosome aberrations	ERHS
#5	Crnich	Dynamic PKCδ-Mediated Trafficking of TRPM4 Regulates Smooth Muscle Excitability	BMS
#6	Denkers	Minor Oral Lesions Facilitate CWD infection	MIP
#7	Disatian	Phenotype-transformed interstitial cells in canine and human myxomatous mitral valves express tryptophan hydroxylase 1	CS
#8	Draine	Decontamination of Medical Radioisotopes from Hard Surfaces using Peelable Polymer-Based Decontamination Agents	ERHS
#9	Duffy	Effective Intranasal Immunization with Liposome Nucleic Acid Vaccine Adjuvants	MIP
#10	Eschelbach	Use of Single Cycle Simian Immunodeficiency Virus (scSIV) to Identify the Mucosal Portals of Transmission and Initial Target Cells of Primate Lentivirus Infection After Oral Challenge	MIP
#11	Gallagher	Cholinergic (starburst) amacrine cells express β-endorphin in the mouse retina	BMS
#12	Gingrich	Intestinal Parasites of Dogs on the Galapagos Islands	CS
#13	Henao-Tamayo	Post-exposure vaccination against Mycobacterium tuberculosis	MIP
#14	Herrera	Phospholipase Cy1 is Required for Pressure-Induced Vasoconstriction of Cerebral Arteries	BMS
#15	Higgins	Localized immuno-suppressive environment during the foreign body to implanted biomaterials	MIP
#16	Jones	Protection from Pneumonic Burkholderia Infection by Inhaled Antibiotic Nanoparticles	MIP
#17	Kiser	IL-10-producing CD4$^{+}$T-cells mitigate malaria-associated anemia	MIP
#18	Krull	Transcriptional profile of day 18 pregnant and non-pregnant equine endometria: an insight into maternal recognition of pregnancy	ANS

#19	Lee	The Effects of Mannose Capped Lipoarabinomannan on Dendritic Cell Function	MIP
#20	Lossing	Roles of transcription factor genes Msx1 and Vgll2 in mouse fetal ovaries	BMS
#21	Lydon	Fine-needle aspiration for the characterization of microvessel density in tumors	BMS
#22	Mathiason	Tracking Prion Infectivity in the Blood of Deer with Chronic Wasting Disease	MIP
#23	Merrick	Indoleamine 2,3 Dioxygenase in Feline Immunodeficiency Virus Infection	MIP
#24	Michel	The Role of Complement Receptor CD21/35 in a Murine Model of Chronic Wasting Disease	MIP
#25	Miles	Investigations of In Utero Vertical Transmission of Chronic Wasting Disease in Deer and Elk	MIP
#26	Partin	The stargazin C terminus encodes an intrinsic and transferable membrane sorting signal	BMS
#27	Quorllo	In vitro antitumor effects of curcumin against osteosarcoma	CS
#28	Rice	Phenotypic Characterization of Equine Mesenchymal Stem Cells	CS
#29	Sagawa	Evidence for a Novel Role of the Oncoprotein Nucleophosmin in mRNA Export and Quality Control	CMB
#30	Scapa	Ischemia in the pathogenesis of primary lesion necrosis in the guinea pig model of tuberculosis	MIP
#32	Shang	Immunological characterization of MDR-TB in guinea pig model	MIP
#33	Silveira	Testicular dysgenesis in Sitka black-tailed deer on Aliulik Peninsula, Alaska: Over expression of genes involved in testicular descent in testes regardless of their descent status	BMS
#35	Troyer	Combining Immunotherapy with Antibiotics for Treatment of Virulent Inhaled Pathogens: Francisella tularensis and Burkholderia pseudomallei	MIP
#36	Ulloa	Knockdown of TRPC proteins in human myometrial cells and their potential role in calcium signaling	BMS
#37	Wyckoff	De Novo Generation of PrPres from PrPc by PMCA	MIP
Clinical Sciences			
#38	Adams	The distribution of bacterial flora on equine limbs at a veterinary teaching hospital	CS
#39	Bucy	Characterization of Lentiviral Neuropathy Using Magnetic Resonance Imaging Techniques	ERHS
#40	Davis	Serum Fructosamine in Cats Receiving an Oral Chondroprotective Agent	CS

#41	DeLuca	Evaluation of heart rate and body temperature as potential indicators of labor in mares	CS
#42	Dudak	Detection of Bacteria in Normal Feline Liver	CS
#43	Duffy	Effectiveness of Hyperimmune Anti-parvovirus Antiserum For Treatment Of Parvovirus Infection In Dogs	CS
#44	Elliot	Determination of optimal DNA isolation methods and real time PCR protocol for detection of bacteremia in dogs	CS
#45	Ferris	The effects of dexamethasone and prednisolone treatment on pituitary and ovarian function in normal cycling mares	CS
#46	Glassner	Clinical, Microscopic, and Phenotypical Characterization of Neoplastic and Non-neoplastic Feline Hepatic Lymphocytic Diseases	Other
#47	Hafeman	Depletion of Phagocytic Cells Using Liposome Encapsulated Bisphosphonates	CS
#48	Halsey	Feline Intestinal Sclerosing Mast Cell Tumor: 50 cases (1997-2008)	MIP
#49	Hartnack	Odds of post-discharge morbidity and mortality in horses from which Salmonella was isolated during hospitalization and in horses housed on the same premises	CS
#50	Hassel	Quantitation of fecal sand clearance with a probiotic/psyllium product in horses with naturally acquired colonic sand accumulation	CS
#51	Hesser	Determination of the Mycoplasma spp. associated with cat bite abscesses	CS
#52	Hollingshead	Development of an ELISA for Analysis by a Densimeter to Quantify Progesterone in Mares	BMS
#53	Hoyt	Evaluation of sucralfate as a phosphate binder in cats with chronic renal disease	CS
#54	Keegan	Oxidative stress in cats with chronic renal failure	CS
#55	Kuhnmuench	The effect of colloid formulation on colloid osmotic pressure in horses with naturally occurring gastrointestinal disease	CS
#56	Magden	CO2 Euthanasia Best Practices Guidelines	MIP
#57	Marquez	Novel Method for a Non Invasive Technique to Assess Gastrointestinal Motility in Dogs	CS
#58	McCord	Culture-independent detection of bacteria in feline inflammatory liver disease.	CS
#59	Quimby	The pharmacokinetics of mirtazapine in healthy cats	CS
#60	Rosenbaum	Assessment of Bedding Change Frequency in IVC Mouse Cages	MIP
#61	Ryan	Radium-223 (Alpharadin™) biodistribution and acute toxicity after IV administration in dogs	CS
#62	Tangtrongsup	Prevalence of Giardia spp. infection in dogs in Chiang Mai, Thailand: preliminary findings	CS
#63	Terry	Evaluation of Hedgehog Signaling in Canine Lymphoma	CS

#64	Virgin	A comparison of sedative effects of caudal epidural detomidine hydrochloride and intravenously administered detomidine hydrochloride in equine standing laparoscopic surgery	CS
#65	Walters	Characterization of Differences in Calculated and Actual Measured Skin Doses to Canine Limbs during Stereotactic Radiosurgery using Gafchromic Film	ERHS
#66	Fenimore	Bartonella spp. associated endocarditis in dogs in Colorado and Wyoming	CS
#67	Palanisamy	Oxidant-antioxidant imbalance during Mycobacterium tuberculosis infection in the guinea pigs	MIP

Departmental Abbreviations

ANS: Animal Sciences
 BMS: Biomedical Sciences
 CMB: Cell and Molecular Biology Program
 CS: Clinical Sciences
 ERHS: Environmental and Radiological Health Sciences
 MIP: Microbiology, Immunology, and Pathology

Thank you moderators and judges!!

Thank you to our sponsor:



HESKA®

for their generous support!

BASIC SCIENCE

Solid-phase tissue electrophoresis enhances sodium dodecyl sulfate-based decellularization of xenogeneic bioscaffolds

S Arai, CMR Lacerda, EC Orton

PURPOSE: Treatment of xenogeneic bioscaffolds with ionic detergents does not completely remove soluble antigenic proteins from candidate xenogeneic scaffolds for tissue engineering. The study objective was to determine if solid-phase tissue electrophoresis enhances removal of antigenic proteins from candidate bioscaffolds. **METHODS:** Porcine aortic valve conduit (PAV) was subjected to hypotonic lysis and treated with 0.25% or 1% sodium dodecyl sulfate (SDS) overnight. Tissues were mounted in 2% agarose gel and subjected to solid-phase gel electrophoresis (SGE) at 0, 60, or 120 V for 4 h. After treatment, soluble proteins were extracted from tissues and assayed for antigenicity by immunoblot (IB) analysis with rabbit anti-PAV immune serum. Three replicate gels were prepared for each treatment. Density of IB bands was measured and relative density (%) was calculated using untreated tissue as control. **RESULTS:** SGE decreased ($p < 0.05$) tissue antigenicity and the effect was voltage dependent. There was no difference between 0.25% and 1% SDS treated tissues at similar SGE voltage. **CONCLUSION:** SGE improves the removal of antigenic proteins from PAV and enhances SDS-based bioscaffold decellularization.

ISG15 is a molecular sentinel that functions to assist mothers in coping with environmental stressors imposed on pregnancy

RL Ashley, LE Henkes, RV Anthony, KC McBroom, JK Pru, TR Hansen

The ubiquitin homolog, ISG15 is up-regulated in the endometrium in response to pregnancy in humans, baboons, ruminants, pigs, and mice. ISG15 is produced in response to type I interferon, becomes covalently attached to intracellular proteins and regulates numerous intracellular responses. The purposes of this study were to: 1) solidify a functional role for Isg15 during pregnancy using Isg15 mutant mice; 2) identify cytokines that regulate Isg15 expression during decidualization; and 3) identify pathways negatively impacted by Isg15 deficiency in vivo. We previously reported up to 70% embryo mortality in Isg15 knockout (KO) female mice when mated to either wild type (WT) or KO males. More recently, and in response to low relative humidity (<30%), the average litter size was reduced 36 % in Isg15 KO females compared to WT. Embryo mortality was also increased 1.5 fold in KO females kept under hypoxic conditions. Our findings, using two different model systems, indicate that ISG15 functions to assist mothers in coping with stressors imposed on pregnancy by the environment. IL-1 β initiates murine and human decidualization responses. It was next hypothesized that IL-1 β induces isgylation in cultured mouse decidual explants and in human uterine fibroblast (HuF) cells. Culture of mouse decidual explants (7.5 dpc) or HuF cells with 10 ng/mL IL-1 β induced an increase in Isg15 mRNA. In parallel, IL-1 β up-regulated expression of enzymes (Herc5, Ubch8) that coordinate the covalent addition of Isg15 to target proteins, as well as the gene that encodes the de-isgylation enzyme UBP43 in HuF cells. In a final series of experiments qRT-PCR was used to validate expression of select genes identified in our previous microarray analysis (~500 genes differentially expressed in Isg15 KO versus WT 7.5 dpc deciduas). We confirmed that Ifi202b, an anti-apoptotic and cell-survival gene is up-regulated and that Adam8 and Adam12 are down-regulated in decidual tissue isolated from Isg15 KO.

Topical imidacloprid and moxidectin prevents flea transmission of Bartonella henselae in cats

CA Bradbury, MR Lappin

Purpose: Bartonella species are common pathogens in cats and people and are considered significant zoonotic agents especially in immunocompromised people. The most common species isolated from cats are Bartonella henselae and Bartonella clarridgeae which are both vectored by fleas. The purpose of this study was to determine whether monthly topical administration of imidacloprid and moxidectin would lessen flea transmission of Bartonella henselae among cats. **Materials and Methods:** Eighteen specific pathogen free cats were housed in three groups of six. The three enclosures were separated by mesh so as to allow fleas to pass among groups yet prevent cats from biting or scratching one another. One group was inoculated intravenously with Bartonella henselae; three weeks later, infection was confirmed in all cats based on positive polymerase chain reaction (PCR) assay results and the cats were then housed in the middle enclosure. The Bartonella henselae infected cat group was flanked by a group that was administered topical imidacloprid and moxidectin monthly for three months and by a group that was not treated. On days 0, 30, and 60, 100 fleas per cat were placed on each of the six cats in the Bartonella henselae infected group. Over a period of thirteen weeks, blood was collected from all cats weekly for Bartonella spp. PCR, serology and culture. **Results:** While Bartonella henselae infection was ultimately confirmed in all of the untreated cats, none of the treated cats became infected. **Conclusion:** In this setting, monthly topical imidacloprid and moxidectin prevents flea transmission of Bartonella henselae in cats.

Resveratrol and muscadine grape extract reduce radiation-induced bone marrow PU.1 gene loss and chromosome aberrations

RE Carsten, AM Bachand, PN Le, SM Bailey, RL Ullrich

PURPOSE: To investigate if resveratrol (RES) or muscadine grape extract (MGE) containing RES could reduce radiation-induced PU.1 gene loss, the optimal dose of RES for reducing radiation-induced chromosome aberrations, and the optimal MGE-RES dose for reducing radiation-induced chromosome aberrations in mouse bone marrow cells. **MATERIALS:** Mice received 1 of the following treatments: no treatment, RES only, radiation only, RES initiated before radiation (Res+RAD), MGE started before radiation (MGE+RAD), and RES 2 hours or 2 days after radiation (RAD>Res 2hrs or RAD>Res 2 days+). The Res+RAD group received RES daily for 3 days prior to radiation exposure, with the third RES dose administered 30 minutes before irradiation. RES administration continued in the drinking water. MGE+RAD received the MGE with a total trans-resveratrol dose of 5.7 mcg/kg by gavage for 3 days prior to irradiation. For the RAD>Res 2hrs, RES was given as a single dose 2 hours after irradiation and for RAD>Res 2 day+, RES was initiated 2 days after irradiation and continued. Bone marrow was collected at 1 and 30 days post-irradiation for FISH PU.1 detection. Doses of 5.7 mcg/kg and 1.5-100 mg/kg of RES or 0.9-10.7 mcg/kg of total trans-resveratrol in the MGE given for 3 days prior to irradiation were used for dose response studies. Bone marrow was harvested at 1 day. **RESULTS:** RES and MGE initiated before irradiation and RES started after irradiation significantly ($p < 0.0001$) reduced PU.1 gene loss at 1 and 30 days. The optimum dose range of RES for reducing chromosome aberrations was 3.1-25 mg/kg and for the MGE it was 2.1-7.1 mcg/kg. **CONCLUSIONS:** RES alone, or as found with other bioactive factors in MGE is capable of reducing radiation-induced PU.1 gene loss. The mcg/kg doses of MGE-RES are superior to RES alone in mg/kg or equivalent mcg/kg doses of RES. Reduced PU.1 gene loss and chromosome aberrations suggests that RES and MGE may protect against radiation-induced acute myeloid leukemia.

Dynamic PKC δ -Mediated Trafficking of TRPM4 Regulates Smooth Muscle Excitability

R Crnich, GC Amberg, AL Gonzales, MT Tamkun, S Earley

The melastatin Transient Receptor Potential (TRP) channel TRPM4 is vital for pressure induced smooth muscle cell (SMC) depolarization and constriction of cerebral arteries. Protein kinase C (PKC) activity contributes to SMC excitability by a number of mechanisms, including TRPM4 activation. Although strong evidence shows a correlation between PKC, TRPM4 activity, and subsequent depolarization, the mechanisms underlying regulation of TRPM4 are unclear. Several TRP channels are regulated by dynamic, directed movement of channel protein into/out of the plasma membrane. Thus, we hypothesized that rapid insertion of TRPM4 into the plasma membrane in response to PKC activity regulates channel dynamics and controls SMC excitability. Consistent with this hypothesis, live-cell fluorescence recovery after photobleaching (FRAP) analysis of GFP-tagged TRPM4 indicate that the channel is mobile. Cell surface biotinylation and total internal reflection (TIRF) microscopy reveal that TRPM4 is rapidly inserted into the plasma membrane in response to PKC δ activity. Pressure-myograph studies of intact cerebral arteries demonstrate that TRPM4 and PKC δ are involved in PKC-induced constriction. We conclude that stimulation of PKC δ activity leads to membrane depolarization and vasoconstriction by increasing the number of TRPM4 channels in the sarcolemma.
AHA0535226N

Minor Oral Lesions Facilitate CWD infection

ND Denkers, GC Telling, EA Hoover

Purpose: Chronic wasting disease (CWD) is a highly transmissible spongiform encephalopathy (TSE) that affects deer, elk and moose. While the exact mechanism of CWD prion transmission, entry, and trafficking remains incompletely elucidated, exposure of the oral and/or nasal mucous membranes seems certain. In this respect, as part of foraging, cervids likely experience minor lesions in the oral mucous membranes; these could have impact on susceptibility to prion entry and subsequent infection. In this study we assess whether or not micro-abrasions to the tongue enhance susceptibility to CWD infection.

Materials and Methods: Transgenic mice expressing the normal cervid PrPC protein [Tg(cerPrP) mice] were inoculated orally with 10 μ l of a 10% w/v brain homogenate from either CWD-positive or negative deer. Two sets of Tg(cerPrP) mice--with or without minor abrasions on the lingual surface--were exposed orally to CWD prions. Mice are being observed and cohorts sacrificed at 1, 2, 12, 52, 78, and 104 weeks post inoculation. Western blot (WB) analysis and immunohistochemistry (IHC) are being used to detect the CWD abnormal prion protein (PrPCWD) in tongue, lymphoid tissue, and the brain.

Results: At 296 and 303 days post inoculation (dpi), two inoculated Tg(cerPrP) mice with lingual lesions developed clinical signs of neurologic dysfunction and were euthanized and analyzed for PrPCWD. Both mice were positive for PrPCWD by western blot and immunohistochemistry. No evidence of PrPCWD was detected in the Tg(cerPrP) mice examined at early time points. All remaining exposed mice are currently under observation at >300 dpi.

Conclusions: These preliminary results indicate that micro-abrasions to the lingual surface may facilitate CWD transmission. The results from animals currently on study should provide the significant numbers needed to substantiate attack rates and determine when and where PrPCWD can be detected after oral mucosal exposure.

Phenotype-transformed interstitial cells in canine and human myxomatous mitral valves express tryptophan hydroxylase 1

S Disatian, CE Orton

PURPOSE: Tryptophan hydroxylase 1 (TPH1) is the limiting enzyme for peripheral serotonin synthesis. Expression of TPH1 by valve interstitial cells (VIC) could implicate an autocrine serotonin signaling mechanism in the pathogenesis of myxomatous valve disease (MVD). The study objectives were to: 1) determine expression of TPH1 in canine normal and myxomatous mitral valves, and 2) identify the VIC phenotype expressing TPH1. **METHODS:** Expression of TPH1 was determined in canine normal (n=4) and myxomatous (n=4) mitral valves by immunoblot (IB) and immunofluorescence microscopy (IFM). IB results were expressed as band density normalized to alpha-tubulin expression. IFM results were expressed as number of TPH1+ cells/high powered field (HPF). TPH1 expression was co-localized with markers of VIC phenotype transformation: alpha-smooth muscle actin (alpha-SMA) and embryonic non-muscle myosin (SMemb) by double IFM staining. **RESULTS:** IFM demonstrated increased ($p < 0.05$) number of TPH1+ VIC in myxomatous mitral valves (14.9 ± 1.2 cells/HPF) compared to normal valves (5.0 ± 0.3 cells/HPF). TPH1 protein expression by IB was increased ($p < 0.05$) in myxomatous valves (2.7 ± 1.18) compared to normal valves (0.53 ± 0.35). Alpha-SMA and SMemb phenotype expression patterns were distinctly different in myxomatous valves. $65.5 \pm 9.2\%$ of SMemb+ VIC were TPH1+, whereas only $16.5 \pm 4.7\%$ of alpha-SMA VIC were TPH1+. **CONCLUSIONS:** TPH1 expression is increased in canine myxomatous mitral valves implicating an autocrine serotonin signaling in the pathogenesis of MVD. TPH1 expression is associated with SMemb VIC phenotype transformation.

Decontamination of Medical Radioisotopes from Hard Surfaces using Peelable Polymer-Based Decontamination Agents

AE Draine, TE Johnson

Medical radioisotopes are typically short-lived, however, down time in a medical facility related to radioisotope contamination is costly and can impact patient care. Although liquid decontamination agents can be used to address this problem, they often require multiple applications which can produce large volumes of low-level radioactive waste. Therefore, research was conducted on the decontamination efficiency of three low-volume peelable decontamination agents: Carboline ALARA 1146 (Agent A), Bartlett TLC Free (Agent B), and Cellular Bioengineering Decon Gel 1101 (Agent C). Testing was performed on vinyl composition and stainless steel tiles. Both hard surfaces can be found in hospitals, research laboratories, and universities. The tiles were contaminated with Tc-99m, TI-201, and I-131. All three agents worked efficiently on stainless steel performing at 97.37% - 99.4% removal, with Agent A outperforming the other two. Vinyl floor tile decontamination ranged from 75.78% - 97.32% removal. Agent C worked best at removing Tc-99m (97.32%) followed by Agent A at 90.49% and Agent B at 75.78%. Agent C also worked best at decontaminating TI-201 (94.00%) followed by Agent B at 89.97% and Agent A at 88.87%. Agent A worked best at removing I-131 (96.20%), followed by Agent C at 94.29% and Agent B at 92.15%. All three agents encapsulated the radionuclide very effectively and residual or cross contamination was never identified. Agent A was the most user friendly in terms of application and peelability. Agent C had the lowest odor and thinnest dry thickness. Overall, all three agents achieved a decontamination percentage of 75% or greater.

Effective Intranasal Immunization with Liposome Nucleic Acid Vaccine Adjuvants

AJ Duffy, R Troyer, and SW Dow

In previous studies we have shown that a vaccine adjuvant comprised of cationic liposomes complexed to non-coding plasmid DNA (CLDC) can elicit very effective cellular and humoral immunity when administered parenterally. Here we have investigated the effectiveness of mucosal immunization using CLDC adjuvants. We found that intranasal immunization with a protein antigen in CLDC adjuvant was able to effectively cross-prime CD8+ T cell responses and also elicit strong humoral immunity. Humoral immune responses were equivalent to those elicited by cholera toxin and superior to CpG based vaccines. We also used labeled CLDC and flow cytometry to assess uptake by antigen presenting cells in the lungs and draining lymph nodes. Intranasal administration of CLDC was associated with recruitment of inflammatory monocytes to the airways and uptake by myeloid DC in draining lymph nodes. Vaccination also elicited local production of MCP- 1 and IFN-g in the lungs. We conclude that CLDC are effective mucosal adjuvants, in part because of their ability to efficiently target mucosal APC in the lung and draining LNs.

Use of Single Cycle Simian Immunodeficiency Virus (scSIV) to Identify the Mucosal Portals of Transmission and Initial Target Cells of Primate Lentivirus Infection After Oral Challenge

E Eschelbach, HG Domingues, L Annamalai, Q Degottardi, C Mische, A Carville, DT Evans, SP O'Neil

PURPOSE: During 2006, new HIV infections occurred in 530,000 children under 15 years of age. Many pediatric infections occur as a result of mother-to-child transmission through exposure of the mucosal surfaces of the alimentary tract to infectious virus or to infected cells that are present in breast-milk; however, the anatomical sites of transmission after oral exposure and the initial targets of infection remain unknown. A principal objective of this project was to investigate whether OCT-embedded sections of frozen tissue could be used to identify the mucosal portals of viral transmission after oral challenge.

MATERIALS/METHODS: We are using single-cycle SIV (scSIV) to investigate the mechanism of oral transmission by primate lentiviruses. Unlike replication-competent viruses, scSIVs are capable of only a single round of virus replication. Thus, any cells that are infected with scSIV represent primary infections, since the virus particles that are produced are defective and unable to initiate new infections. Four pig-tailed macaques were orally inoculated with a scSIV cocktail that included 9 ug of each of three different scSIV constructs. Macaques were sacrificed at 1, 2, 3, and 4 days after oral inoculation and complete necropsies were performed, collecting alimentary tract mucosa, draining lymphoid tissues, and systemic lymphoid tissues. RNA was extracted from cryosections of alimentary tract tissue obtained from the macaque sacrificed 3 days after inoculation, and RT-nPCR was performed to detect SIV_{gag} sequences.

RESULTS/CONCLUSIONS: Both buccal mucosa and proximal colon were positive for SIV_{gag} sequences by RT-PCR, indicating that both the oral cavity and the gastrointestinal tract served as portals of viral transmission after oral inoculation. This study proved that frozen OCT tissue sections could be used as a substrate for identifying the anatomic sites of mucosal transmission. Supported by NIH grants DE012936, RR00168, and RR007000.

Cholinergic (starburst) amacrine cells express β -endorphin in the mouse retina

SGallagher, P Witkovsky, K English, M Low, V Otero-Corchon, S Hentges, J Vigh

The proopiomelanocortin (POMC) gene encodes a large precursor polypeptide that yields β -endorphin, adrenocorticotrophic hormone (ACTH), melanocyte-stimulating hormone (MSH), and other diverse biologically active peptides. Using a transgenic model in which enhanced green fluorescent protein (eGFP) or DsRed is expressed under control of the mouse POMC gene promoter, we sought to: characterize the precise morphology of POMC expressing cells in the mouse retina; investigate whether POMC colocalizes with any of the other commonly described retinal cell markers; see if the final POMC peptide products are also present in the retina. Using confocal microscopy, we were able to identify POMC fluorescent signaling in cholinergic (starburst) amacrine cell somas located at the inner border of the inner nuclear layer (INL) and in the ganglion cell layer (GCL), with two bands in the inner plexiform layer (IPL).

Immunohistochemical techniques showed that: POMC-positive cells were clearly negative for GAD 65, but colocalized GAD 67; most POMC-positive cells colocalized ChAT at both soma and the bands in sublaminae 2 and 4 in the IPL; POMC-positive cells colocalized calbindin and calretinin calcium binding proteins; few POMC-positive cells are also positive for β -endorphin. Additional staining confirmed that wild-type mouse starburst amacrine cells colocalize ChAT and β -endorphin. Although endogenous opioid peptides have previously been identified in the retina, to our knowledge this is the first evidence of endogenous β -endorphin expression in the mammalian retina. While the function of such expression has not yet been elucidated, the evidence shows that in the mouse retina starburst amacrine cells express β -endorphin.

Intestinal Parasites of Dogs on the Galapagos Islands

EN Gingrich, AV Scorza, MR Lappin, EL Clifford

Purpose: Dogs in the Galapagos Islands are a unique population created by isolation from the mainland and regulations prohibiting further importation. The effect of infectious agents of these domestic dogs on the indigenous fauna is largely unknown. The purpose of this study was to determine the prevalence of intestinal parasites in dogs on the Galapagos Islands.

Materials/Methods: Fecal samples were collected from 97 dogs presented during the neutering campaigns on Santa Cruz (n=51), San Cristobal (n=17), and Isabela (n=29) islands. Feces were evaluated for parasites by microscopic examination after zinc sulfate centrifugation flotation as well as by a commercially available IFA for *Cryptosporidium* spp. and *Giardia* spp. Polymerase chain reaction for *Cryptosporidium* spp. DNA and *Giardia* spp. DNA was performed on all positive samples to provide the infecting genotypes.

Results: *Ancylostoma caninum* (57.7%) and *Toxocara canis* (16.5%) were most commonly detected, followed by *Giardia* spp. (5.2%), *Isospora canis* (4.1%), *Sarcocystis canis* (3.1%), and *Cryptosporidium* spp. (1%). Adequate DNA for sequencing was available for one *Giardia* spp. which was shown to be assemblage D.

Conclusions: Despite being isolated, the dogs on the Galapagos have many of the same enteric parasites detected on the mainland of South America. These dogs are not routinely administered anthelmintics or other drugs, but are often allowed to roam the streets and live in close proximity to humans. Parasite prophylaxis is necessary to decrease the parasite burden within the population and to lessen the risk of spread to humans or other animals also inhabiting the islands.

Post-exposure vaccination against *Mycobacterium tuberculosis*

M Henao-Tamayo, GS Palanisamy, EE Smith, CA Shanley, B Wang, IM Orme, RJ Basaraba, NM DuTeau, D Ordway

Enhancing or facilitating immunity to tuberculosis in animal models after exposure to the infection has proved extremely difficult. We report here the results of a screening exercise in which we attempted to change the course of infection in low dose aerosol infected guinea pigs, by giving a single intradermal inoculation of vaccine ten days after exposure. In this study we used a newly described flow cytometric technique to monitor changes in cell populations accumulating in the lungs of guinea pigs challenged by low dose aerosol infection with *Mycobacterium tuberculosis* and vaccinated ten days later. On day forty after infection, the fusion protein F36 and a pool of Ag85A and ESAT-6 vaccines induced a significant decrease of the bacterial load, showed increased expression of the activation marker CD45+ on CD4+ T cells, and reduced numbers of heterophils. Lung pathology and pathology scores were marginally improved in animals given these vaccines, but lymph node pathology was not influenced. Despite early effects, no changes in long term survival were seen. These results suggest that a single post-exposure vaccination can initially slow the disease process. However, this effect is transient, but this could be of use in an multi-drug resistant/extremely drug resistant outbreak situation because it could potentially slow the infection long enough to complete drug susceptibility testing and initiate effective chemotherapy.

Phospholipase Cy1 is Required for Pressure-Induced Vasoconstriction of Cerebral Arteries

CE Herrera, R Crnich, and S Earley

Phospholipase C (PLC) hydrolyzes the phosphodiester bond of the membrane phospholipid phosphatidylinositol (4,5)-bisphosphate (PtdIns(4,5)P₂) to generate the second messengers diacylglycerol (DAG) and inositol 1,4,5-trisphosphate (IP₃). A number of PLC isoforms are present in vascular smooth muscle cells, including members of the PLC β , PLC γ , and PLC δ families. Pharmacological inhibition of PLC activity blocks both pressure- and agonist-induced vasoconstriction. To test the hypothesis that specific PLC isoforms influence discrete vasoconstrictor pathways, we used small interfering RNA (siRNA) to silence PLC γ 1 expression in intact cerebral resistance arteries. Expression of PLC γ 1 in intact cerebral arteries treated with siRNA was reduced by approximately 70% compared to controls. Arteries treated with PLC γ 1 siRNA failed to constrict in response to increases in intraluminal pressure. In contrast, vasoconstriction in response to the purinergic receptor agonist uridine triphosphate (UTP) did not differ between PLC γ 1 siRNA-treated arteries and controls. These findings demonstrate that PLC γ 1 is required to regulate myogenic responsiveness, whereas other PLC isoforms regulate agonist-induced vasoconstriction. AHA0535226N.

Localized immuno-suppressive environment during the foreign body to implanted biomaterials

DH Higgins, RJ Basaraba, AC Hohnbaum, DW Grainger, M Gonzalez-Juarrero

The implantation of synthetic biomaterials initiates the foreign body response (FBR), characterized by macrophage infiltration, foreign body giant cell (FBGC) formation and fibrotic encapsulation of the implant. The FBR is orchestrated by a complex network of immune modulators including diverse cell types, soluble mediators and unique cell surface interactions. The specific tissue locations, expression patterns, and spatial distribution of these immune modulators around the site of implantation are not clear. This study describes a new model for studying the FBR in vivo and specifically evaluates the spatial relationship of immune modulators during this response. We modified a biomaterial implantation murine in vivo model which allowed for cross-sectional in situ analysis of the FBR. A mesh nylon implant was inserted under the skin on the dorsal side of C57BL/6 mice (n=4). Immunohistochemical techniques were then used to determine the localization of the soluble mediators (IL-4, IL-13, IL-10, IL-6, TGF-beta, TNF-alpha, IFN-gamma and MCP-1), specific cell types (macrophages, neutrophils, fibroblasts, lymphocytes) and cell surface markers (F4/80, CD11b, and CD11c), at early, middle and late stages of the FBR in subcutaneous implant sites. Cytokines IL-4, IL-13, IL-10 and TGF-beta were localized to implant-adherent cells including macrophages and FBGCs. These results demonstrate localized expression of immuno-suppressive factors around the biomaterial implant that creates a privileged site for opportunistic infections. Furthermore, a better understanding of the FBR in vivo can facilitate the development of novel strategies to enhance biomaterial implant design for better performance functions and safety.

Protection from Pneumonic Burkholderia Infection by Inhaled Antibiotic Nanoparticles

A Jones, R Hansen, D Gustafson, D Allison, A Goodyear, K Propst, S Dow

Purpose: *Burkholderia pseudomallei* is a category B select agent that is a potential bioweapon. *B. pseudomallei* is resistant to many antibiotics and effective treatment requires extensive i.v. antibiotics initiated quickly after infection. We hypothesized that a single inhaled dose of slow release nanoparticles containing antibiotics could effectively control pneumonic *B. pseudomallei* infection. Materials/ Methods: Nanoparticles containing ceftazidime or doxycycline were produced by microemulsion encapsulation. Drug release characteristics in vitro and in vivo were determined by analyzing particle supernatants and tissue samples of mice given particles by HPLC/MS. Particle antibiotic activity was assessed in vitro. Mice treated with nanoparticles were challenged with *B. pseudomallei* and survival was monitored. Results: The nanoparticle supernatants contained measurable antibiotic concentrations as determined by HPLC/MS and contained antibiotics capable of inhibiting the growth of *B. thailandensis* in vitro. Concentrations of both antibiotics were detectable in serum and lung homogenates after intranasal administration, though concentrations of doxycycline in tissues were much higher than ceftazidime. Treatment with nanoparticles provided partial protection against lethal inhaled *B. pseudomallei* infection resulting in a delayed mean time to death in ceftazidime and doxycycline treated groups. Conclusions: Our data indicate that polylactic acid nanoparticles containing ceftazidime or doxycycline release active local concentrations of antibiotics in the lung. Moreover, nanoparticle delivery of antibiotic appears to be sufficient to provide significant protection against *B. pseudomallei* aerosol challenge. Our future directions are to improve the nanoparticle formulation for better entrapment and release characteristics for pulmonary protection from acute bacterial challenge.

IL-10-producing CD4+T-cells mitigate malaria-associated anemia

P Kiser, J Perry, A Avery

Purpose: Malaria is an infectious disease caused by protozoan parasites from the genus *Plasmodium*. These parasites infect and destroy red blood cells (RBC), however, the amount of RBC loss during infection is often disproportionate to parasitemia. This discrepancy is likely to be immune mediated. The immunosuppressive cytokine IL-10 has been shown to be protective against severe manifestations of malaria infection and our lab has found that IL-10 deficient (IL-10KO) mice become more anemic than wild-type mice (C57Bl/6) despite lower parasitemia during murine *Plasmodium yoelii* infection. Furthermore, our lab and others have reported that malaria-specific IL-10 producing CD4+ T cells (IL-10+CD4+ T cells) arise during *P. yoelii* infection. The purpose of this study was to determine whether IL-10+CD4+ T cells mitigate malaria-associated anemia. **Materials and Methods:** CD4+ T cells isolated from *P. yoelii*-infected and recovered IL-10KO or C57Bl/6 mice were transferred to athymic nude mice. Recipient nude mice were infected with *P. yoelii* and both anemia and parasitemia were monitored. RBC production and destruction in infected mice were monitored by enumerating RBC precursors and RBC clearance, respectively, in both strains of mice. **Results:** Nude mice that received CD4+ T cells from IL-10KO mice experienced greater RBC loss relative to parasitemia than nude mice that received T cells from C57/Bl6 mice. **Conclusions:** CD4+ T cells that express IL-10 conferred greater protection against anemia than those that are deficient in this cytokine. These data suggest that IL-10 is protective against immune-mediated anemia during malaria infection. Our results may help elucidate host mediated mechanisms of anemia in other diseases involving erythrocyte parasites.

Transcriptional profile of day 18 pregnant and non-pregnant equine endometria: an insight into maternal recognition of pregnancy

AL Krull and JE Bruemmer

Purpose: Maternal recognition of pregnancy is an essential physiological response that allows the dam to maintain pregnancy. In the pregnant mare recognition of a conceptus is required to prevent the release of prostaglandin F₂α (PGF) to allow for survival of the corpus luteum (CL) and continued production of progesterone. However, the mechanisms behind recognition of pregnancy in the mare are poorly understood. Because PGF is a pro-inflammatory hormone we hypothesized that differential gene expression in the endometrium at the time of maternal recognition will be an anti-inflammatory event leading to the decrease in PGF secretion. **Materials and Methods:** Three mares were used in a simple crossover design in which each mare served as her own non-pregnant control. The mares were inseminated every other day until ovulation was detected. On day 18 post-ovulation, embryos were recovered and endometrial biopsies were taken. Each mare's subsequent cycle was followed, without insemination, to day 18 and endometrial biopsies were taken for the non-pregnant control cycle. mRNA was isolated for microarray analysis conducted using an Affymetrix equine GeneChip specific to inflammatory processes and the results were confirmed using semi-quantitative real time PCR. **Results:** At a cut off of 1.5, microarray analysis identified 118 genes that were significantly ($p=0.001$) up regulated and 93 significantly down regulated genes in pregnant versus non-pregnant samples. RT-PCR confirmed the microarray results for 4 up and 6 down regulated genes. Pathway analysis indicated participation of these genes in pathways related to disease, cancer, cellular growth and proliferation and cell death. **Conclusions:** Although our data does not support our hypothesis and indicates that recognition of pregnancy occurs through an alternative method, the results from this study provide important new insights into gene expression in the equine endometrium during early pregnancy.

The Effects of Mannose Capped Lipoarabinomannan on Dendritic Cell Function

EJ Lee, DM Higgins, AG Rosas-Taraco, J Sanchez-Campillo, IM Orme, and M Gonzalez-Juarerro

Purpose: Mycobacterium tuberculosis (Mtb) derived mannose capped lipoarabinomannan (ManLAM) is a major component of the bacterial cell wall. ManLAM has been shown to have a negative effect on the function of dendritic cells (DCs), thus it is the purpose of this study to examine how ManLAM affects DC function through IL-10, an anti-inflammatory cytokine, and nitric oxide (NO), an anti-microbial product. **Materials/Methods:** Bone marrow derived DCs were cultured for 6-8 days in cRPMI and 20ng/mL GMCSF. Cells were treated with 1mcg/mL Mtb purified ManLam, 20ng/mL LPS, or left untreated. DC phagocytic capacity was measured using 1µm fluorescent beads and CD4+ T cell stimulatory capacity was measured by mixed lymphocyte reaction. In addition cells were analyzed by immunohistochemistry (IHC) and flow cytometry for IL-10 and NO production. Mice were treated via intra-pulmonary delivery of ManLAM directly into the lungs, and the tissue was analyzed by IHC. **Results:** DCs treated with ManLAM show reduced phagocytic capacity and an inability to stimulate CD4+ T cell proliferation in a mixed lymphocyte reaction, while LPS stimulated DCs are highly phagocytic and can stimulate CD4+ T cell proliferation. In response to ManLAM, DCs show positive staining for intracellular IL-10, though only a small amount of IL-10 is secreted. IL-10 expressing DCs are also found within the lungs of ManLAM treated mice. ManLAM treated DCs are unable to maintain NO expression both after ManLAM treatment and after H37Rv Mtb infection. **Conclusions:** These experiments show that ManLAM alters the ability of DCs to activate CD4+ T cells and to initiate a proper immune response. Even though IL-10 is not secreted by ManLAM treated DCs, its intracellular production serves an autocrine function. IL-10, a major anti-inflammatory cytokine, serves to alter the functionality of DCs preventing proper activation and expression of stimulatory receptors on the cell surface.

Roles of transcription factor genes Msx1 and Vgll2 in mouse fetal ovaries

RM Lossing, JC da Silveira, GJ Bouma

Background & Purpose: Little is known about the transcriptional regulation of mammalian fetal ovarian development. Moreover, the underlying cause of many cases of abnormal fetal gonad development is still unknown. To obtain a better understanding of the transcriptional control of mammalian fetal ovarian development, a gene profiling microarray experiment was conducted on a unique precursor somatic cell population (precursor granulosa and Sertoli cells in fetal ovaries and testes, respectively). Two transcription factors, Vgll2 and Msx1, were identified as candidate genes and expressed at significantly higher levels in precursor granulosa compared to Sertoli cells, suggesting they play a role in fetal ovarian differentiation. Vgll2 (vestigial-like 2) has been implicated in ventromedial hypothalamic and skeletal muscle development, whereas Msx1 (msh homeobox homolog 1) has been implicated in cardiac and craniofacial formation, including odontogenesis and cranial neural crest differentiation, and limb development and suppression of tumor growth. **Material & Methods:** Real time RT-PCR was conducted to confirm the Vgll2 and Msx1 expression during fetal ovarian development. In situ hybridization and immunohistochemistry were performed to examine their cellular localization pattern in fetal ovaries. **Results:** Dynamic expression patterns for Vgll2 and Msx1 were observed during fetal gonadal development in mice. Significantly higher expression was found in fetal ovaries compared to fetal testes near the time of primordial germ cell differentiation. **Conclusion:** These preliminary data reveal that the transcription factors Vgll2 and Msx1 play a role in fetal ovarian development. Future studies will focus on the role of these transcription factors in precursor granulosa cell differentiation.

Fine-needle aspiration for the characterization of microvessel density in tumors

MM Lydon, JL Sottnik, AM Guth, SW Dow

Purpose: Tumor angiogenesis is a requirement for tumor development and an important marker for assessing tumor aggressiveness. Immunohistochemical (IHC) staining of endothelial cells is the classical method for determining microvessel density (MVD). Fine-needle aspiration (FNA) cytology is a promising method for characterizing tumors, and analysis using flow cytometry is an accepted method for tumor evaluation. However, it has yet to be determined if tumor sample analysis by flow cytometry is equally representative of MVD as compared to IHC.

Hypothesis: Flow cytometry is comparable in the characterization of angiogenesis to IHC, thus allowing for the use of flow cytometry to assess changes in MVD over time and to determine the efficacy of anti-tumor agents. **Methods:** Syngeneic and immunocompetent BALB/c and C57BL/6 mice were challenged with 4T1 mammary adenocarcinoma and MCA-205 fibrosarcoma cells respectively. Mice underwent a FNA and samples were analyzed by flow cytometry. Tumor tissue was analyzed by IHC and tumor single cell suspensions were subjected to flow cytometry analysis. Endothelial cells were defined as being CD45-CD11b-CD31+PI-. Tumor sections from OCT were characterized by CD31 IHC staining. **Results:** Repeated experiments across tumor models have shown that MVD analysis as assessed by FNAs are comparable to MVD analysis of the whole tumor by flow cytometry. Ongoing experiments are being performed to assess the relationship between MVD analysis using flow cytometry verses IHC. **Conclusion:** FNAs for tumor angiogenesis have been shown to be representative of the overall tumor using flow cytometry for analysis. If angiogenesis measured by flow cytometry and IHC are correlative this would prove that flow cytometry is a reliable method for measuring tumor angiogenesis. Since FNAs have been found to be representative of the overall tumor, it is plausible angiogenesis can be reliably measured over time using repeated FNAs.

Tracking Prion Infectivity in the Blood of Deer with Chronic Wasting Disease

CK Mathiason, SAHays, J Hayes-Klug, JG Powers, GL Mason and EA Hoover.

Purpose: The blood and saliva of deer infected with chronic wasting disease (CWD) contain infectious prions (Mathiason, et. al. Science 2006). The goal of these studies was to identify the blood components responsible for prionemia in CWD infection. **Methods:** Two bioassay studies containing cohorts of n=4 CWD-naïve white-tailed deer/cohort were conducted. Study A cohorts were inoculated intravenously with cellular vs. cell free components of blood from CWD+ deer. In Study B purified leukocyte subsets comprised of either CD21+ B cells, CD14+ monocytes or CD41/61+ platelets were assessed. Additional cohorts received whole blood from either CWD + or CWD negative deer and served as controls for both studies. CWD infection status was monitored by immunohistochemistry (IHC) and western blotting (WB) for PrPCWD in tonsil biopsies collected at 0, 3, 6, 12, and 15 months post inoculation (mo. pi). At study termination (18 mo pi) a wider array of lymphoid tissues and the brain were examined. **Results:** Study A: IHC and WB analysis of tonsil biopsies and terminal tissues revealed PrPCWD in 4/4 deer inoculated with the leukocyte + platelet fraction of blood from CWD+ donors. By contrast 0 of 4 deer receiving plasma from the same donors became CWD infected. Study B: Current results based on tonsil biopsies indicates PrPCWD detection in 2/4 deer receiving CD21+ B cells, 1/4 recipients of CD41/61+ platelets, and 0/4 CD14+ deer receiving monocytes. All 8 deer serving as positive controls became PrPCWD+ in tonsil biopsies between 6 and 12 mo. pi while negative controls remained PrPCWD negative. **Conclusions:** We report for the first time associaton of infectious CWD prions with the cellular, B cell, and platelet enriched fractions and not with cell-free plasma fraction of blood from CWD+ deer. These results have bearing on the trafficking of CWD prions in deer and help direct efforts to develop an antemortem blood test to detect CWD in live cervids or other species.

Indoleamine 2,3 Dioxygenase in Feline Immunodeficiency Virus Infection

CH Merrick, KP O'Halloran, TL Lehman, PR Avery

Dendritic cells (DC) are antigen presenting cells that play a crucial role in the regulation of cell mediated immune responses. Indoleamine 2,3 dioxygenase (IDO) expression is induced in DC by interferon-gamma (IFN-g) and lipopolysaccharide (LPS) secondary to contact with viruses, bacteria, parasites or neoplastic cells. IDO catalyzes the degradation of the essential amino acid tryptophan (TRP) into the metabolite kynurenine (KYN) and the local depletion of TRP and accumulation of KYN can result in immunosuppression. Increased IDO expression during human immunodeficiency virus (HIV) infection has been demonstrated and we sought to determine if this was true in cats infected with feline immunodeficiency virus (FIV). This study compares IDO levels in feline DC from naïve and FIV-infected cats and measures serum levels of TRP and KYN in cats during the acute phase of FIV infection. Surprisingly, we found that IFN-g induced IDO expression was decreased in DC from FIV infected cats as compared to controls. Despite these in vitro results, acute FIV infection caused a significant increase in serum KYN and a significant decrease in TRP/KYN beginning as early as 3 weeks post-infection. Future studies blocking IDO activity during the acute phase of FIV infection will help to elucidate the role of IDO in lentiviral-associated immunosuppression.

The Role of Complement Receptor CD21/35 in a Murine Model of Chronic Wasting Disease

BA Michel, B Pulford and MD Zabel

Prion accumulation and replication occur in lymphoid follicles or inflammatory foci containing follicular dendritic cells (FDCs). FDCs accumulate immune complexes through their complement receptors CD21/35 and Fc receptors. These receptors, specifically CD21/35, have also been shown to play a critical role in peripheral prion pathogenesis in mouse scrapie models. In this study we evaluated the role of CD21/35 in peripheral accumulation of PrPCWD by analyzing the spleen at 15, 30, 70 and 140 days post inoculation using Western Blot and protein misfolding cyclic amplification (PMCA). We also examined feces from mice at 0, 1, 3, 6, and 8 days after oral inoculation with PrPCWD to determine whether prion retention and shedding depend on complement receptors CD21/35.

Investigations of In Utero Vertical Transmission of Chronic Wasting Disease in Deer and Elk

L Miles, C Mathiason, A Nalls, T Spraker, J Powers, E Hoover

Chronic Wasting Disease (CWD) is a fatal, neurodegenerative condition first identified in cervid populations of Colorado and Wyoming in the United States. The disease is caused by accumulation of an abnormal, partially protease-resistant form of the prion protein (PrPCWD). While horizontal transmission of CWD has been substantiated and continues to be extensively studied, vertical transmission has yet to be confirmed or heavily investigated. It is unknown whether vertical transmission should be considered as a factor in the high incidence of CWD spread through dense populations of animals. Thus, research of in utero infection is of particular importance because pre-natal transmission of CWD would impact how the disease is managed. In this study, we assess whether evidence of in utero vertical transmission of CWD is present in deer and elk. Maternal and fetal target tissues—brain at the obex region, retropharyngeal lymph node, spleen, placentome and/or cotyledon—were collected from CWD-positive and CWD-negative deer (*Odocoileus virginianus*) and elk (*Cervus elaphus*). These samples are being tested using a CWD-specific ELISA (HerdCheck, IDEXX) which identifies the amount of PrPCWD in the tissue.

The stargazin C terminus encodes an intrinsic and transferable membrane sorting signal

MA Bedoukian, JD Whitesell, EJ Peterson, CM Clay, and KM Partin

Activity-dependent plasticity of alpha-amino-3-hydroxy-5-methylisoxazole-4-propionic acid receptors is regulated by their auxiliary subunit, stargazin. Association with stargazin enhances alpha-amino-3-hydroxy-5-methylisoxazole-4-propionic acid receptor surface expression and modifies the receptor's biophysical properties. Fusing the cytoplasmic C terminus of stargazin to the C-terminal domains of either GluR1 or the gonadotropin-releasing hormone receptor permits efficient trafficking from the endoplasmic reticulum and sorting to the basolateral membrane without altering other properties of either receptor.

In vitro antitumor effects of curcumin against osteosarcoma

BA Qurollo, B Rose, DH Thamm

Purpose: Osteosarcoma (OSA) is the most common primary bone tumor in humans and dogs and is typified by aggressive local bone destruction as well as a high rate of metastasis. Novel therapies are needed. Curcumin, a derivative from the popular spice turmeric, has been reported to act against several cancer-associated molecular targets such as AKT, ERK, VEGF, and IGF-1. The goal of this study was to evaluate the potential antitumor effect of curcumin against a panel of canine and human OSA cell lines. Materials and Methods: Antiproliferative effects were evaluated using a bioreductive fluorometric assay. Alterations in ERK and AKT signaling were evaluated using western analysis. Results: Curcumin inhibited OSA cell proliferation in a dose-dependent fashion, with an EC50 of approximately 10 micromolar for a 72-hour exposure, well above reported achievable serum concentrations from human clinical trials. Western blot analysis showed no inhibition of ERK or AKT phosphorylation in lysates from OSA cells exposed for two hours to 5, 10, or 40 micromolar curcumin. Conclusions: Curcumin exhibited a dose-dependent antiproliferative effect against canine and human OSA cells, which did not seem to be associated with alterations in ERK or AKT phosphorylation. The concentration of curcumin necessary to inhibit OSA proliferation is probably unachievable in vivo.

Phenotypic Characterization of Equine Mesenchymal Stem Cells

DM Rice, SW Dow, JD Kisiday

Purpose: It is important to characterize equine mesenchymal stem cells (MSC) through cell surface antigen markers. Phenotypic characterization of MSC can help identify their undifferentiated state. The importance of this is due to the fact that MSC have the capacity to differentiate into a multitude of cell lineages. Materials/Methods: Equine bone marrow was isolated and seeded in low-Glucose DMEM with 10% FBS and 5% CTM/Pen-Strep for 7-10 days until colonies of MSC formed. After being trypsinized the MSCs were placed in alpha-MEM that contained 10% FBS and 5% CTM/Pen-Strep for expansion. The MSC were then analyzed using a panel of antibodies: CD34, CD117, CD44, CD133, CD105, CD73, CD90, CD166, and CD271. Results: Equine MSC stained positive for CD44, CD90, and CD105. Interestingly, there was a sub-population that stained positive for CD117, CD133, and CD166. This sub-population may represent a progenitor population with higher proliferative capacity. Conclusion: Equine MSC share some similar cell surface markers with other species such as CD44, CD105, and CD90. Equine MSC have a sub-population of cells which exhibit a more immature phenotype. Future investigations will further identify the sub-population seen as well as determine the phenotypic differences between early and late passaged equine MSC.

Evidence for a Novel Role of the Oncoprotein Nucleophosmin in mRNA Export and Quality Control

F Sagawa, H Ibrahim, A Morrison, CJ Wilusz, J Wilusz

Processing of the 3' end of most mRNAs in mammalian cells includes cleavage of pre-mRNAs and the subsequent addition of 150-200 adenylate residues. Previously we have shown the 32 KDa nucleophosmin (NPM) protein is deposited on the 3' untranslated region of mRNAs as a direct result of 3' end processing. Therefore NPM effectively 'marks' mRNAs that have undergone successful 3' end processing. NPM is overexpressed in most cancer cells and has been implicated as a major cause of oncogenic transformation in non-translocation lymphomas. Now the key question is what the functional consequences of NPM deposition on mRNAs are. To address this, we have used shRNA technologies to create transient and stable HeLa NPM knockdown cell lines. In these cells, we find that the length of the poly(A) tail on multiple mRNAs is significantly extended in these NPM knockdown cell lines. Furthermore, Fluorescence In Situ Hybridization (FISH) assays demonstrate that mRNAs accumulated in nucleus in of NPM knock-down cells. These data strongly suggest that NPM deposition plays a role in RNA quality control and/or the export of mRNAs out of the nucleus. Finally, we have successfully recapitulated the mRNA hyperadenylation phenotype observed in NPM knockdown cells in in vitro polyadenylation assays using nuclear extracts prepared from these cells. In addition to providing us with a powerful tool to study mechanistic aspects of NPM regulation of poly(A) tail length, this in vitro assay also suggests that NPM may be only one member of a protein complex or 'mark' that is deposited on mRNAs upon polyadenylation. We are currently identifying these components to provide additional insights into the role of NPM and the polyadenylation mark complex in hyperadenylation, mRNA export, and nuclear mRNA surveillance.

Ischemia in the pathogenesis of primary lesion necrosis in the guinea pig model of tuberculosis

J Scapa, D Ackert, N Kirk, G Palaisamy, C Shanley, I Orme, R Basaraba

Observation: Tuberculosis is a chronic inflammatory disease of humans caused by *M. tuberculosis*. Like in humans with natural infection, experimentally infected guinea pigs develop hypoxic lesions with necrosis that harbor drug-tolerant bacilli. The pathogenesis of lesion necrosis likely involves both host and pathogen factors but is poorly understood. **Hypothesis:** We hypothesize that inflammatory cell infiltrates disrupt local blood supply to lesions resulting in ischemic necrosis. **Methods:** The capillary density in lesions was compared to unaffected lung parenchyma using fluorescently labeled antibodies to endothelial cells. Blood supply to lesions compared to unaffected lung parenchyma by measuring total hemoglobin concentrations spectrophotometrically in tissue homogenates. Regional perfusion of lesions compared to unaffected lung was measured using immunofluorescent microspheres injected intravenously. **Results:** Endothelial cell density was shown to decrease in lesions versus uninfected tissue using an antibody to Factor VIII related antigen. Preliminary data from lung tissue homogenates showed hemoglobin concentrations at an average of 180.9mg/dL/gram of tissue, in normal lung tissue, as compared to 60.8mg/dL/gram of tissue, in lesions. **Conclusions:** Preliminary findings indicate vascularity is limited in lesions with necrosis as compared to normal guinea pig lung tissue and likely contributes to the pathogenesis of lesion necrosis.

Immunological characterization of MDR-TB in guinea pig model

SB Shang, M Harton, C Shanley, M Caraway, C Ruiz, R Basaraba, IM Orme, DJ Ordway

Worldwide the rate of multi-drug and extensively drug resistant TB (MDR/XDR TB) has acutely risen. A significant percentage of new clinical isolates of Mycobacterium tuberculosis (TB) are of extremely high virulence. Very little is currently known about these clinical isolates in terms of basic biology including virulence, pathogenicity and immune modulation of the host. We demonstrate that the hypervirulent strain of M.tuberculosis TN14149 shows increased bacterial growth, organ pathology and suppressed host immunity compared to the H37Rv and MDR-TB strains. We hypothesize that the virulence of strain TN14149 is associated with suppression of the protective host immune responses

This work was supported by NIH grant AI-040091, CRC grant-1-49131.

Testicular dysgenesis in Sitka black-tailed deer on Aliulik Peninsula, Alaska: Over expression of genes involved in testicular descent in testes regardless of their descent status

JC Silveira, GJ Bouma, ME Legare, RP Amann, DNR Veeramachaneni

We found that 74% of male Sitka black-tailed deer (SBTD), hunted during 1999-2007 on the Aliulik Peninsula (major affected area; southern Kodiak Island), were without scrotal testes (bilateral cryptorchid; BCO). Most male SBTD on northern Kodiak and Afognak Islands were unaffected and had scrotal testes (non-cryptorchid; NCO). Analyses of mitochondrial and microsatellite DNA revealed that SBTD on the Aliulik Peninsula reveal that inbreeding is not the cause for BCO. Based on previous studies with different species, it is likely that an endocrine disruptor might affect testicular descent in male fetuses gestating on the Aliulik Peninsula. To uncover molecular changes underlying BCO, we examined expression of genes involved in regulating testicular descent. Testicular tissue from hunter-killed deer was placed into RNAlater in the field during fall 2005-2007. SBTD gene-specific primers were designed based on available sequences in GenBank, and RT-PCR products were sequenced to confirm specificity. Real time RT-PCR analyses were performed to examine expression of *Insl3*, *Lgr8* (Great), *ERa*, and *AR* in testes from SBTD residing on Afognak Island (n=6 NCO) or the affected area (n=17 NCO, 40 BCO). Expression of all 4 genes was higher in NCO from the affected area than NCO in unaffected area; *Insl3* ~19 fold (P=0.10), *Great* ~11 fold (P=0.12), *AR* ~5 fold (P=0.20), and *ERa* ~ 4 fold (P<0.02). In the affected area, expression of *Great* and *ERa* was ~14 and ~8 fold higher in BCO compared to NCO testes (P=0.09 and 0.12, resp.). To examine the role of mutations or epigenetic factors in altered gene expression, we started to isolate, clone, and sequence promoter regions of genes in SBTD. Sequence analysis of the *Insl3* promoter region showed a conserved CpG island, which may be involved in regulating *Insl3* expression. We conclude that adult testes of SBTD in the affected area displayed greater expression of certain genes than those from an unaffected area.

Combining Immunotherapy with Antibiotics for Treatment of Virulent Inhaled Pathogens: *Francisella tularensis* and *Burkholderia pseudomallei*

R Troyer, L Kellihan, K Propst, S Dow

Purpose: *Francisella tularensis* and *Burkholderia pseudomallei* are highly virulent inhaled bacterial pathogens. In this study we sought to determine whether antibiotic therapy for these pathogens could be enhanced by immunotherapy with cationic lipid-DNA complexes (CLDC), a potent innate immune stimulant. **Methods:** We compared the susceptibility of *F. tularensis* and *B. pseudomallei* to combination immuno-antibiotic therapy using both in vitro and in vivo model systems. We infected a macrophage cell line (AMJ cells) with bacteria and then treated the cells with antibiotic, supernatant from CLDC-treated mouse spleen cells, or a combination of antibiotic plus CLDC supernatant. The effect of therapy was quantified at 24 hours post infection by lysing cells and plating intracellular bacteria on agar. Immuno-antibiotic therapy was assessed in vivo by intranasal infection of BALB/c mice followed by intraperitoneal antibiotic therapy alone or combined with CLDC immunotherapy. **Results:** In macrophages, treatment of *F. tularensis* with subtherapeutic levels of four different antibiotics combined with CLDC supernatant produced modest additive reductions in intracellular bacteria. In contrast, treatment of *B. pseudomallei* infection with a subtherapeutic level of ceftazidime combined with subtherapeutic CLDC supernatant produced a highly synergistic three log reduction in bacterial burden. In *F. tularensis* infected mice, CLDC immunotherapy slightly enhanced subtherapeutic gentamicin treatment by increasing median mouse survival time by 2 days. In *B. pseudomallei* infected mice, CLDC immunotherapy combined with ceftazidime to significantly increase mouse survival compared to ceftazidime or immunotherapy alone. **Conclusions:** CLDC immunotherapy moderately enhanced the efficacy of antibiotic therapy for *F. tularensis*. In contrast, CLDC immunotherapy synergized with ceftazidime antibiotic therapy to provide greatly enhanced treatment for *B. pseudomallei*.

Knockdown of TRPC proteins in human myometrial cells and their potential role in calcium signaling

A Ulloa, A Gonzales, S Earley, and BM Sanborn

Canonical transient receptor potential (TRPC) proteins may play a role in regulating changes in intracellular calcium ($[Ca^{2+}]_i$). Human myometrium expresses TRPC4, TRPC1 and TRPC6 mRNAs in greatest relative abundance. Contributions of TRPC4 to increases in $[Ca^{2+}]_i$ were assessed in human myometrial cells using short hairpin RNAs (shRNAs). The present data show that knockdown of endogenous TRPC4 specifically attenuates GPCR-stimulated, but not thapsigargin- or OAG-stimulated extracellular calcium-dependent increases in $[Ca^{2+}]_i$. Moreover, the oxytocin-stimulated increases in current activity are markedly attenuated in the presence of a TRPC4 knockdown. To further determine the functions of other TRPCs, knockdown of TRPC1 is being pursued. Reporter assays used to screen the most effective TRPC1-shRNA constructs show a 76-92% knockdown in the psiCHECK-2 system. Production of the adenoviral construct TC1sh1 under the control of the U6 promoter is in process. Additionally, a modified pAdTrack-CMV (pAdTCMV-MCS) vector containing new multiple cloning sites for the cloning of up to 6 shRNAs inserted between the CMV promoter and the start site for GFP protein, was produced. pAdTCMV-MCS backbone is used to produce adenovirus by homologous recombination with pAdEasy-1. Infected cells display GFP expression which decreases with increasing number of shRNA constructs cloned prior to the GFP transcription start site, due to shRNA processing. Previously tested TRPC4 and TRPC1 shRNA sequences were each cloned into this new adenoviral vector to induce knockdown of each specific protein (TRPC4 or TRPC1), and in combination (TRPC4 and TRPC1) to induce knockdown of both proteins with a single vector. RT-qPCR and immunoblotting data obtained from the adenoviral expression of TC4sh1 in this new system suggests the potential for obtaining a stronger and more effective knockdown using this novel adenoviral approach. Supported by NIH HD38970, T32-HD0703 and the March of Dimes.

De Novo Generation of PrPres from PrPc by PMCA

Christy Wyckoff, Bruce Pulford Tracy Nichols, Crystal Myerett, Kurt VerCauteren and Mark Zabel

Protein Misfolding Cyclic Amplification (PMCA) is a highly sensitive method of detection for pathogenic prion protein (PrPres). Using normal brain homogenate with excess PrPc mixed with PrPres material as a seed, the samples are run through alternating cycles of incubation at 37°C and sonication, resulting in amplification of PrPres. The sensitivity of PMCA has made it useful in the study of prions and it will likely continue to be applied to prion research. However, as with many diagnostic techniques, there is concern of false positives. Studies have demonstrated that PMCA can generate PrPres from minimal components and the concern has been raised that the PMCA procedure may be capable of producing PrPres from PrPc with out any PrPres seed present. We used a new sonicator in a prion free lab to test the hypothesis of de novo PrPres PMCA generation from PrPc alone. Three separate replicates of 20 samples of normal brain homogenate (NBH) from transgenic mice expressing cervid PrPc were sonicated for 40 seconds with a 30 minute incubation at 37°C over 24 hours; this was repeated 7 times for each of the three replicates. Each sample volume was 50 ul, with 25 ul of sonicated NBH transferred into 25 ul of new unsonicated NBH upon each additional 24-hour cycle of PMCA. After 4 PMCA rounds 1 of 60 samples was positive for PrPres (1.6%), after 5 rounds a total of 3 of 60 samples were positive (5.0%), and after 7 rounds a total of 4 of 60 samples were positive (6.7%). A total of 8 PMCA rounds were run. Sensitivity of this PMCA assay was also tested using infected elk brain homogenate (IBH) D10. Sensitivity trials yielded an increased detection of PrPres at a dilution of 9×10^2 and a sensitivity out to 2.4×10^4 after 1 round. Our results demonstrate that the PMCA procedure of incubation and sonication does result in low levels of de novo PrPres formation, or false positives. Researchers must be aware of this potential when designing studies and using PMCA.

CLINICAL SCIENCE

The distribution of bacterial flora on equine limbs at a veterinary teaching hospital

MK Adams, DA Hendrickson, DS Bolte, S Rao, FJ Olea-Popelka

Purpose: To map the distribution of the bacteria on the equine limb, compare bacterial profiles of the proximal and distal limb, and assess the implications of any differences in bacterial profiles. This will guide the equine practitioner in the selection of location-specific antimicrobial protocols for joint infection prophylaxis and treatment.

Materials/methods: Cultures were taken from twenty horses admitted to the Colorado State University College of Veterinary Medicine and Biomedical Sciences in May-June, 2008 for routine elective surgery. Samples were collected from the left mid-thorax and the dorsal aspect of 9 joints on the left side of each horse: front and hind coffin and fetlock joints, carpi, elbows, shoulders, hocks, and stifles. Culturettes were submitted to the Veterinary Diagnostic Laboratory, cultured aerobically and identified to species when possible.

Results: The likelihood of isolating gram-positive bacteria was 1.23 times ($p=0.0124$) higher at proximal sites above the fetlock than at distal sites. The likelihood of isolating coliform bacteria was 1.32 times ($p<0.05$) higher at distal sites than at proximal sites above the fetlock. The likelihood of isolating one of the common septic arthritis agents in horses was 1.16 times ($p<0.05$) higher at distal sites than at proximal sites above the fetlock. Coagulase-positive Staphylococcus was not isolated in this study.

Conclusion: There were significant differences between the bacterial profiles of the proximal and distal limb, but not enough to be clinically relevant. These findings suggest that prophylactic antibiotic strategies targeted at preexisting normal flora should be the same across the limb. The inability to isolate coagulase-positive Staphylococcus from 200 sites in this study suggests that joint infections caused by that organism are due to bacteria from a source other than pre-existing bacteria at the site.

Characterization of Lentiviral Neuropathy Using Magnetic Resonance Imaging Techniques

D Bucy, J Thompson, M Brown, L Sestina, J Elder, H Bielefeldt-Ohmann, S VandeWoude, S Kraft

NeuroAIDS is a syndrome of cognitive and motor disorders that occurs in as many as thirty percent of patients infected with Human Immunodeficiency Virus (HIV). NeuroAIDS has a complex pathogenesis that is poorly understood and only partially controlled by anti-retroviral therapies. Feline Immunodeficiency Virus (FIV), the feline analogue of HIV, shares a similar pathogenesis to HIV including neurologic dysfunction resembling NeuroAIDS. Evidence suggests that viral genotype may play a role in the severity of neuropathogenesis in both FIV and HIV infection. Three FIV genotypes were used in this study of lentiviral neuropathy: FIV-A-PPR, which has greater neurologic manifestations than other strains; FIV-C36, which causes more severe systemic disease, but has limited neurologic manifestations; and FIV-C-env, which is an FIV-A-PPR backbone with the C36 viral envelope. Experimental groups ($n=5$ per group) consisted of cats infected with equivalent doses of FIV-A-PPR, FIV-C36, FIV-C-env, or uninfected controls. Brain MRIs, including diffusion weighted imaging and MR spectroscopy, were performed at 30 days post inoculation (PI) to detect neuropathophysiology. Blood and bone marrow aspirates were also taken at regular intervals to track viremia, proviral load, and CD4+ T-cell counts. Data were also compared with a preliminary study, in which MRIs were performed at 127 days PI. In that study, there was a significant increase in tissue water diffusion in FIV-infected cats. No significant MRI differences were seen between experimental groups 30 days PI, suggesting that the initial detectable neuropathology occurs between 30 and 127 days PI.

Serum Fructosamine in Cats Receiving an Oral Chondroprotective Agent

KF Lunn and KT Davis

Purpose: Glucosamine and chondroitin sulfate (Glu/CS) are commonly used in combination to manage degenerative joint disease in humans and companion animals. Glucosamine is an amino monosaccharide derivative of glucose, and when given intravenously in high doses it causes insulin resistance in experimental animals. Studies in humans have shown that oral Glu/CS supplementation does not cause insulin resistance or affect regulation of diabetes mellitus however, similar studies in companion animals have yet to be documented. In cats, serum fructosamine concentrations reflect the average blood glucose concentrations over a period of two to three weeks. Accordingly, elevated fructosamine levels in healthy cats receiving Glu/CS supplementation would suggest that this medication may affect blood glucose regulation in cats. This study was designed to examine the effects of Glu/CS supplementation on fructosamine levels in healthy cats. **Methods:** Eight healthy research cats were enrolled, after receiving a full physical examination, serum chemistry profile, complete blood count and urinalysis. All were treated with oral Glu/CS once daily for three weeks. Serum fructosamine was measured on day 0 and day 22 at the CSU VTH. **Results:** Eight cats were treated with Glu/CS however, one cat developed conjunctivitis during the study and was excluded from data analysis. The mean serum fructosamine levels before and after Glu/CS supplementation were 241.8 and 258.0 $\mu\text{mol/l}$ (normal range: 150-325 $\mu\text{mol/l}$). A paired t-test revealed no significant difference in serum fructosamine levels before and after Glu/CS supplementation ($P=0.178$). **Conclusions:** These results suggest that oral Glu/CS supplementation does not significantly affect serum fructosamine concentrations in healthy cats. These findings may help decrease concerns about the effects of Glu/CS on glucose regulation in diabetic cats, and improve the confidence of veterinarians in using chondroprotective agents in these patients.

Evaluation of heart rate and body temperature as potential indicators of labor in mares

CA DeLuca, JM Bright, A Latimer, PM McCue

Purpose: The objective of this study was to monitor body temperature in mares treated with a prostaglandin analogue and to monitor body temperature and heart rate in prepartum mares. We hypothesized that 1) body temperature would decrease following the administration of a prostaglandin analogue, 2) body temperature would decrease prior to or during the onset of Stage I of Labor and 3) heart rate would increase with the onset of Stage II of Labor. **Materials and Methods:** Experiment 1: 5 Quarter Horse mares aged 7-16 years were used. Mares 1, 2 and 3 were intact. Mares 4 and 5 were ovariectomized. A sterilized temperature logger (Stowaway Tidbit Underwater Data Logger) was placed in the vaginal vault and body temperature was recorded for 24-48 hours before and 24 hours after administration of cloprostenol, a prostaglandin analogue (Estrumate®, 250 μg , I.M.). Experiment 2: 5 client-owned mares in late gestation were used. When milk calcium levels were = 150 ppm, indicating that the mare would likely foal within 48-72 hours, a sterilized temperature logger was placed vaginally and a Holter monitor (Ronzinn Electronics) was fitted. **Results:** Experiment 1: All mares experienced a decrease in body temperature following injection of cloprostenol. The temperature decrease ranged from -0.86 to -1.91°C (mean = -1.35°C). Experiment 2: No mare showed a change in body temperature during the study period. Heart rate data was available for 3 mares. One mare foaled before the Holter monitor could be placed. The other mare's ECG strip contained excessive noise and could not be interpreted. No mare showed an increase in heart rate with the onset of Stage II of Labor.

Conclusion: In conclusion, all mares in Experiment 1 experienced a decrease in body temperature following administration of PGF_{2a}, presumably due to heat loss following peripheral vasodilation and sweating. The onset of active labor in mares was not associated with changes in body temperature or heart rate.

Detection of Bacteria in Normal Feline Liver

J Dudak, KW McCord, KW Simpson, DC Twedt

Purpose: The etiopathogenesis of feline inflammatory liver disease (ILD) is unclear. The isolation of bacteria from ILD and a response to antibiotics supports a possible infectious etiology. Using fluorescent in situ hybridization (FISH) assays we have shown the presence of bacteria in some cats with ILD suggesting bacteria may play a role in this disease (see companion abstract). The purpose of this study was to determine the presence and spatial distribution of bacteria within the normal feline liver. **Materials/methods:** Twenty-two histologically normal liver samples were identified; 11 from necropsy and 11 surgical samples. Sections were obtained from archived paraffin embedded blocks. Unstained hepatic tissue sections were made and subjected to fluorescence in situ hybridization (FISH) with a 16S rDNA probe that recognizes bacteria in the family Enterobacterace (EUB338) and a non-EUB probe used as a control. Fluorescent antibodies against cytokeratin and factor VIIIa were used to enable distinction between bile ducts and vascular structures respectively. Tissues were examined with a fluorescence microscope for the presence and location of bacteria. **Results:** 0/11 surgical liver biopsies positive for bacteria and 1/11 necropsy samples positive for bacteria. Bacteria that were identified in some samples was located primarily over the liver capsule suggesting most likely bacterial contamination. **Conclusion:** The results of this study found that the presence of bacteria in the normal feline liver to be uncommon and, if present, it is likely a contaminant.

Effectiveness of Hyperimmune Anti-parvovirus Antiserum For Treatment Of Parvovirus Infection In Dogs

A Duffy, T Hackett, V Campbell, J Quimby, J Veir, D Chung, F Dececco, M Lappin, S Dow

Background: Administration of hyperimmune parvovirus antiserum has been recommended for treatment of dogs with parvovirus infection, in addition to standard supportive care. However, the effectiveness of this treatment has never been clinically proven. **Hypothesis:** We hypothesized that administration of hyperimmune serum to dogs with parvovirus infection would improve hematologic recovery and suppress viral replication. **Study Objectives:** To determine whether treatment with hyperimmune serum decreases viral titers, increases neutrophil and monocyte recovery rates, decreases hospitalization, and increases survival of parvovirus infected dogs treated with hyperimmune serum compared to control animals not receiving immune serum. **Study Design:** Randomized, open-label, controlled clinical trial involving dogs with confirmed parvovirus enteritis. **Materials and Methods:** Three control dogs and 4 anti-parvovirus hyperimmune serum treated dogs have been entered into the study to date, out of 20 total dogs proposed for the trial. All patients were treated with standard supportive care. The treatment group received a 12 ml intravenous infusion of hyperimmune serum, while the control group received standard supportive care only. Blood samples were collected prior to hyperimmune serum treatment and every 24 hours thereafter until death or discharge from the hospital. **Results:** Interim analysis of the data indicated that level of viremia, neutrophil counts, and days of hospitalization and overall survival times were not significantly different between the two groups. Dogs treated with hyperimmune serum had significantly lower monocyte counts. **Conclusions and Clinical Relevance:** The interim data analysis suggests that treatment with hyperimmune serum is not likely to induce significant improvement in several key parameters in dogs with parvovirus enteritis.

Determination of optimal DNA isolation methods and real time PCR protocol for detection of bacteremia in dogs

JK Veir, MS Elliott, TB Hackett, MR Lappin

Purpose: Bacterial infections and septicemia are serious complications of critical illness. Animals with severe disease were 10 times more likely to die if they had concurrent bacteremia. While isolating bacteria from the blood is essential to document bacteremia it takes days for results of standard blood culture to be available. Polymerase chain reaction (PCR) has been used to identify the presence of microbial DNA in clinical specimens. By using primers directed at sequences conserved throughout the eubacterial kingdom, PCR has been used to quickly amplify bacterial 16S ribosomal DNA making it possible to identify minute quantities of microbial specific DNA. The eubacterial DNA load in a blood sample can be quantified by use of real time PCR. The objective of this study was to determine the optimal extraction method and quantitative PCR protocol for detection of a broad range of bacterial species. Materials/Methods: Four commercially available extraction methods were evaluated both with and without enzymatic or physical cell wall disruption. The analytical efficiencies of the extraction methods were determined using dilution series of three representative gram positive and gram negative clinical isolates. Two previously published real time PCR protocols were then evaluated using the representative dilution series and Ct values were determined. Results: An automated, commercially available extraction method without pretreatment in conjunction with a previously published broad range primer/probe set proved to be the most effective with gram-negative organisms. A manual, commercially available extraction with an enzymatic pretreatment was superior for gram positive organisms but decreased recovery of DNA from gram negative organisms. Residual bacterial DNA was detected in reagents with all protocols. However, treatment of reagents with a restriction endonuclease prior to extraction significantly decreased the sensitivity of the assays evaluated.

The effects of dexamethasone and prednisolone treatment on pituitary and ovarian function in normal cycling mares

RA Ferris, PM McCue

Objective: Post mating induced endometritis (PMIE) is one of the most common causes of infertility in the mare. Recently glucocorticoids have been used to modulate the inflammatory event associated with PMIE. The objective of this study was to evaluate the effects of glucocorticoids on pituitary and ovarian function. Materials and Methods: Eighteen cycling Quarter Horse-type mares in early estrus were randomly assigned to one of three treatment groups: dexamethasone 0.05 mg/kg IV BID for 5 days, prednisolone 0.5 mg/kg PO BID for 5 days, or placebo (5 mls of molasses) PO BID for 5 days. Mares were examined by transrectal ultrasound daily to determine the day of ovulation. Blood samples were collected daily to measure luteinizing hormone (LH), progesterone, and cortisol levels. A GnRH stimulation test was administered between days 3 and 5 of treatment. Values are presented as the mean \pm SEM. Results: Dexamethasone treated mares had a greater suppression of endogenous cortisol release (9.4 ± 1.1 ng/ml) than prednisolone (41.9 ± 4.0 ng/ml) or control mares (55.6 ± 23.4 ng/ml). Follicular development of dexamethasone treated mares diverged from prednisolone and treated mares after day 2 of treatment. This divergence led to a greater number of dexamethasone treated mares failing to ovulate (4/6) than prednisolone (1/6) or control (0/6) treated mares. The percent change in pre- versus post- GnRH stimulation LH levels were similar for all treatment groups. Circulating LH levels were reduced in the dexamethasone group after two days of treatment compared to prednisolone or control groups. Mares that failed to ovulate had LH levels that remained less than 1 ng/ml (ie no LH surge occurred). Conclusion: Dexamethasone administration resulted in alteration of pituitary and ovarian function. Caution should be used when using chronic administration of dexamethasone to modulate the inflammatory event associated with PMIE.

Clinical, Microscopic, and Phenotypical Characterization of Neoplastic and Non-neoplastic Feline Hepatic Lymphocytic Diseases

K Glassner, DA Kamstock

Distinguishing between neoplastic and non-neoplastic hepatic lymphocytic diseases in cats often presents a histopathologic diagnostic challenge yet carries a significant impact with regard to treatment and prognosis. This retrospective study sought to further characterize clinical, microscopic, and phenotypical features associated with both non-neoplastic (lymphocytic cholangitis, cholangiohepatitis, and portal hepatitis) and neoplastic (portal lymphocytic lymphoma) hepatic disease in cats. Forty cases microscopically diagnosed with any of the above mentioned inflammatory hepatic diseases (20) or portal lymphocytic lymphoma (20) were acquired through the CSU Diagnostic Laboratory database. All slides were reviewed along with clinical history, treatment, and clinical follow-up. Original diagnosis was deemed appropriate or inappropriate based on response to therapy. The majority of cases revealed favorable clinical responses thus supporting accurate original diagnoses. The primary and consistent finding supporting lymphoma was the monomorphic, as well as dense and compact, population of portal lymphocytes as compared to a mixed, often more rarefied, inflammatory cell population in the inflammatory diseases which, at times, contained only few scattered neutrophils admixed with a marked population of lymphocytes. Portal bridging was more often associated with, but not limited to, inflammatory disease. Variable degrees of portal fibrosis, biliary sclerosis, biliary hyperplasia, and biliary infiltration by neoplastic or inflammatory cells were features of both. Mitotic figures were not frequently noted in the portal lymphomas. Results of this study indicate that the most significant parameter to assist in microscopically differentiating neoplastic and non-neoplastic portal lymphocytic hepatic disease in cats is the presence of a pure, monomorphic, population of dense and compact lymphocytes which may or may not infiltrate or efface associated bile ducts.

Depletion of Phagocytic Cells Using Liposome Encapsulated Bisphosphonates

SD Hafeman, RM Troyer, SW Dow

Purpose: Tumor-associated macrophages help promote tumor growth and increased numbers of these cells have been associated with a poor prognosis in many tumors. Liposomal clodronate (LC; dichloromethylene bisphosphonate encapsulated in phosphatidylcholine liposomes) has been effectively used for macrophage depletion in the treatment of IMHA in dogs, and in anti-tumor studies. However, the influence of the type of liposome used for delivery of clodronate on the efficiency of macrophage depletion has not been extensively studied. Therefore, we assessed the effects of LC prepared with different characteristics on the effectiveness of macrophage killing both in vitro and in vivo with the goal of finding the most effective formulation. Methods: Liposomes with different charges (positive, negative, neutral) as well as those containing the mannose targeting ligand were prepared containing either clodronate or phosphate buffered saline. The effects of the different liposomes on macrophage killing were assessed using murine macrophage cell lines and the MTT assay to assess cell viability. We also used fluorescently labeled liposomes and flow cytometry to assess the efficiency of macrophage uptake of liposomes. The effectiveness of in vivo depletion of phagocytic cells was also assessed by flow cytometry after i.v. administration of different LC types. Results: The liposome formulation had a significant impact on efficiency of macrophage killing in vivo, as did the origin of the macrophage cell line (monocyte-derived vs mature macrophages). Neutral, negatively charged, and mannosylated LC showed the most consistent cell killing in vitro. All three LC formulations also demonstrated significant depletion of all phagocytic cells in vivo, with the mannosylated LC being the most effective. Conclusions: Mannosylated LC elicits the most effective macrophage depletion. This suggests that mannosylated LC would be used for depletion of macrophages in anti-tumor studies.

Feline Intestinal Sclerosing Mast Cell Tumor: 50 cases (1997-2008)

C Halsey, BE Powers, DA Kamstock

The purpose of this cases series is to introduce the clinical and histopathologic features of a unique sclerosing variant of intestinal mast cell tumor (sMCT) in the cat. Splenic and intestinal mast cell tumors are the most common visceral forms of mast cell tumor in the cat and typically display similar microscopic features. Fifty cases of feline intestinal mast cell tumors with unique histological features including atypical cell morphology, a marked stromal component, and significant eosinophilic infiltrates were reviewed. Case evaluation included age, breed, sex, anatomical and microanatomical location, presence or absence of mucosal ulceration, cell pattern and morphology, mitoses, eosinophilic infiltrate, and metastasis. Ages ranged from 2-18 years (median=8). Eleven different breeds were represented with no breed or sex predilection. Lesions most often involved the small intestine 35/46 (76%) with transmural involvement in 46/50 cases (92%) and mucosal ulceration in 29/50 (58%). Cell morphology varied with a predominance of spindled variants. Poorly discernible intracytoplasmic granules which demonstrated enhanced visibility with special stains (Giemsa, Toluidine Blue), were identified in all cases. Neoplastic cells were arranged in sheets but more often formed a trabecular pattern (47/50; 94%) admixed with moderate to abundant amounts of dense stromal collagen (sclerosis). Eosinophilic infiltrates were moderate to marked in 44/50 cases (88%). Metastasis was present in ~67% of the cases involving mesenteric lymph nodes (67%) and liver (66%). Treatment and clinical outcome was available in 25/50 cases and included resection and anastomosis (R/A) only (13/25), R/A and corticosteroids (9/25), or R/A followed by treatment with CCNU (1/25), radioactive iodine (1/25), or vinblastine (1/25). With exception of the single case treated by R/A followed by vinblastine, all animals died or were euthanized within 3 months of initial diagnosis. R/A followed by vinblastine yielded a 3.5 year disease free interval. This is the first case series to characterize a sclerosing variant of intestinal mast cell tumor in the cat.

Odds of post-discharge morbidity and mortality in horses from which Salmonella was isolated during hospitalization and in horses housed on the same premises

AK Hartnack, PS Morley, DC Van Metre

Purpose: To evaluate whether horses that shed Salmonella at the CSU-VTH have a higher incidence of gastrointestinal disease following hospitalization when compared to horses that do not shed Salmonella during hospitalization. Materials/Methods: Retrospective cohort study. Horses eligible for the study were admitted as inpatients to the JLV-VTH from 2002-2008 and subsequently discharged alive. Horses allocated to the Salmonella study group had =1 fecal sample from which Salmonella was isolated during hospitalization. Horses allocated to the control group had no fecal cultures from which Salmonella was isolated and =3 fecal samples from which Salmonella was not isolated during hospitalization. Eighty-two horses were enrolled in the Salmonella group. For each horse allocated to the Salmonella group, 3 control horses (n=244) were enrolled, matched for the Salmonella-group horse by month and year of admission. A scripted interview was developed to collect data regarding health of these patients, as well as the health of horses from the same premises, during the 6 months after discharge from the JLV-VTH. Results: Owners of 221 (68%) horses were successfully contacted and agreed to participate in the study. 59/82 (72%) owners of Salmonella (+) horses participated; 162/244 (66%) owners of Salmonella (-) horses participated. Odds of the occurrence of colic (OR=1.9, 95%CI=0.8-4.4) and diarrhea (OR=1.6, 95%CI=0.7-3.4) in hospitalized horses for a 6-month period after discharge were not significantly different between the 2 groups (P>0.10, respectively). Similarly, for horses from the same premises on which horses in the study were housed after discharge, odds of the occurrence of diarrhea (OR=0.8, 95%CI=0.2-3.2) was not different for the two groups. Conclusions: No statistically significant relationship was found between Salmonella shedding status and development of subsequent gastrointestinal disease in hospitalized horses or their stablemates.

Quantitation of fecal sand clearance with a probiotic/psyllium product in horses with naturally acquired colonic sand accumulation

M Maher, DM Hassel, AE Hill, AD Landes

Purpose: To examine the efficacy of Assure™ (prebiotic, probiotic) and Assure Plus™ (prebiotic, probiotic, psyllium) on clearance of sand from horses with naturally occurring colonic sand accumulation. **Materials and Methods:** Ten adult horses were selected via radiographic screening from two local farms with known sandy environments. Pre-treatment and post-treatment cranioventral abdominal radiographs were used to quantitate sand accumulation and clearance within the large colon. All horses began receiving 132g of a concentrate mix feed, 1 week prior to the onset of the pre-treatment period and throughout the study. Approximately 200g of feces was collected and weighed on days -6, -3 and 0 to document natural sand clearance. A fecal sand serial decanting process was performed on the fecal material collected from each horse. The 10 horses were randomly divided into 2 groups and then received either the Assure and Assure Plus product, or concentrate mix alone. The treatment consisted of feeding 15g Assure powder in the am and 8 oz Assure Plus pellets in the pm as a daily supplement for 30 days. Starting on the first day of treatment, fecal samples were collected from all horses every 3 days for 30 days for fecal sedimentation analysis. **Results:** Fecal sedimentation sand clearance data was not normally distributed ($p < 0.001$ on Shapiro-Wilk testing). Zero-skewness log transformation created a new variable equal to $\ln(\text{sand clearance} - 0.2804351)$. That variable was normally distributed ($p = 0.63$), and was used for the remainder of the analyses. Pre-treatment sand clearance did not differ between treatment and control groups or between horses, but did differ by day. Post-treatment sand clearance did not differ significantly by group or horse, but did differ by day. **Conclusions:** There was no significant effect of administration of Assure and Assure Plus on sand evacuation in horses with naturally acquired sand accumulation.

Determination of the Mycoplasma spp. associated with cat bite abscesses

JM Hesser, C Torres, MR Lappin

Introduction: Mycoplasma spp. are cell wall deficient organisms that also are normal flora of the cat mouth. It is possible that these organisms are commonly associated with cat bite abscesses and may contribute to failure of common prescribed beta-lactam class antibiotics.

Purpose: To determine the prevalence of Mycoplasma spp. within cat bite abscesses before and after beta-lactam antibiotic therapy. **Materials and Methods:** Aerobic, anaerobic, and Mycoplasma spp. bacterial culture, antibiotic susceptibility testing (aerobic bacteria), and Mycoplasma spp. PCR on discharges from cutaneous abscesses formed secondary to cat bites were offered at no charge to select veterinarians in Larimer County. All abscesses were opened and drained at the discretion of the attending veterinarian, and all cats were administered amoxicillin-clavulanate drops or tablets. A recheck a day 14 was required to assess healing. Lesions that did not properly respond to initial therapy were to be sampled as before and then administered an antimicrobial drug with an anti-Mycoplasma spectrum. **Results:** To date, 13 cats have been enrolled. Anaerobic bacteria were cultured from 12 of 13 cats; Peptostreptococcus anaerobius and Fusobacterium spp. were most common. Aerobic bacteria were cultured from 11 of 13 cats; Pasturella multocida, coagulase negative Staphylococcus spp., and Enterococcus spp. were most common. Mycoplasma spp. was cultured and amplified by PCR from 1 of 13 cats before and after failure to respond to amoxicillin-clavulanate. This cat responded to enrofloxacin and clindamycin administration.

Conclusions: In this study, Mycoplasma spp. were infrequently isolated or amplified from cat bite abscesses. However, results from the cat that failed beta lactam antibiotic administration suggest a pathogenic role of the Mycoplasma spp. isolated.

Development of an ELISA for Analysis by a Densimeter to Quantify Progesterone in Mares

S Hollingshead, TM Nett, PM McCue

Measurement of circulating concentrations of progesterone is crucial for understanding early pregnancy status as well as pathological conditions involving luteal tissue. Currently progesterone in the serum is quantified using radioimmunoassay (RIA); however, this technique is time consuming and cannot be performed in the clinical setting. Previous research has shown that a microtitre plate enzyme-linked immunosorbent assay (ELISA) can be used to quantify progesterone in serum with similar specificity, sensitivity and precision compared to RIA. The objective of this research project is to adapt the ELISA protocol for use on cuvettes which can then be analyzed using a densimeter currently available on breeding farms to evaluate sperm concentrations. A capture ELISA procedure is being utilized; cuvettes are coated with the goat anti-rabbit IgG then rabbit anti-progesterone is added along with a serum sample and progesterone conjugated to horseradish peroxidase (HRP). The competitive reaction takes place for 90 min before unbound steroid is separated from antibody-bound steroid by a washing step. Finally the substrate reagent ABTS is added to the cuvette and allowed to react for 1 hour causing a visible color change. The ELISA protocol is being evaluated in order to achieve a sensitivity, specificity, accuracy and precision comparable to what is achieved by RIA. Development of a cuvette ELISA that can be read by a densimeter will allow for a rapid, reliable assay that can be performed in a clinical setting and at farms. The intention of this research is to develop an assay that quickly provides information to aid in determining whether pregnant mares need additional progesterone supplementation to maintain their pregnancies.

Evaluation of sucralfate as a phosphate binder in cats with chronic renal disease

JM Quimby, L Hoyt and MR Lappin

Purpose: Control of hyperphosphatemia is an important part of the management of CRD. Sucralfate is used as a gastric protectant in cats, but may also bind phosphorus. The purpose of this study was to determine the effect of sucralfate administration on serum phosphorus concentration, urine phosphorus fractional excretion, and fecal concentration of phosphorus of cats with CRD. **Materials/Methods:** Eight normophosphatemic cats with stable CRD were used. Five cats were administered 500 mg of sucralfate as an oral slurry, three times daily for 14 days. Two cats served as controls and did not receive sucralfate. Blood and urine samples were collected twice during the week prior to sucralfate administration, and twice during sucralfate administration. Fecal samples were collected for phosphorus levels on three cats that received sucralfate once the week prior to sucralfate administration and once 7 days after starting sucralfate. Concentrations of phosphorus, calcium, potassium, sodium and creatinine were measured on all serum and urine samples. Fractional excretion of phosphorus in urine was calculated. **Results:** Three of five cats had apparent clinical decompensation as evidenced by vomiting, anorexia and constipation after sucralfate administration. No control cats exhibited such signs. It was suspected that these abnormalities were a result of sucralfate administration and the study was discontinued. Changes in fecal phosphorus concentrations were not observed. The effect of sucralfate administration on serum phosphorus concentration or urinary excretion of phosphorus was difficult to determine because of dehydration and worsening azotemia associated with decompensation. **Conclusion:** The phosphate binding ability of sucralfate in cats is still unknown. Administration of sucralfate to cats with CRD appears to have significant side effects and cannot be recommended.

Oxidative stress in cats with chronic renal failure

R Keegan & CB Webb

Purpose: Oxidative stress is an important component in the progression of chronic renal failure (CRF) in humans, and neutrophil function may be impaired by oxidative stress in these patients. This study was designed to test the hypothesis that cats with CRF have increased oxidative stress and decreased neutrophil function when compared to Control cats. **Materials/methods:** A biochemical profile, complete blood count, urinalysis, blood pressure, plasma antioxidant capacity, erythrocyte lysate superoxide dismutase enzyme (SOD) level, whole blood reduced-to-oxidized glutathione ratio (GSH:GSSG), and neutrophil phagocytosis and oxidative burst were measured in 20 cats with CRF and 10 Control cats. Statistical comparisons (two-tailed t-test) are reported as mean \pm standard deviation. **Results:** There was no difference in age or body weight between Control and CRF cats. The CRF cats had significantly greater serum BUN, creatinine, and phosphorus concentrations than Control cats, and significantly lower PCV and urine specific gravity than Control cats. The GSH:GSSG ratio was significantly greater in the CRF group (177.6 ± 197 , 61.7 ± 33 ; $p < 0.02$), while the SOD level and antioxidant capacity were not significantly different between groups. Neutrophil oxidative burst following *E. coli* phagocytosis was significantly greater in CRF cat than Control cats (732 ± 253 , 524 ± 54 ; $p < 0.05$). **Conclusions:** The significantly greater GSH:GSSG ratio in CRF cats is consistent with an activation of antioxidant defense mechanisms in this disease state. It remains to be determined if supplementation with antioxidants beyond the level of Control cats would be of benefit in cats with CRF.

The effect of colloid formulation on colloid osmotic pressure in horses with naturally occurring gastrointestinal disease

T Kuhnmuench, ES Hackett, TB Hackett

Purpose: Protein loss secondary to gastrointestinal disease is the primary indication for colloid administration in adult horses. Information on the effects of colloidal formulations on colloid osmotic pressure (COP) and survival is currently not available for veterinarians providing primary care of critical equine patients. We hypothesized that intravenous hydroxylethylstarch colloid supplementation would raise the COP in horses with low protein secondary to gastrointestinal disease, regardless of the formulation used. **Methods:** Horses were enrolled, with client consent, if they developed a serum total protein < 5.0 g/dL or albumin < 2.2 g/dL during hospitalization for gastrointestinal disease. Horses were assigned at random to one of two treatment groups. 5 horses were treated with 10 ml/kg hydroxylethylstarch in saline (Hetastarch®) and 5 horses treated with 10 ml/kg hydroxylethylstarch in lactated ringers solution (Hextend®). Continuous data were reported as mean and 95% confidence interval. A paired t test was used to evaluate changes in COP pre- and post-colloid administration in both groups. A two sample t test was used to assess differences between groups in COP change following colloid administration. Level of significance for all comparisons was $p < 0.05$. Analysis was conducted using commercially available software (StataCorp, College Station, TX). **Results:** For both groups, average COP prior to treatment was 9.8 mmHg [7.6 – 12.0 mmHg] and post colloid treatment was 12.2 mmHg [10.1-14.3 mmHg]. COP was significantly increased with colloid treatment ($p < 0.0001$) but this increase was not significantly different between treatment groups. Survival did not differ between treatment groups ($p = 0.1779$). **Conclusion:** Colloid supplementation improved COP by nearly 25%, regardless of the formulation used. Further enrollment of horses is needed to confirm these preliminary conclusions.

CO₂ Euthanasia Best Practices Guidelines

ER Magden and S VandeWoude

CO₂ euthanasia is a primary mechanism of rodent euthanasia; however, the administration of CO₂ is controversial and the precise methods of delivery vary across campus. In order to determine the most humane method of CO₂ administration as a euthanasia agent we evaluated the current CO₂ euthanasia practices, performed in-lab observations of different techniques being utilized, and conducted a thorough review of all relevant literature. Using this information we developed a recommended protocol for the humane use of CO₂ in rodent euthanasias at CSU. We concluded that the “best” method of CO₂ euthanasia is to use a flow meter to displace 20% of the cage volume per minute with CO₂ gas. With this flow rate we can achieve the gradual effects of sedation, analgesia, and anesthesia, followed by death of the animal. With this sequence of events we can help to ensure a true eu-thanasia, or death without distress. Following a report outlining these findings and providing a video demonstration, this method was adopted by the CSU IACUC.

Novel Method for a Non Invasive Technique to Assess Gastrointestinal Motility in Dogs

M Marquez, A Bradley, K McCord, K Dowers, P Boscan and D Twedt

Purpose: Current diagnostic techniques for gastrointestinal motility disorders in veterinary practice are cumbersome, invasive, subjective and expensive. The purpose of the present study is to validate a novel, non-invasive method to measure gastrointestinal transit time, motility and pH in dogs (SmartPill®).

Materials/methods: A computerized SmartPill® capsule was ingested with food by 10 walker hound dogs. Transit time, pressure, pH and temperature were recorded through out the gastrointestinal tract. The data were downloaded and analyzed using the SmartPill® software.

Results: The SmartPill® proved to be a useful method to assess gastrointestinal transit time, pressure patterns and pH in dogs. The mean transit time was 10.93 ± 1.22 hours for the stomach, 3.4 ± 0.16 hours for the small bowel and 13 ± 1.16 hours for large bowel. Pressure patterns for the stomach were 2.9 ± 0.08 contractions per min and 12 ± 0.7 mmHg; for small bowel 1.6 ± 0.09 contractions per minute and 39 ± 1.81 mmHg and for large bowel 2.2 ± 0.05 contractions per minutes and 10 ± 0.3 mmHg. Gastric pH was 1.64 ± 0.05 during meals and 0.77 ± 0.02 between meals. The pH increased to 7.5 when the capsule entered the small bowel and later decreased to 6 when entered the large bowel. Temperature was used as an indicator for body entrance and exit.

Conclusion: The SmartPill® is a useful method to assess gastrointestinal transit time, motility and pH in dogs.

Culture-independent detection of bacteria in feline inflammatory liver disease.

KW McCord, J Dudak, JM Cullen, KW Simpson, DC Twedt

Purpose: The etiopathogenesis of feline inflammatory liver disease (ILD) is unclear. Isolation of bacteria from the liver and response to antibiotics supports an infectious etiology. This study sought to demonstrate the presence of bacteria within the liver of cats with ILD by use of culture-independent methods. **Materials:** 37 archived samples from cats with ILD changes were obtained. Routine histopathology and culture were performed. Unstained tissues were subjected to fluorescence in situ hybridization (FISH) with a 16S rDNA probe that binds DNA of bacteria in family Enterobacteriaceae (EUB338) and a non-EUB probe (control). In culture positive samples, a FISH probe for that specific bacterium was used. Fluorescent antibodies were used to distinguish between bile ducts and vascular structures. Tissues were examined with a fluorescence microscope for the presence of bacteria. Histopathology was classified as reactive hepatopathy (RH, n=15), acute neutrophilic cholangitis (ANC, n=2), chronic neutrophilic cholangitis (CNC, n=12) and lymphocytic cholangitis (LC, n=8). **Results:** Bacteria were observed in 19/37 (56%) tissue sections. Intrahepatic bacteria were visualized within portal vessels or venous sinusoids of 7 (3 CNC, 4 RH), the bile duct of 1 (CNC), and the hepatic parenchyma of 4 (1 LC, 3 RH) cats. Bacterial colonization was highest in 3 sections with CNC and 1 with RH. In 8 sections bacteria were restricted to the outer surface of the liver capsule (3 RH, 3 LC, 2 CNC) and may represent contaminants. Bacterial culture was positive in 11/23 samples. FISH and culture concurred in 14/23 cases and revealed E.coli in 3/3 CNC with invasive bacteria and 3/6 sections with capsular bacteria. 3 FISH positive samples were culture negative. **Conclusions:** The results of this study suggest that bacteria may play a role in ILD. The localization of intrahepatic bacteria to portal veins, venous sinusoids and adjacent to or within bile ducts suggests translocation of enteric bacteria to be a likely source of infection.

The pharmacokinetics of mirtazapine in healthy cats

JM Quimby, DL Gustafson, BJ Samber, KF Lunn

Purpose: To determine the pharmacokinetics of mirtazapine in clinically normal cats after oral administration of a single 3.75 mg (0.62 +/- 0.10 mg/kg) high dose (HD), or 1.88 mg (0.43 +/- 0.05 mg/kg) low dose (LD).

Materials/Methods: Ten healthy cats (2.3 +/- 0.9 years) with normal CBC, chemistry and urinalysis were used. Blood samples were collected prior to and 0.25, 0.5, 1, 4, 8, 24, 48, and 72 hours after oral administration of 3.75 mg (5 cats), or 1.88 mg (5 cats) of mirtazapine. Serum was harvested, frozen and later analyzed by high performance liquid chromatography and tandem mass spectrometry. Mirtazapine, 8-hydroxymirtazapine and glucuronide metabolite concentrations were measured. Non-compartmental pharmacokinetic modeling was performed. **Results:** No cats experienced adverse effects, although increased vocalization and affection was noted. Mean half-life was 15.4 +/- 4.7 hours (HD) and 10.2 +/- 2.2 hours (LD). Mean peak plasma concentration was 156.5.0 +/- 92.4 ng/ml (HD) and 73.1 +/- 45.5 ng/ml (LD). Mean time to maximum plasma concentration was 1.4 +/- 1.3 hr (HD) and 1.5 +/- 1.2 (LD). Mean clearance was 18.0 +/- 3.1 ml/min/kg (HD) and 10.5 +/- 3.6 ml/min/kg (LD). Mann-Whitney test was used to compare groups and there was a statistically significant difference in half-life and clearance (p = 0.03 for both) between HD and LD. Therefore, the drug does not display dose proportionality. This may be due to delay in metabolism at the higher dose as there was no significant difference between groups in the amount of glucuronidated metabolite. The limited glucuronidation ability of cats may explain this observation.

Conclusion: A single low dose of mirtazapine was well tolerated and resulted in a half-life that is compatible with a 24 hour dosing intervals in healthy cats. Higher doses may result in delayed metabolism of the drug.

Assessment of Bedding Change Frequency in IVC Mouse Cages

MD Rosenbaum, S VandeWoude, T Johnson

The frequency of mouse cage changing has significant implications not only for the animals themselves, but also for the personnel who care for the animals, and facility managers overseeing time management and per diem rates. The objective of this study was to determine the impact of microisolator bedding volume and cage change interval on microenvironmental conditions, mouse health, and behavior. A total of 15 cages housing ICR mice female (n=5/cage) were monitored for 17 days. Three different volumes of autoclaved aspen bedding chips were used: low volume (250ml); high volume (550ml); or 'normal' medium volume (400ml). Mice were evaluated (physical exam, weight) on days 7, 10, 14, and 17, and a qualitative assessment of cage soiling was photographed at these timepoints. Pooled feces was collected for corticosterone analysis, and bedding mass was also measured at these timepoints. On day 17, one mouse from each cage was euthanized and bronchoalveolar lavage was performed for cytologic analysis. Mice were videotaped for 10 minutes during the active periods on days 1, 8, and 15. Atmospheric analysis was performed daily to determine intra-cage ammonia, particulate matter, and cage humidity/temperature using a hygrometer and photo-ionization detector. Particulate size and number were recorded by an Aerodynamic Particle Sizer. Findings included variations in humidity, ammonia, and particulate depending upon cage bedding volume. Edification of cage appearance and actual intra-cage environment was obtained. No changes were recorded indicating animals were stressed, experienced adverse health effects, or were exposed to detrimental levels of particulates or adverse environmental conditions during the 17 day period. This study demonstrates that a 2-week interval between cage changes did not impact measurable animal welfare indices, despite the appearance of excessive soiling by this timepoint.

Radium-223 (Alpharadin™) biodistribution and acute toxicity after IV administration in dogs

SD Ryan, N Ehrhart, P Steyn, D Gustufson, M Dornish

A pre-clinical biodistribution and acute toxicity study was conducted to assess radium-223 for the treatment of skeletal metastases. A single IV injection of radium-223 at 3 doses (50, 150 or 450 kBq/kg) or 0.9% saline was administered to 16 dogs. Biodistribution in blood, urine and fecal samples was determined. Weekly clinical pathology samples were collected for hematology, serum biochemistry and urinalysis. Weekly body weight and fecal consistency scores were measured. Necropsy and histopathology was done 30 days after injection. Injection of radium-223 was well tolerated and adverse clinical events were rare. Radium-223 was rapidly eliminated from the blood with an alpha half-life of 10.8 minutes. Elimination of radium-223 was via both the urinary and gastrointestinal routes. A dose-dependent decrease in total WBC, granulocyte and platelet counts with nadir at 10-14 days was observed. An elevation in body temperature was seen in high dose group dogs with the granulocyte nadir. One dog in the highest dose group developed aspiration pneumonia and a grade 4 neutropenia and was euthanized prior to study completion. No abnormalities in serum biochemical or urinalysis parameters were detected. No treatment effect was observed on body weight or fecal consistency. Selective radioactivity concentration was observed by autoradiography and tissue levels in the bone specimens of all radium-223 treated dogs compared to soft tissues. A dose related decline in bone marrow hematopoietic cellularity was seen histologically in the treatment group dogs. Intravenous injection of radium-223 was well tolerated in normal beagle dogs. A dose limiting myelotoxicity in dogs was observed at the 450 kBq/kg dose. No adverse clinical events were noted in the clinically relevant 50 and 150 kBq/kg dose groups. These findings are in agreement with phase I and II European human trials and support the safety profile of the clinically used dose of 50kBq/kg in people.

Prevalence of Giardia spp. infection in dogs in Chiang Mai, Thailand: preliminary findings

S Tangtrongsup, AV Scorza, LR Ballweber, JS Reif, MD Salman, MR Lappin

Purpose: Giardia spp. is a common cause of waterborne diarrhea and is zoonotic in human, pets and wildlife animals worldwide. However, the prevalence of this organism in dogs in Thailand and the potential for dogs to serve as a reservoir host is unknown. This study was conducted to explore the prevalence of Giardia infection in dogs in this province. Establishment of a reliable diagnostic procedure in the province was considered as secondary purpose of this study. The study results then will be used to determine prevention strategies in Chiang Mai.

Materials/methods: A cross-sectional study was designed and 82 canine fecal samples were obtained from client owned dogs, breeding farms and a shelter during June and July 2008.

Demographic and geographic data were recorded. Fecal samples were scored using a standardized system. Giardia infections were diagnosed using zinc sulfate flotation, an immunofluorescent assay (IFA) and a PCR targeting the GDH gene. Associations of age category (<1 year, 1-7 years and >7 years), type of housing (client owned, breeding farms, and shelter), fecal score (1 to 7), and Giardia PCR positive results were analyzed using Fisher's exact test and odds ratios were estimated. **Results:** The prevalence of Giardia infections were 31.7%, 24.4%, and 15.9% by flotation, IFA, and PCR, respectively. Positive results were significantly associated with the age categories ($p=0.04$). When compared to dogs of more than seven years of age, the odds ratio of dogs less than one year of age was of 3.54 (95%CI: 1.06-11.83) and the odds ratio of dogs one to seven years of age was 3.36 (95%CI: 0.18-64.1). Fecal score and type of housing were not significantly associated with the Giardia positive results. **Conclusion:** Giardia infection in young dogs in Chiang Mai was common. These data suggested that dogs could be a potential reservoir for the zoonotic transmission of Giardia spp. The genotypes of the positive Giardia samples are currently being determined.

Evaluation of Hedgehog Signaling in Canine Lymphoma

JL Terry, DH Thamm, LA Wittenburg, B Rose

Purpose: The Hedgehog (Hh) cell signaling pathway plays a key role in cell differentiation, growth and localization. Activation of the pathway appears to be a key mechanism by which cancer cells avoid apoptosis, particularly in B-cell lymphoma (LSA). In our study we are exploring the importance of the Hh pathway in canine LSA as it may offer a novel therapeutic target.

Materials/Methods: Canine LSA cells were grown under normal conditions (RPMI), bone marrow conditioned media thought to be high in Hh ligands or with the Hh pathway agonist purmorphamine. Relative viable cell number was determined using a bioreductive fluorometric assay (Alamar Blue, Promega). Trizol/chloroform and Qiagen RNeasy protocols were used to obtain RNA extracts from LSA samples from the CSU Animal Cancer Center tissue archive. Extracts were DNase treated and reverse transcribed using Qiagen RT-PCR kit. PCR using GAPDH primers was performed on the samples with and without reverse transcriptase to ensure uncontaminated cDNA. Using primers specific for the Hh membrane receptor Patched (PTC), PCR was then performed. **Results:** The canine LSA 1771 cell line of B-cell origin showed a statistically significant increase in viability when grown in media containing purmorphamine while the OSW cell line of T-cell origin did not. 3 of 4 B-cell LSA cultures from primary canine LSA samples showed a statistically significant increase in viability when cultured with purmorphamine. 6 of 7 canine B and T-cell LSA samples grew significantly better in bone marrow CM. Hh membrane receptor PTC was expressed in 67% (6/9) of B-cell LSA biopsies and the 1771 cell line. The single T-cell sample and the OSW cell line did not express PTC.

Conclusions: Canine B-cell LSA cell viability is consistently higher when grown in the presence of Hh pathway agonist purmorphamine. Both T and B-cell LSA samples grow better in bone marrow conditioned media. Hh membrane receptor PTC is expressed on B but not T cell LSA samples.

A comparison of sedative effects of caudal epidural detomidine hydrochloride and intravenously administered detomidine hydrochloride in equine standing laparoscopic surgery

JE Virgin, DA Hendrickson, T Wallis, S Rao

Objective- To compare the level of sedation achieved in horses undergoing standing laparoscopic ovariectomy with continuous intravenous detomidine infusion or caudal epidural detomidine. **Study Design-** A double blind prospective study. **Animals-** 12 mares undergoing bilateral ovariectomies. **Methods-** Mares were divided into two administration groups; 6 were sedated using continuous detomidine infusion and 6 were sedated with caudal epidural detomidine. Serum cortisol measurements were taken at 4 time points for each horse: a baseline cortisol measurement when the horse was received at the clinic, 10 minutes prior to surgery, at the removal of the 2nd ovary, and 10 minutes post surgery. Two surgeons performed the surgery and an objective score was assigned at each procedure (a total of 8 within each surgery) based on a visual analogue scale for pain assessment with 0 indicating no pain and 10 indicating the worst possible amount of pain. **Results-** There were no statistical differences found among serum cortisol levels among the two administration groups. Seven of the procedures within the surgeries did not differ significantly in visual analogue scores between the two administration groups. The initial grasp of the left ovary (the first ovary) in the continuous infusion group had a significantly higher ($p=0.05$) median visual analogue scale score compared to the caudal epidural group. **Conclusions-** Continuous detomidine infusion provides as consistent and effective sedation as caudal epidural detomidine for standing laparoscopic ovariectomies in mares.

Characterization of Differences in Calculated and Actual Measured Skin Doses to Canine Limbs during Stereotactic Radiosurgery using Gafchromic Film

J Walters, JF Harmon, SD Ryan, and SM LaRue

Currently stereotactic radiosurgery (SRS) is being used as an alternate limb sparing treatment in canines with localized limb tumors that would normally undergo amputation. SRS uses high doses of radiation in a small number of fractions in an effort to kill tumor cells while sparing critical healthy tissue. During SRS of the limb the critical healthy tissue is the skin and therefore becomes the limiting factor of delivered dose. Currently, there is uncertainty in the calculated skin dose provided by treatment planning systems. This uncertainty leads clinicians to err on more conservative dosing to patients. The aim of this study is to use gafchromic film and a constructed limb phantom to characterize differences between actual measured dose and dose calculated by of the Varian Eclipse treatment planning system's algorithm as a function of distance from the skin surface. By measuring the actual dose during limb sparing SRS treatments with gafchromic film in a constructed phantom as well as on patients, and then comparing differences with calculated dose estimates clinician may be provided with the potential to increase tumor dose and likelihood of tumor control.

Bartonella spp. associated endocarditis in dogs in Colorado and Wyoming

A Fenimore, M Lappin, R Maggi, M Varanat, E Breitschwerdt

Purpose. Since the mid 1990's, several species of Bartonella, including *B. vinsonii*, *B. quintana*, and *B. clarridgeiae* have been identified in dogs diagnosed with infectious endocarditis (IE). The prevalence of Bartonella spp. infection in dogs in the referral area for Colorado State University is unknown. The purpose of this study was to evaluate the heart valves of dogs with suspected IE for the presence of Bartonella spp. DNA by polymerase chain reaction (PCR).

Materials and methods. The medical records system at the Veterinary Medical Center was searched for dogs with a clinical diagnosis of endocarditis that had been admitted from January 1990 to June 2008. DNA was extracted from the available formalin fixed valvular tissues and assessed for Bartonella spp. DNA by three PCR methods. The Bartonella spp. was determined by genetic sequencing or fluorogenic PCR.

Results. Of these 119 patients with a presumptive diagnosis of endocarditis, 22 had IE based on valvular histopathology results. The histopathology blocks and complete medical records were available from 9 dogs. Bartonella henselae DNA was amplified from the tissues of seven dogs; *B. vinsonii* DNA was amplified concurrently from three dogs. Of the seven dogs, six were from Colorado and one was from Wyoming (*B. henselae* only) and all were greater than five years of age. The dogs were not known to have left the region and fleas or ticks were reported on some dogs.

Conclusions. This is the first report of *B. henselae* associated IE in dogs. The results suggest that Bartonella spp. infection can occur in dogs in the western states and these agents should be on the differential list for dogs with suspected IE in the region.

Oxidant-antioxidant imbalance during Mycobacterium tuberculosis infection in the guinea pigs

G Palanisamy, N Kirk, F Ackart, C Shanley, I Orme, R Basaraba

Observation: In humans and guinea pigs with Mycobacterium tuberculosis (Mtb) infection, granulomatous lesions become necrotic and harbor a population of extracellular bacilli that persist even following aggressive antibiotic therapy. A better understanding of what factors contribute to lesion necrosis may improve our understanding of the mechanisms of Mtb persistence and drug tolerance. We hypothesize that altered host antioxidant defense mechanisms contribute to the oxidant-antioxidant imbalance and thus Mtb persistence. **Materials and methods:** Using the BCG vaccinated and unvaccinated guinea pig model of tuberculosis the oxidant-antioxidant imbalance is evaluated in tissues by immunohistochemistry and spectrophotometry. **Results:** As a consequence of progressive granulomatous inflammation, excessive reactive oxygen species deplete host antioxidant defense mechanism. We have observed that vaccination of guinea pigs with *M. bovis* BCG prior to aerosol infection prevents lesion necrosis and restores host antioxidant defenses. Moreover, malondialdehyde (an end product of lipid peroxidation) and the essential antioxidant transcription factor Nrf2 were increased in inflammatory and parenchymal cells in vivo. Despite the increase in cytoplasmic expression, Nrf2 function may be impaired due to the lack of cytoplasm to nuclear translocation. Nrf2 dysfunction during Mtb infection was further supported by a lack of NQO1 (Nrf2 downstream target) expression within granulomata. **Conclusion:** We conclude that the lesion necrosis occurring during overwhelming oxidative stress conditions during Mtb infection may be due to failed antioxidant defense mechanisms regulated by the host transcription factor Nrf2.

Oral Presentations

**Session I & II ~ Salon I, V
1:00-5:45PM**

BASIC SCIENCE

Pathogen seroprevalence among bobcat (*Lynx rufus*) and puma (*Puma concolor*) populations in the western United States

SN Bevins, JA Tracey, SP Franklin, VL Schmit, KL Gage, ME Schrieffer, KA Logan, LL Sweanor, MW Alldredge, WM Boyce, SPD Riley, LM Lyren, EE Boydston, C Krumm, DO Hunter, ME Roelke, MR Lappin, KR Crooks, and S VandeWoude

Relatively little is known about how habitat fragmentation affects disease dynamics in wildlife populations. Large carnivores are categorized as ecologically pivotal organisms, and we are investigating how anthropogenic disturbances might influence interactions between fragmented habitat and infectious disease. Here, we present an overview of our study on infectious disease seroprevalence in two North American carnivores -- bobcats (*Lynx rufus*) and pumas (*Puma concolor*) -- across multiple habitat types that vary in degree of urbanization. Blood samples were obtained opportunistically in Colorado and California. Preliminary data include the seroprevalence of *Yersinia pestis*, Feline immunodeficiency virus, *Bartonella henselae*, and *Toxoplasma gondii* in populations of *L. rufus* and *P. concolor*. Samples were screened for *Yersinia pestis* using a hemagglutination assay, feline immunodeficiency virus was analyzed via western blot, and the remaining pathogens were analyzed using ELISAs. Adult animals were more likely to be seropositive for all pathogens than sub-adult animals. Age, sex, species, and capture season differences were found as well. Further evaluations will model correlative relationships between response variables. This analysis of a diverse group of pathogens in multiple species will aid our understanding of the interaction between urbanization and disease transmission in wildlife.

Pre-existing immunity to related flaviviruses protects against infection by Japanese encephalitis virus in hamsters

AM Bosco-Lauth, RA Bowen

Purpose: Japanese encephalitis virus (JEV) is a mosquito-borne virus in the family Flaviviridae. It is closely related to West Nile virus (WNV) and St. Louis encephalitis virus (SLEV) and can cause severe encephalitic disease in humans and horses. JEV is endemic in Southeast Asia and the surrounding Pacific Islands and most recently emerged in Australia. If JEV were to invade the U.S. it is necessary to determine whether or not prior infection with WNV or SLEV can confer any immunity against JEV. The focus of this experiment is to examine cross-protection between flaviviruses and flaviviral vaccines against JEV in the hamster model. **Materials and Methods:** Juvenile male Golden Syrian Hamsters were divided into groups and injected with one of the following: WNV, SLEV, Yellow fever 17D vaccine strain live virus, Prevenile™ chimeric WNV vaccine, Recombitek™ recombinant WNV vaccine, Sindbis virus as a non-flavivirus control, and lastly an untreated control group. After 28 days, all hamsters were inoculated with JEV. Hamsters were bled daily for five days and humanely euthanized 14 days post-inoculation. Virus isolation was performed using Plaque Assays and antibody titers determined using Plaque Reduction Neutralization Assays, both on Vero cells. **Results:** The WNV, SLEV, and Prevenile™ vaccine groups were all negative for JEV infection as determined by absence of viremia (virus in blood.) The Recombitek™ vaccine protected 3/9 hamsters. For both Sindbis virus and Yellow fever 17D, 5/6 hamsters developed viremia. At the end of 14 days, all but 2 hamsters had neutralizing JEV antibodies and the WNV infected hamsters all had boosted WNV antibodies after JEV infection. **Discussion:** While an introduction of JEV into the U.S. is possible, these results indicate the likelihood that existing immunity against WNV and SLEV could mitigate the impact of JEV on susceptible hosts. Furthermore, vaccination against WNV could protect against JEV as well.

The Effects of Short RNAs and the Recruitment of Decay Enzymes on Sindbis Viral RNA Stability

E Chaskey, CJ Wilusz, J Wilusz

Sindbis Virus (SinV) is a positive-sense, single-stranded RNA virus in the genus Alphavirus. The viral RNA has a 5' cap and a 3' poly(A) tail, making it very similar to cellular mRNAs. Although this allows for exploitation of cellular factors to augment gene expression and replication, it also leaves the viral RNAs vulnerable to degradation by cellular mRNA decay pathways. Our laboratory has previously shown that SinV RNAs are degraded during an infection without prior reduction in the length of their poly(A) tails. This suggests that pathways for mRNA decay other than the conventional deadenylation-dependent exonuclease pathways appear to be specifically targeting viral RNAs. We hypothesize that the RNAi pathway may be playing a role in SinV RNA decay in HeLa cells. Therefore we predict that the half-lives of SinV RNAs will be increased by inhibiting the RNAi machinery in HeLa S3 cells. This hypothesis is being tested in two ways. A major component of the RNAi pathway is Dicer1, which processes the dsRNA into siRNAs. Therefore, knocking down Dicer1 may stabilize viral RNAs and facilitate replication. Our second approach is expression of the Flockhouse virus B2 protein. The B2 protein binds dsRNA, a potent activator of the RNAi pathway, and prevents its recognition during viral replication. Expression of B2 protein during SinV infection may therefore also stabilize viral RNAs. Our laboratory is also interested in exploiting viral interactions with the cellular RNA decay machinery as a therapeutic approach to treat viral infections. In a separate set of 'proof of principle' studies, we hypothesize that actively directing cellular RNA decay enzymes to viral transcripts will enhance viral RNA turnover and effectively reduce viral replication. This hypothesis is currently being tested by tethering two factors that are known to destabilize RNAs, tristetraprolin and hUpf3b, to SinV RNA using an MS2 coat protein approach.

Attenuation of TRPC6 expression specifically reduced the diacylglycerol-mediated increase in intracellular calcium in human myometrial cells

D Chung, Y-S Kim, JN Phillips, A Ulloa, HL Galan, BM Sanborn

An increase in intracellular Ca^{2+} ($[Ca^{2+}]_i$) as a result of release of Ca^{2+} from intracellular stores or influx of extracellular Ca^{2+} contributes to the regulation of smooth muscle contractile activity. Human uterine smooth muscle cells exhibit receptor-, store- and diacylglycerol (OAG)-mediated extracellular Ca^{2+} -dependent increases in $[Ca^{2+}]_i$ (SRCE) and express TRPC mRNAs (predominantly TRPC1, 4, and 6) that have been implicated in SRCE. To determine the role of TRPC6 in human myometrial SRCE, short hairpin RNA (shRNA) constructs were designed that effectively targeted a TRPC6 mRNA reporter for degradation. One sequence was used to produce an adenovirus construct (TC6sh1). TC6sh1 reduced TRPC6 mRNA but not TRPC1, 3, 4, 5 or 7 mRNAs in PHM1-41 myometrial cells. Compared to uninfected cells or cells infected with empty vector, the increase in $[Ca^{2+}]_i$ in response to OAG was specifically inhibited by TC6sh1, whereas SRCE responses elicited by either oxytocin or thapsigargin were not changed. Similar findings were observed in primary pregnant human myometrial cells. When PHM1-41 cells were activated by OAG in the absence of extracellular Na^+ , the increase in $[Ca^{2+}]_i$ was partially reduced. Furthermore, pretreatment with nifedipine, an L-type calcium channel blocker, also partially reduced the OAG-induced $[Ca^{2+}]_i$ increase. These findings suggest that OAG activates channels containing TRPC6 in myometrial cells and that these channels act in both an indirect manner via enhanced Na^+ entry coupled to activation of voltage-dependent Ca^{2+} entry channels and directly to promote elevation of intracellular Ca^{2+} . Supported by HD38970.

Comparison of dose and injection frequency using porcine FSH and recombinant FSH for superovulating mares

EL Cullingford, JP Verver, EL Squires, PM McCue, GE Seidel Jr.

Purpose: To date, results from superovulating mares have been disappointing. Recently, a recombinant FSH (reFSH) has become available with covalently linked alpha and beta subunits, giving it a longer half-life than endogenous FSH. Also, there have been conflicting data on the effectiveness of porcine FSH (pFSH) as a superovulatory treatment. The purpose of this study was to compare the dose and frequency of administration of pFSH and reFSH on ovulation rates in mares. **Materials/methods:** In phase I, 29 mares received injections of 25, 50, 100 or 150 mg pFSH or .5mg reFSH 2x/day. Mares were used up to three times, with the second cycle being a control cycle without administered FSH. In phase II, 12 different mares were administered 25 or 50 mg pFSH or .25 or .5 mg reFSH 4x/day. All treated mares were administered PGF2 alpha on the second day of treatment and given 2500 IU of hCG 24-36 h after the majority of follicles were > 30 mm. Control mares were also given PGF2 alpha, but received deslorelin to induce ovulation. **Results:** Mares receiving .5mg of reFSH 4x/day had a higher ovulation rate ($P < 0.05$) than control mares (mean 4.4, SEM 1.248 versus 1.26 SEM .094 ovulations per cycle). No other treatments were different ($P > 0.05$) from the controls; mean ovulations per cycle ranged from 1.0 to 2.6. **Conclusions:** pFSH did not increase ovulation rates at any dose or frequency of injection compared to the controls ($P > 0.05$). For mares treated with reFSH, 4x/day injections resulted in higher ovulation rates than any other treatment group ($P < 0.05$). However, four of the 18 mares administered reFSH still failed to ovulate. While reFSH may be a powerful superovulatory treatment, further research is needed to establish optimal protocols and to determine if failed ovulations are due to insufficient LH receptors or overstimulation of the ovaries.

Molecular Regulation of the Developing Trophoblast

B Fromme, J Bouma, Q Winger

Trophoblast stem (TS) cell differentiation is required for the development of a healthy placenta. TS cells can be grown in culture and provide a good model for studying stem cell differentiation. TS cells proliferate under the control of FGF-4, removing FGF-4 leads to differentiation into trophoblast giant cells (TGCs). An Affymetrix microarray performed on proliferating and differentiated trophoblast cells grown in culture revealed genes that may be involved in regulating the differentiation of TS cells. Lin-28 and Hmga2 were both found to be expressed at significantly higher levels in the proliferating cells. Lin-28 is an RNA binding protein that is expressed in many undifferentiated tissues but downregulated later in development. Hmga2 is a transcription factor involved in cell cycle regulation that is highly expressed in developing tissues. Lin-28 and Hmga2 are upregulated in some cancers, and both are regulated by the microRNA (miRNA) family Let-7. The Let-7 family is expressed in differentiated tissues, regulating gene expression and function by degrading mRNA transcripts. Conversely, LIN-28 is known to play a role in regulating Let-7 processing by binding to double stranded stem-loop precursor-miRNAs. Therefore, we would expect to detect decreased expression of Lin-28 and Hmga2, but increased Let-7s, in differentiated TGCs. Real-time PCR showed a significant decrease in Lin-28 expression in TGCs. LIN-28 protein expression and localization was examined by immunofluorescence. LIN-28 protein is found in cytoplasm, and has been detected in the nucleus in myogenic cells acting as a translational enhancer by forming protein-RNA complexes. In TS cells we found LIN-28 in cytoplasm of proliferating cells, and in cytoplasm and the nucleus of differentiated TGCs, where it may be involved with regulating RNA processing. Our studies indicate a role for Lin-28 and Hmga2 in TS cell differentiation.

Sustainable TRPM4 Channel Activity in Freshly-Isolated Cerebral Artery Smooth Muscle Cells

AL Gonzales, GC Amberg, R Crnich, S Earley

Localized control of cerebral blood flow and arterial constriction in response to changes in intraluminal pressure are dependent on the intrinsic regulation of smooth muscle cell membrane potential. The melastatin transient receptor potential (TRP) channel TRPM4 is highly selective for monovalent cations, is activated by elevated levels of intracellular Ca^{2+} , and is a critical regulator of smooth muscle membrane depolarization, which serves to open voltage dependent Ca^{2+} channels (VDCC), and resulting in myocyte contraction. Interestingly, Ca^{2+} activates and inactivates TRPM4, causing the channel to rapidly inactivate under conventional whole-cell patch clamp conditions. When the slow Ca^{2+} buffer, ethylene glycol-bis(2-aminoethylether)-N,N,N',N'-tetraacetic acid (EGTA), was included in the pipette solution, we identified a transient tetraethylammonium (TEA)-insensitive inward Na^{+} current in freshly isolated cerebral arterial myocytes. siRNA-mediated silencing of TRPM4 and the recently described TRPM4 inhibitor, 9-phenanthrol, both diminish the open probability (NPo) compared to controls, strongly suggesting the molecular identity of the channel to be TRPM4. This study demonstrates a practical method to record sustained TRPM4 activity and may be used to study other TRPM4-like Ca^{2+} sensitive channels in other excitable tissues, such as neurons. AHA0535226N; F31HL094145-01.

MyD88 dependent production of IFN-g is critical for controlling infection with Burkholderia mallei

AW Goodyear, H Bielefeldt-Ohmann, R Troyer, SW Dow

Purpose. Burkholderia mallei is a gram negative bacteria which causes glanders in horses, and is a potential biological weapon. Our group and others have shown that activation of innate immunity is required for control of acute infection with B. mallei. Therefore, we have now investigated the role of adapter protein myeloid differentiation factor 88 (MyD88), which is a key component of the Toll like receptor signaling pathway, in controlling B. mallei infection.

Methods. TLR4^{-/-}, TLR2^{-/-} and MyD88^{-/-} C57BL/6 mice were used to investigate the role of TLR signaling in response to B. mallei infection. To determine differences in survival, bacterial burden and pathology, mice were infected intranasally (i.n.) with 0.5LD50 B. mallei. Proinflammatory cytokine production was assessed by cytometric bead array or ELISA. To specifically investigate the role of IFN-gamma (IFN-g) MyD88^{-/-} mice received intraperitoneal IFN-g treatment after i.n infection with B. mallei. **Results.** When compared to WT mice, MyD88^{-/-} mice were found to be highly susceptible to B. mallei infection. In contrast, TLR4^{-/-} mice were not different from wild type mice, whereas TLR2^{-/-} were actually protected from infection. MyD88^{-/-} mice had increased pathology and bacterial burden in all major organs. When cytokine levels are normalized to bacterial burden the production of multiple cytokines was dependant on MyD88 signaling. But the only cytokine that correlated with the survival of WT mice was IFN-g. Furthermore, treatment of MyD88^{-/-} mice with IFN-g provided significant protection against acute respiratory B. mallei infection. **Conclusions.** The inability to signal via MyD88 rendered mice extremely susceptible to B. mallei infection. This effect appeared to be mediated primarily through suppression of IFN-g production.

Systemic Depletion of Tumor-Associated Macrophages and Myeloid Suppressor Cells by Liposomal Clodronate Controls the Growth of Established Tumors

AM Guth, S Hafeman, JL Sottnik, S Dow

Background: Expansion of the numbers of tumor-associated macrophages (TAMs) and myeloid suppressor cells (MSCs) are associated with inhibition of antitumor immune responses. TAMs arise from monocytes, which are recruited from the blood into tumor tissues while MSCs consist of monocytes and neutrophils released from the bone marrow that take on an immunosuppressive function. Both populations inhibit immune responses and promote tumor growth. **Hypothesis and Aims:** We hypothesized that systemic depletion of MSCs and TAMs would improve antitumor immunity and control tumor growth. In Aim 1, we assessed the effects of mannosylated liposomal clodronate (MLC) treatment on depletion of TAM and MSC in mouse tumor models. In Aim 2, we assessed the effects of MLC treatment on tumor growth and immune responses. **Materials and Methods:** To deplete MSC and TAMs, we used liposomes containing the bisphosphonate drug clodronate (MLC), which is a very effective macrophage depletion agent. Tumors were established s.c. in C57BL/6 mice. After tumors were established, i.v. once weekly treatment with MLC was initiated. Control mice were treated with liposomes containing PBS. Tumor growth was monitored using two-dimensional measurements. Total numbers of monocytes, MSCs and TAMs in tumor tissues, spleen, and blood were assessed by flow cytometry. **Results:** We found that injection of MLC was effective in significantly depleting both TAM and MSC populations in the spleen. The drug also significantly reduced circulating monocyte numbers. Treatment of tumor-bearing mice with MLC resulted in significant and sustained inhibition of tumor growth in different tumor models. **Conclusions:** MLC was an effective agent for depleting both MSCs and TAMs. Treatment with MLC i.v. was efficient in controlling the growth of established tumors and thus represents a potentially effective new approach to tumor immunotherapy and one that could be readily combined with conventional therapeutics.

Disruption of Tcfap2c in Primordial Germ Cells using Blimp1-Cre Prevents Germ Cell Production

J Guttormsen and Q Winger

Purpose: The formation of germ cells during embryonic development is driven by a complex pattern of gene expression. The transcription factor AP-2gamma (Tcfap2c) is necessary for germ cell development and fertility. Our previous mutation studies have revealed that Tcfap2c is necessary for oocyte and spermatocyte production. In this study we investigated the role of Tcfap2c during germ cell development. **Materials and Methods:** To investigate Tcfap2c we utilized the Cre/loxP conditional gene mutation strategy to overcome the early embryonic lethality of the Tcfap2c mutation. We created Tcfap2c mutant mice using the germ cell specific Blimp1-Cre model. **Results:** Tcfap2c mutant ovaries resulted in a lack of germ cells. Blimp1-Cre begins expression in the primordial germ cell population at specification around embryonic day 7 (E7). This creates Tcfap2c mutants deleted specifically in the germ cell population, allowing other tissues to develop normally. Ovaries were collected at 26 days post partum (dpp) and analyzed, mutant ovaries were noticeably reduced in size when compared to littermate controls. Histology revealed that mutant ovaries lack primary and secondary follicles at 26dpp. Therefore, to determine the time of the germ cell loss, embryos were analyzed at E8 and E12 by immunofluorescence for germ cell makers Stella and Pecam. The mutant showed decreased numbers of germ cells at both stages. **Conclusions:** This data confirms that Tcfap2c is necessary for germ cell development. The lower number of germ cells seen at E8 and E12 in mutants indicates that Tcfap2c is necessary very early in germ cell development. Tcfap2c could be regulating germ cell specification which would result in fewer initial germ cells or germ cells could be specified but decrease due to lack of proliferation or increased apoptosis. These discoveries establish the Tcfap2c mutation as a potential genetic cause for reproductive failure in humans.

Ultrasensitive Detection of PrPCWD in CWD-exposed, Conventional Test Negative Deer

NJ Haley, CK Mathiason, MD Zabel, GC Telling, EA Hoover

Purpose: Chronic wasting disease (CWD), a prion disease affecting captive and free-ranging cervids (e.g. deer, elk, and moose), is distinguished by its high level of transmissibility. Bodily fluids and excretions are thought to play an important role in the transmission of CWD. Using cervid bioassay and established CWD detection methods, we have previously identified infectious prions in saliva and blood but not urine or feces of CWD+ donors. This contrasted with more recent findings, in which CWD prions were detected in urine using a cervid transgenic mouse (Tg[CerPrP] mouse) bioassay. We sought to identify the abnormal CWD prion protein (PrPCWD) and prion infectivity in brains of CWD-exposed, though conventional test-negative deer. **Materials/Methods:** Brain and retropharyngeal lymph nodes of negative deer were reanalyzed for PrPCWD using serial protein misfolding cyclic amplification (sPMCA) and cervid transgenic mouse bioassay. **Results:** PrPCWD was detected by sPMCA and Tg[CerPrP] bioassay in the brain and retropharyngeal lymph nodes of exposed, CWD-negative deer. The concentration of infectious prions was low, as indicated by: undetectable PrPCWD levels in traditional assays (western blot, ELISA) and extended incubation periods in test brain-inoculated vs. positive control Tg[CerPrP] mice (250+/- 19 vs. 149 +/- 11days, respectively). **Conclusions:** Very low levels of CWD prions can be detected in the tissues of CWD-exposed but conventional test negative deer. The finding of subclinical infection in deer exposed to urine and feces extends our understanding of CWD transmission and highlights the potential for infectious prions in body fluids in other prion infections, while demonstrating the sensitive and specific application of sPMCA in the diagnosis of prion diseases.

Trans-species amplification of CWD and correlation with 170N of substrate PrP

TD Kurt, GC Telling, MD Zabel, EA Hoover

Purpose: Chronic Wasting Disease (CWD) is an efficiently transmitted prion disease of cervids. Whether CWD could represent a threat to non-cervid species remains speculative. We previously demonstrated in vitro amplification of CWD prions (PrP-CWD) by serial protein misfolding cyclic amplification (sPMCA) using brain substrate from transgenic mice [Tg(CerPrP) mice] expressing normal cervid prion protein (PrP-C). Here we attempted to amplify CWD prions in brain substrates from several non-cervid species to test the hypothesis that sPMCA can be used to predict potential susceptibility to CWD.

Methods: We diluted PrP-CWD from infected deer into brain substrate from several species including Mus mice, Peromyscus mice, prairie voles, prairie dogs, cats, coyotes and transgenic mice [Tg(HuPrP) mice] expressing human PrP-C. The samples were loaded into a 96-well plate and alternately sonicated/incubated for 48 hrs, then subjected to protease digestion and western blotting. Successful amplification was indicated by newly formed protease-resistant bands in samples seeded with PrP-CWD but not in non-PrP-CWD-seeded controls. Non-seeded control samples were used as a guide to assure complete PrPC digestion.

Results: Brain homogenates from several CWD-susceptible non-cervid species supported amplification of PrPCWD by sPMCA, whereas brain homogenates from several CWD-resistant species did not. Analysis of PrP sequence suggests that the ability to support amplification of PrPCWD by trans-species sPMCA is correlated with the presence of asparagine at position 170 of the substrate species PrP.

Conclusion: Our results suggest that sPMCA may offer insights into barriers to transmission of CWD, including the effects of host PrP sequence.

Differential protein expression between normal and myxomatous canine mitral valves

CMR Lacerda, EC Orton

Purpose: Each year, valvular heart disease accounts for over 20,000 deaths in the U.S. Myxomatous valve disease (MVD) is the most common heart valve disease in humans and dogs. MVD is pathologically identical in these species, and its pathogenesis is poorly understood. The study objectives were to 1) develop proteomic methodology suitable for analysis of extracellular matrix-rich heart valve tissues, and 2) survey over- and under-expressed proteins that could provide mechanistic clues into the pathogenesis of MVD.

Methods: Normal, early-stage and late-stage myxomatous mitral valves from dogs were studied. A shotgun proteomic analysis of extracted proteins with iTRAQ labeling to determine differential protein quantification was employed. Proteins were classified by function and clustered according to differential expression patterns.

Results: More than 300 proteins, with almost 100 of those being differentially expressed were identified. Hierarchical sample clustering of differential protein profiles showed that early- and late-stage valves were closely-related. This finding suggests that fast proteome changes occur in early degeneration stages and these changes persist in late stages, characterizing a diseased proteome that is distinct from normal.

Conclusions: Shotgun proteomic analysis of matrix-rich canine heart valves is feasible, and should be applicable to human heart valves as well. Differential protein expression provides a basis for future investigations into the pathogenesis of canine and human MVD.

Identification of novel targets of the RNA binding protein, CUGBP1

JE Lee, J Wilusz, CJ Wilusz

Myotonic Dystrophy Type 1 (DM1) is an autosomal dominant disorder caused by a trinucleotide (CTG) repeat expansion in the 3' UTR of the DMPK gene. Much of the disease pathology, including myotonia, muscle wasting and insulin resistance, results directly from toxic effects of the repeat-containing RNA. The mutant RNA sequesters several cellular proteins into nuclear foci. DM1 cells commonly show altered expression and/or function of several RNA-binding proteins, including CUGBP1. CUGBP1 has been implicated in the first step of mRNA degradation, namely deadenylation. Our previous results¹ have shown that CUGBP1 binds to the 3'UTR of the Tumor Necrosis Factor (TNF) mRNA and recruits the PARN deadenylase to mediate rapid poly(A) shortening. Consistent with this, depletion of CUGBP1 from muscle cells results in stabilization of TNF mRNA. Moreover, expression of mutant CUG-repeat containing DMPK sequences in muscle cells also induces TNF mRNA stabilization as well as changes in CUGBP1 phosphorylation status². Based on these results we hypothesize that there are other clinically relevant mRNAs whose decay is regulated by CUGBP1 and PARN. We have initiated global analyses of mRNA decay rates in CUGBP1 and PARN knockdown muscle cells, with the goal of identifying such targets.

Chronic feline immunodeficiency virus infection alters bone marrow-derived myeloid dendritic cell function

T Lehman, K O'Halloran, E Hoover, P Avery

Purpose: As dendritic cells (DC) are potent antigen presenting cells integrating the innate and cell-mediated immune responses to infection, DC-lentivirus interactions could be fundamental to the persistent immune dysfunction that marks FIV, SIV, and HIV infections. **Materials/methods:** We have developed methods to generate large numbers of feline myeloid DCs (mDC) from bone marrow precursors, which can be collected via needle biopsy and differentiated in vitro in the presence of feline granulocyte macrophage colony stimulating factor. Utilizing serial bone marrow (BM) collections, we have compared mDC generated from naïve and chronically FIV-infected cats to determine whether differences in BM mDC growth, phenotype, maturation, or function are present. **Results:** These studies have shown that feline BM-derived mDC from FIV-infected cats: (a) appear to be productively infected by FIV and (b) are impaired in their ability to stimulate CD4⁺ T cell proliferation, as measured by allogeneic mixed leukocyte reaction (MLR). This mDC dysfunction does not appear to be associated with altered ex vivo mDC growth or maturation as determined by enumerating CD11c and MHC class II double-positive cells, measuring expression levels of CD11c, CD80, CD1a, and MHC class II, and measuring endocytic capacity. The impaired ability to stimulate T cells appears to be specific to the DC-T cell interaction (immunological synapse) as T cells from the MLR assay proliferate with subsequent mitogenic stimulation. **Conclusions:** Given that the mDC are differentiated from BM precursors, these results suggest that FIV infection of myeloid cell precursors may impart long lasting functional defects in the differentiated progeny. Further studies into the mechanisms of FIV-induced DC impairment are ongoing.

Potential alternative to the avian influenza vaccine: Assessment of shRNA plasmids targeting viral and avian proteins

L Linke, J Triantis, GA Landolt, S Bennett, K Pabilonia, MD Salman

Purpose: Losses due to avian influenza (AI) outbreaks are devastating and estimates of potential loss are enormous. Vaccination is not a sound control strategy. Consequently, research to develop more effective methods should be a priority. The aim of this study is to use RNA interference (RNAi) to insert short hairpin RNA (shRNA) into chicken cells, silencing AI and chicken genes associated with AI viral replication to confer resistance to infection. A low-pathogen AI (LPAI) isolate will be used to test and refine the proposed approach. Subsequent studies will use high-pathogenic AI (HPAI). This is the first step in establishing resistance to AI replication in an avian tissue model intended for future prevention in poultry. Materials/Methods: LPAI H8N4 pathogenicity will be established in chicken hepatocellular carcinoma epithelial (LMH) cells. shRNA will be designed to target specific viral and chicken genes associated with AI infection. LMH cells will be transfected with a shRNA-plasmid and challenged with H8N4. Viral reduction will be assessed via immunocytochemistry (ICC) specific for the viral nucleoprotein antigen, quantitative real-time PCR specific for the viral matrix gene, TCID50 and the hemagglutination assay (HA). Results: H8N4 was adapted to optimally infect the LMH cells after 3 serial passages in culture, showing an increase in viral production as determined by ICC, HA and RRT-PCR. Eight chicken and 3 AI target genes have been identified and shRNA oligonucleotides have been designed using BLOCK-it RNAi Designer. Conclusions: Demonstrating the pathogenicity of H8N4 in vitro verifies that this avian model is suitable for future work, including optimizing transfection protocols to evaluate each shRNA plasmid in vitro. Subsequent shRNA transfection and H8N4 challenge assays will be conducted. This project will establish a proof of concept for designing a more powerful control method with potential to reduce the risk of AI infection in susceptible poultry.

Are Salmon Farms in British Columbia Currently Managed for Sustainability?

BM Munk, E Di Cicco, C Stephen

Sustainability, defined as meeting “the needs of the present without compromising the ability of future generations to meet their needs,” is the goal for salmon farm management in British Columbia. In practice, the sustainable management of food production systems should meet the economic, environmental and social attributes of sustainability as defined by the food production system itself and the production unit to be measured. We adapted sustainability models from resource management and food production systems to salmon farming and reviewed the current licensing and management requirements to assess whether salmon farming in BC is currently managed for sustainability. We concluded that BC salmon farming is not regulated for sustainability because (1) there are no explicit indicators in use to address the economic and social attributes; (2) the indicators used for environmental attributes suffer from scientific uncertainty and tend to measure impact rather than sustainability; (3) community involvement is inadequate to define meaningful regulations; and (4) there are no programs to integrate the economic, environmental and social attributes of sustainability. We recommend an integrated approach where experts engage stakeholders and community members to define specific, measurable and meaningful sustainability criteria and indicators to move towards sustainable salmon farming practices.

Receptor Binding Affinity of Recent Canine Influenza A Viruses

H Pecoraro, S Bennett, G Landolt

First isolated from racing greyhounds in Florida, canine influenza virus (CIV) has since caused outbreaks of respiratory disease throughout the US. Phylogenetic analyses indicated that the canine isolates evolved from contemporary equine H3N8 influenza viruses. Although influenza A viruses are occasionally transmitted from one host species to another, the viruses are only rarely maintained in the new host species. The viral hemagglutinin (HA) protein is thought to be a major contributor to host-range restriction because of its role as the viral receptor binding protein. Compared to equine H3 virus sequences, the canine isolates differ in five amino acid residues including the residue at position 222 (W222L). As residue 222 is located near the receptor binding pocket, it has been thought that the substitution of leucine for tryptophan at this position alters the canine viruses' receptor binding affinity. We hypothesize that the maintenance of influenza virus in canines is a result of a switch in receptor binding specificity from SA-a2,3-Gal to SA-a2,6-Gal linkage between sialic acid and oligosaccharides on the host cell surface. To evaluate the receptor binding affinity of recent canine influenza viruses, we performed solid-phase binding assays based on the binding of immobilized virus to biotinylated polymers. Our results demonstrate that both canine and equine H3N8 influenza viruses have the highest affinity to a2,3 linked sialic acids. More specifically, the equine and canine viruses share a high binding affinity for 3'SLN terminated sialylglycopolymers (3'SLN-PAA) (NeuAc-a2,3Gal-b1,4GlcNAc-PAA). These findings are supported by previous sialic acid staining results demonstrating the presence of mainly a2,3-linked receptors in the respiratory tract of dogs. We conclude that the W222L mutation in HA has not resulted in a switch in receptor binding preference and that HA does not appear to be a major determinant in maintenance of CIV.

Biomarkers of metastasis and resistance to chemotherapy in canine osteosarcoma

LE Pfaff, AA Ptitsyn, RS Thomas, J Seibert, DL Duval

Purpose: Osteosarcoma (OSA) is the most common bone tumor in dogs and roughly 80% of OSA tumors arise in the appendicular skeleton of large and giant breed dogs. The majority of patients experience rapid lung metastasis following tumor removal and chemotherapy while a minority remains disease-free for six months or longer. Characterization of OSA with regard to its metastatic potential and chemotherapeutic resistance would improve both prognostic capabilities and treatment modalities. **Methods:** We analyzed gene expression in archived primary OSA tissue from dogs that were treated with limb amputation followed by doxorubicin or platinum-based drug chemotherapy. Study samples were selected from two groups: dogs with a disease free interval (DFI) of less than 100 days (n=8) and those with a DFI greater than 300 days (n=8). Gene expression was screened with Affymetrix Canine 2.0 genome chips and analyzed with a two-tailed t-test following transformation and algorithm application. Array data were also analyzed for gene ontology. Quantitative RT-PCR was performed on 27 significantly changed genes (uncorrected $p < 0.05$) with an expanded sample set (n=10 from each group) and predictive models were built. **Results:** Gene ontology analysis revealed alterations in pathways associated with cytoskeletal remodeling, hedgehog and PTH signaling among others. Quantitative RT-PCR studies confirmed significant ($p < 0.05$) expression changes in 10 genes including IGF2, one of its binding proteins IGF2BP1, and the putative tumor suppressor gene NDRG2. Classification models were able to predict cohort with up to 95% accuracy. **Conclusion:** Our results reflect the multifactorial nature of the disease and suggest that gene expression has a strong predictive value for metastatic potential and/or chemotherapeutic resistance in OSA. The observed changes in gene expression and pathway regulation can lead researchers to more targeted chemotherapeutic regimens and expand clinicians' prognostic toolsets.

Genetic Deletion of the purM Gene from Burkholderia pseudomallei Renders the Strain Completely Avirulent

KP Propst, KH Choi, T Mima, SW Dow, and HP Schweizer

Purpose: *Burkholderia pseudomallei* causes the disease melioidosis and the disseminated form has a mortality rate close to 100%. This pathogen is classified as a category B select agent due to potential use as a biological weapon. Scientific research utilizing this agent is highly regulated and must be conducted within Biosafety Level 3 (BSL-3) facilities. The purpose was to create an attenuated strain of *B. pseudomallei* that is fully attenuated in animal models of melioidosis. Creation of an avirulent *B. pseudomallei* strain exempt of such federal regulations would greatly increase studies of this pathogen by researchers who do not have access to BSL-3 facilities.

Methods: A defined purM- mutant of *B. pseudomallei* strain 1026b was created that is deficient in purine biosynthesis. The virulence of this mutant strain compared to the fully virulent parental 1026b strain was characterized in both murine and hamster melioidosis models following pneumonic challenge.

Results: While the parental 1026b strain was highly lethal in all animals tested, the attenuated mutant strain was completely avirulent to BALB/c, SCID, IFN-gamma KO, and 129 Sv/Ev mice. In addition, the mutant was also non-lethal to Syrian hamsters, which demonstrate hyper-susceptibility to *B. pseudomallei* infection. Animals infected with the virulent 1026b strain had rapid dissemination of the bacteria and contained large numbers of bacteria in the lungs, liver and spleen at time of death. However, the attenuated mutant was rapidly cleared from the lungs of infected animals, and all organs were sterile at 30 days post-infection.

Conclusions: The attenuated strain created in this study was completely avirulent to all animal models of *B. pseudomallei* tested. Due to this avirulence, we are planning to file a request with the Centers for Disease Control and Prevention for exemption of this strain from federal regulations and BSL-3 classification.

Toll-like receptor and antimicrobial peptide expression in the equine respiratory tract A Quintana

Purpose: The equine airway epithelium is the first line of defense from invading respiratory pathogens such as equine influenza virus (EIV) and equine herpesvirus-1 (EHV-1). While much progress has been made in understanding the adaptive immunity to these viruses, our understanding of the innate immunity is in its infancy. The goal of this study was to examine if toll-like receptors (TLRs), important for the induction of the innate immune response, are present in the equine respiratory tract. Additionally, we studied expression of the antimicrobials MxA, beta-defensin-1 (BD1) and 2'5' oligoadenylate synthetase (OAS), which play important roles in pathogen defense.

Materials/methods: Tissues were collected and homogenized from six standard locations of the upper and lower respiratory tract while epithelial cells were isolated from five standard locations through enzymatic digestion. RNA was isolated from both tissues and epithelial cells followed by reverse transcription and PCR, using sequence-specific primers. TLR9 protein expression was examined in the epithelial cells through FACS staining and analysis.

Results: Our results demonstrate mRNA expression of TLRs 1-4 and 6-10 as well as MxA, 2'5'OAS and BD1 throughout the respiratory tract and in cultured epithelial cells. TLR 9 protein was also expressed in the epithelial cells.

Conclusion: Characterization of the equine airway epithelium will be the first step towards the understanding of host-pathogen interactions at this site. In the future this information will be used comparatively for the development of an in vitro equine respiratory epithelial cell culture system to study the innate immune response to EIV and EHV-1.

Pathogenesis of Chronic Wasting Disease in Transgenic Mice

DM Seelig, GL Mason, GC Telling, EA Hoover

Chronic Wasting Disease (CWD) is a naturally occurring prion disease of cervids in which the normal prion protein (PrP^c) is transformed to a misfolded isoform (PrP^{Sc}). We are utilizing a line of cervid prion protein (CerPrP) expressing transgenic (Tg[CerPrP]) mice to determine the tissue tropism and pathogenesis of CWD. These studies are designed to: 1) generate an effective immunohistochemical (IHC) protocol for the detection of PrP^c in transgenic mice, 2) characterize the susceptibility of Tg[CerPrP] mice to CWD infection, and 3) evaluate the usefulness of enhanced IHC strategies in the detection of PrP^{Sc} in inoculated Tg[CerPrP] mice. We evaluated the distribution of PrP^c in naïve Tg[CerPrP] mice and of PrP^{Sc} in multi-route inoculated Tg[CerPrP] mice using a combination of paraformaldehyde-lysine-periodate (PLP) fixation and monoclonal and polyclonal antibodies. The susceptibility to CWD was evaluated in mice by the inoculation of groups (n=10) of mice via the intracerebral (IC), intraperitoneal (IP), intravenous (IV), and oral (PO) routes. In naïve mice, PrP^c was identified in a wide variety of tissues, including those of the nervous, lymphoid, gastrointestinal, and endocrine systems. CWD-infectivity was documented following inoculation via the IC, IV, IP, and PO routes of exposure. In inoculated mice, PrP^{Sc} was detected in a variety of nervous, lymphoid, hematopoietic, and gastrointestinal tissues (including the salivary gland). Using multiple IHC, we have shown that this line of Tg[CerPrP] mice express PrP^c in a manner similar to the native cervid species and that these mice are susceptible to CWD infection via multiple routes of infection. We have detected PrP^{Sc} in a number of tissues, including the neural and extraneural (pancreas, salivary gland, and bone marrow) tissues. These results confirm the utility of this line of mice as a CWD model species and may provide a histologic basis for the infectivity of cervid saliva and blood.

Characterization of Upland Gamebird Facilities in the United States

KE Slota, AE Hill, RA Bowen, TJ Keefe, KL Pabilonia

Purpose: Highly pathogenic avian influenza (HPAI) has emerged as an important zoonotic disease and disease of economic importance to the global poultry industry. In order to prepare for an incursion of this virus into the United States, it is important to understand different facets of the US poultry industry. The objective of this study was to measure the scope of the upland gamebird industry and to identify bird movement patterns and characterize human-bird interactions within the industry. **Methods:** A list of people that held current, state-issued permits to keep, breed or release upland gamebirds in the United States was constructed. Randomly selected permit holders were surveyed over the telephone. Responses were received from 218/500 upland gamebird permit holders (UGPH). **Results:** Subjects reported many different reasons for holding an upland gamebird permit, including release of birds for hunting (48.2%), dog training (33.9%), sale to clients (32.1%), hobby (26.6%), and meat to sell for consumption (6.4%). Other purposes for upland gamebird permits included meat or eggs for family, meat for other animals, and exhibition. 82.7% of the subjects obtained birds from outside sources in the past 12 months. Birds traveling to commercial facilities traveled the farthest distances, with a median distance of 167.5 miles. The median numbers of family members and poultry workers that had regular contact with birds were 2 and 0, respectively. **Conclusions:** Our results suggest that several populations of UGPHs may be at risk for infection if there was an HPAI outbreak in the United States. Permit holders obtain birds from many different locations and facilitate interaction of their birds with various other bird populations. There is also the potential for zoonotic disease spread from these bird populations to humans, including upland gamebird raisers who have daily contact with the birds and hunters who prepare birds for consumption.

Mosquito RNA-Binding Proteins Modulate Deadenylation of Alphavirus RNAs

KJ Sokoloski, NL Garneau, CJ Wilusz & J Wilusz

Alphavirus RNAs resemble cellular mRNAs in that they are capped and polyadenylated. We showed previously that despite this resemblance alphaviral transcripts are not degraded by the same pathway as cellular mRNAs whose decay initiates with poly(A) shortening. Alphaviral RNAs are resistant to this deadenylation process and resistance is conferred by elements within the 3' untranslated region (UTR). Through the use of a cell-free system using mosquito cell extracts, we are able to recapitulate all aspects of cytoplasmic mRNA decay, including the viral 3'UTR specific repression of deadenylation. Using this in vitro system we have been able to determine that the modulation of deadenylation is due to multiple elements within the 3'UTR, including the Repeat Sequence Elements and the U-Rich Region. The binding of a 38kD protein, ELAV, to the U-rich sequence correlates with inhibition of deadenylation. Furthermore, competition of ELAV, induces deadenylation and allows binding of a 32kD factor, Squid, to the viral 3' UTR. Interestingly the binding of Squid and ELAV is conserved in other alphaviruses despite poor sequence homology in this region. Both Squid and ELAV have previously characterized roles in mRNA metabolism. We present a potential mechanism by which alphaviruses usurp cellular factors to selectively stabilize viral transcripts. Currently we are in the process of defining the roles that squid and ELAV play in the repression of deadenylation and viral replication.

Activation of innate immunity links bone infection and inhibition of osteosarcoma growth

JL Sottnik, LW U'Ren, DH Thamm, SW Dow

Introduction: Canine and human osteosarcoma patients treated by limb salvage surgery that develop a postoperative infection have increased overall survival compared to uninfected patients. We therefore developed and characterized a mouse model of bacterial osteomyelitis to investigate the mechanisms responsible for this phenomenon.

Methods: A luciferase-transfected *Staphylococcus aureus* strain was established as a biofilm on silk suture and introduced into the medullary cavity of the tibia of C3H mice. The DLM8 murine osteosarcoma cell line was used to assess the antitumor effects of infection in syngeneic, immunologically competent mice, and was introduced three days post-infection. Kinetics of infection were monitored using in vivo bioluminescent imaging and tumors were measured thrice weekly. Flow cytometry and immunohistochemistry were used to evaluate changes in peripheral blood cell populations, tumor angiogenesis, and immune infiltrate.

Results: DLM8 osteosarcoma growth was significantly delayed in mice with bacterial osteomyelitis, and infection was confined to the limb at all time points. Monocyte and NK cell depletion negated this effect. Infected tumor-bearing mice had a significant decrease in circulating endothelial cells and tumor microvessel density. Significant increases in blood monocytes and tumor associated macrophages in infected mice suggest an anti-tumor role of these cells.

Conclusions: A mouse model of osteomyelitis was found to recapitulate the antitumor effects associated with infection of limb spare surgeries in humans and dog. Depletion experiments indicated that the effect was mediated by both NK cells and monocyte/macrophages. Inhibition of angiogenesis was also observed to play a role. We are currently investigating whether other bacterial pathogens can mediate a similar effect.

MicroRNA's in Ovine Reproduction

KJ Torley, JC da Silveira, RV Anthony, GJ Bouma

The underlying cause of many cases of abnormal fetal gonad development in mammals is unknown. In addition, the regulation of gene expression and function during fetal gonad development in females and males remains elusive. Our overall goal is to identify mechanisms of gene regulation during mammalian fetal ovarian and testicular development. MicroRNAs (miRNAs) have been shown to regulate gene expression in tissues throughout the body and likely play a role in mammalian fetal gonad development. MiRNAs are small non-coding RNAs, which regulate gene expression and function. The sheep is a good model to study human gonad development, as there are many similarities in the expression patterns of gonadal sex determining (GSD) genes during fetal development between these two species. In this study, we test the hypothesis that miRNAs are expressed during sheep fetal gonadal development, and predict they play a role in controlling GSD gene function. Gene expression analysis revealed differential expression of a select set of miRNAs in fetal sheep gonads. Using bioinformatics approaches, we identified several known GSD genes as predicted targets for differentially expressed miRNAs. Subsequently, we examined the expression of a number of these GSD genes, and verified their sexually dimorphic expression in sheep fetal gonads. Results indicate that the mammalian testis determining gene, Sox9, was significantly higher expressed in fetal testes compared to ovaries (17 fold and 40 fold at gestational day (GD) 42 and 75, resp.). Furthermore, the ovarian specific genes Wnt4 and Foxl2 were significantly higher expressed in fetal ovaries compared to testes (GD 42 and 75, resp.) In addition, miRNAs potentially targeting these GSD genes were examined for their localization using in situ hybridization, and revealed distinct cellular localization patterns. These studies provide important new insight into the regulation of GSD gene function by miRNAs during fetal gonadal development.

CUG-BP1 RNA binding protein binds to TNF mRNA and regulates its stability

L Zhang, JE lee, A Dickson, J Wilusz, CJ Wilusz

CUG-BP1 RNA binding protein is one of the founding members of the CELF family comprising key factors that determine the fates of a number of mRNAs. Recently, it has been shown that CUG-BP1 elicits the decay of mRNAs with GU-rich element (GRE) in their 3'UTRs. Here, we show that CUG-BP1 binds to TNF 3'UTR with high affinity. Gel-shift and footprinting experiments suggest that CUG-BP1 not only recognizes AU-rich element in TNF 3'UTR, which is a major binding site, but also other sequences within the TNF 3'UTR. We further demonstrate that RRM3 of CUG-BP1 is the principle RNA-binding domain involved in recognition of the TNF 3'UTR. Depletion of CUG-BP1 from mouse myoblasts results in increased abundance of TNF mRNA through stabilization of the transcript. Moreover, activation of the protein kinase C pathway by treatment with phorbol ester, which has been shown previously to result in CUGBP1 phosphorylation, also causes TNF mRNA stabilization. Cytoplasmic CUG-BP1 is phosphorylated when C2C12 cells are treated with phorbol ester or induced to express the CUG repeat RNA. We are currently investigating how CUG-BP1 phosphorylation affects its interactions with the TNF mRNA and with other factors. Taken together, our results demonstrate that CUG-BP1 binds to TNF mRNA and regulates TNF mRNA stability and this regulation may have important implications for disease.

Associations of Intracystic Biochemicals and Markers of Inflammation with Breast Cancer Risk in Women with Benign Cystic Breast Disease – a Prospective Study

M Walling, J Peel, J Burch, R Wells, W Craven

Breast cancer is diagnosed in 1.3 million women worldwide each year. Certain women with benign cystic breast disease are at an increased risk for breast cancer compared to the general population, but recommendations culminating from over three decades of study regarding which cysts signify the greatest risk, and in which women, have been vague and conflicting, leaving clinicians without a clear protocol for dealing with this risk group. Studies have focused on biochemical compounds in breast cyst fluid believed to be associated with breast cancer but have fallen short of identifying markers related to the breast carcinogenesis process. A notable example is cyst classification by intracystic electrolyte levels, which have no mechanistic association with breast tumorigenesis. We will examine two biochemicals in breast cyst fluid that are also implicated in breast cancer, the steroid hormone 17-beta-oestradiol and the potent growth agent epidermal growth factor, and their relationship to cyst types by electrolyte levels and to breast cancer risk. We will also examine cellular components of breast cyst fluids that may be indicative of an immune system response to breast anomalies capable of culminating in tumor. An increasing body of evidence supports a role for the immune system not only in modifying the behavior of existing clinical cancers but also in surveillance and even elimination of pre-clinical cancers, evidence which has been noticeably understudied in benign breast disease. We will assess in a cohort of women with benign cystic breast disease associations between steroidal, hormonal, and inflammatory components of breast cyst fluids and breast cancer risk. The determination of biomarkers of breast carcinogenesis in breast cyst fluid may assist clinicians in the identification of benign masses of the breast that impose a true increased risk of breast cancer, resulting in increased surveillance and preventative treatments for this breast cancer risk group.

Oral Presentations

Session III ~ Salon IV

1:00-5:45PM

CLINICAL SCIENCE

Use of SmartPill technology to assess effects of Iberogast and ondansetron on gastrointestinal motility

A Bradley, P Boscan, K Dowers, M Marquez, K McCord, D Twedt

Purpose: Diagnosis of gastrointestinal (GI) disorders can be challenging, especially when motility is an underlying factor. Treatment options are limited, often based on trial and error, and monitoring is difficult. There are a number of drugs used for treatment of gastrointestinal (GI) motility disorders in humans, but few have adequately been evaluated in the dog. Iberogast (stw 5) is a combination of herbs and is reported to affect GI motility in humans. Ondansetron is a 5-HT₃ receptor antagonist used in dogs for antiemetic properties, but there are also a number of reports showing effects on GI motility in humans. The objective of this study was to determine the effects of Iberogast and ondansetron on GI motility using SmartPill technology. The SmartPill™ is a noninvasive wireless sensor capsule that is given orally and transmits data on gastric and small and large bowel pressures, transit time, luminal pH and temperature. Materials and Methods: Ten healthy adult dogs were used in a cross-over placebo controlled design. All dogs received either ondansetron (0.5 mg/kg PO TID), Iberogast (1 ml PO TID) or placebo (saline 1 ml SQ SID). Transit time (TT), pH, maximum pressure (MP), mean peak amplitude (MPA), contractions/minute (CPM) and motility index (MI, calculated AUC/time) for the stomach, small intestine (SI) and large intestine (LI). Data was analyzed using multivariable linear regression analysis with significance of $p < 0.05$. Results: Total TT was significantly longer for Iberogast and ondansetron compared to placebo. Treatment with ondansetron led to significantly higher pH in each GI segment. Treatment had no significant effect on MP, MPA, CPM or MI. Conclusions: Both Iberogast and ondansetron increase TT, but given the lack of individual segmental parameter differences, the mechanism of action is unclear. Iberogast and ondansetron may be beneficial in the management of disorders in dogs associated with decreased GI transit time.

Effects of Daily Low-Dose Cyclophosphamide on Regulatory T-cells in Dogs with Cancer

JH Burton, A Guth, BJ Biller

Purpose: Regulatory T-cells (Tregs) are a subset of T lymphocytes that play an important role in the prevention of autoimmune disease. Tregs have recently been demonstrated to be increased in humans and dogs with cancer and are thought to suppress cellular immune responses against tumors. Low-dose cyclophosphamide has been shown to decrease the number and function of Tregs in mice and in humans with end-stage cancer. The purpose of this study was to evaluate whether daily low dose cyclophosphamide administered at doses commonly used in veterinary metronomic chemotherapy protocols decreases the number of Tregs in the blood and lymph nodes of dogs with cancer. **Materials/methods:** In this pilot study, client owned dogs with various tumor types, having either gross or microscopic disease, were administered cyclophosphamide 10 mg/m² orally once daily for 28 days. A complete blood count, peripheral blood mononuclear cells, and lymph node aspirates were collected at day 0, 14 and 28 were immunostained with antibodies to CD4 and intracellular FoxP3 and analyzed by flow cytometry to quantify the Treg population. Side effects were reported by the clients and recorded in a standard adverse events collection form. For patients with gross disease, tumor measurements were recorded at each visit. Treg levels at the three time points were analyzed by one-way ANOVA. **Results:** Six dogs were enrolled in this trial. No gastrointestinal or hematological side effects were identified in any of the patients during the course of the study. All patients had stable disease throughout the study. The mean total number of CD4+/FoxP3+ cells in peripheral blood was 78.9, 30.1, and 93.6 cells/ul while the mean percentage of CD4+/FoxP3+ cells was 5.1, 4.3, and 7.8% on day 0, 14, and 28, respectively. Sufficient lymph node aspirates were unable to be obtained consistently for evaluation. **Conclusions:** Cyclophosphamide given orally at 10 mg/m²/day for 28 days did not significantly change the number of circulating Tregs at any time point evaluated in this study. Dose escalation of daily cyclophosphamide is currently being investigated to determine the dose required to selectively deplete Tregs.

Detection of infectious agents and anti-erythrocyte antibodies in cats with anemia

AG Miller, KL Dowers, CB Webb, RF Keegan, AC Avery, PK Kiser, MR Lappin

Purpose: To determine the prevalence of infectious agents and anti-erythrocyte antibodies in cats with acute anemia and to evaluate flow cytometry for detection of anti-erythrocyte antibodies. **Materials and Methods:** Blood from 29 anemic cats and 4 control cats was prospectively evaluated using complete blood count, Coombs' test at 37C and 4C, flow cytometry, Bartonella spp. antibody titers and PCR for DNA amplification from Mycoplasma hemofelis, 'Candidatus M. haemominutum', 'Candidatus M. turicensis', Bartonella spp, Ehrlichia spp and Anaplasma phagocytophilum. The prevalence of anti-erythrocyte antibodies in cats with and without evidence of infections was compared using Fishers' exact test. **Results:** DNA from infectious agents was amplified in 62% of cats. The Coombs' test was positive in 14% of cats at 37C and 24% at 4C. Anti-erythrocyte antibodies were detected by flow cytometry in 17% of cats. All cats (5/5) with positive flow cytometry and 75% (3/4) with a positive Coombs' test had DNA from an infectious agent amplified. The prevalence of anti-erythrocyte antibodies did not differ between cats with or without infectious agents. There was 40% agreement between flow cytometry and the Coombs' test at 37C and 60% between flow cytometry and the Coombs' test at 4C. **Conclusions:** Anti-erythrocyte antibodies are detected in some cats with selected infectious agents. Most cats with positive flow cytometry or Coombs' results concurrently were positive for an infectious agent, therefore, the presence of anti-erythrocyte antibodies did not distinguish between infectious and primary immune mediated anemia.

Mechanical Comparison of Two Suture Materials for Extra-Capsular Stifle Stabilization

NR Cabano, KT Troyer, RH Palmer, BG Santoni, CM Puttlitz

Purpose: To mechanically evaluate crimped interlocking loop configurations (ILC) of 45kg Nylon Leader Line (NLL) and Orthofiber (OF) for extra-capsular stifle stabilization. **METHODS:** Double-loop, single-strand ILC's of each material tightened to 100N and crimp secured. Ramp to failure (n=10/group) -- Initial loop tension, yield force, ultimate force, peak elongation, stiffness, and failure mode were recorded. Stress-relaxation testing (n=10/group) -- loops loaded to 300N and held at resultant displacement. Loop load, displacement and percent relaxation were recorded. Incremental, cyclic loading (n=10/group) -- ILC's were loaded in sets of 5 cycles starting at 100N and increased by 50N (1 and 3Hz protocols). Resting loop elongation and tension were recorded after each set. **RESULTS:** Ramp to failure -- the initial tension in the NLL (75.5 ± 9.5 N) and OF (68.7 ± 10.4 N) suture loops was not significantly different ($p=0.140$). Statistically significant differences ($p=0.001$) were present between suture groups for yield load (NLL 193.6 ± 13.8 / OF 137.3 ± 94.3 N), peak load (NLL 873.7 ± 68.6 / OF 653.6 ± 80.2 N), stiffness (NLL 125.7 ± 4.0 / OF 234.6 ± 25.0 N/mm) and elongation at failure (NLL 19.1 ± 1.4 / OF 5.2 ± 1.0 mm). Yield in NLL ILC's was manifested as variable knot tightening/crimp slippage, but pure crimp-suture slippage in OF ILC's. Stress-relaxation -- OF relaxed at a higher rate with greater total relaxation. Incremental, cyclic loading -- loop elongation increased and residual tension decreased in both groups after each set, independent of load frequency. NLL lost tension at a lower rate but elongated more than OF. **CONCLUSION:** Neither construct exhibited ideal mechanical performance characteristics for LFTS application. The tested 45 kg NLL construct is recommended over the tested OF construct. The stiffness of OF ILC's compared to NLL loops is of interest, but yield via slippage of OF within the crimp clamps occurred at such low loads that the currently designed crimp clamps are not recommended for clinical application. Yield via tightening of the NLL interlocking loop knot suggests that loop configurations that employ an interlocking knot may negate some of the benefits of crimp clamp fixation on 45 kg NLL. **ACKNOWLEDGMENT:** Funding by CSU-CVMSB Research Council and Securos.

Comparison of the efficacy of an oral transmucosal buprenorphine and sustained release subcutaneous buprenorphine in cats post surgical ovariohysterectomy

D Catbagan, J Quimby, J Bratley, C Sonius, PM Mich, P Vogel, K Mama

Buprenorphine provides analgesia for 6 – 12 hours following oral transmucosal administration (OTM) in cats. This study evaluated the efficacy and safety of an alternative subcutaneously administered sustained release (SR) buprenorphine formulation and compared it to BID administration of OTM buprenorphine in cats undergoing surgical ovariohysterectomy (OHE). Twenty-one healthy female DSH cats [5.5 months and 2.5 ± 0.54 kg] were studied. As anesthetic premedication 11 cats received a subcutaneous injection of the SR buprenorphine (120 mcg/kg), and 10 cats received 20 mcg/kg OTM buprenorphine with additional doses at 12, 24, 36, 48 and 60 hours. All other medications and protocols were standard. Two blinded evaluators independently performed pain assessments using a 100 mm visual analogue scale (VAS) and a 0-4 CSU pain and comfort scale (Hellyer et al) prior to drug administration, during anesthetic recovery (1 evaluator) and at 12, 24, 36, 48, 60 and 72 hours. Von Frey filaments were also applied peri-incisionally and fiber size (1.65 to 6.65) at which the cat first responded was recorded. Body temperature (T), heart rate (HR) and respiratory rate (RR) were also recorded. Data were summarized as mean \pm SD. The T, HR and RR were within clinically acceptable ranges for cats at all times, though HR increased from a baseline of 139 ± 14.5 and 144 ± 21.7 to 202 ± 35.7 and 212 ± 41 during anesthesia recovery in the SR and OTM groups respectively. Von Frey scores were similar through all time periods and between groups with overall SR mean of 4.92 ± 0.72 and OTM mean of 4.86 ± 0.60 . CSU and VAS were also similar between groups, rising post-operatively with mean VAS of 16.4 ± 8.73 and 24 ± 16 and mean CSU of 1.59 ± 0.65 and 1.65 ± 0.78 for SR and OTM groups. These scores declined over time. Results of this clinical study suggest that SR buprenorphine has comparable efficacy to BID dosing of OTM buprenorphine for cats undergoing OHE.

Prevalence of Bartonella and haemoplasma DNA in samples from non-owned free-roaming cats admitted to animal shelters in Colorado and Florida

JN Eucher, M Brewer, MR Lappin

Introduction: Bartonella spp. and the haemoplasmas (Mycoplasma haemofelis, 'Candidatus M. turicensis', 'Candidatus M. haemominutum') are common feline pathogens. A flea vector has been demonstrated for Bartonella spp, while the transmission of haemoplasmas is still unclear. It has been hypothesized that Bartonella spp. and haemoplasmas may be transmitted between cats by bites or scratches. **Purpose:** To compare the prevalence of Bartonella spp. and haemoplasma spp. in blood, salivary glands, and tonsils of free-roaming cats admitted to animal shelters in a state where fleas are rare (Colorado) or common (Florida). **Materials and Methods:** Blood, salivary glands, and palatine tonsils were collected from non-owned, free-roaming shelter cats in Colorado and Florida within 24 hours after euthanasia. DNA was extracted by use of commercially available kits and then assessed for Bartonella spp. and haemoplasma spp. DNA using previously published polymerase chain reaction assays. **Results:** The prevalence rates for Bartonella spp. DNA in blood (CO = 0 of 20 [0%]; FL = 10 of 18 [55.6%] $p < 0.0001$), salivary gland (CO = 0 of 24 [0%]; FL = 5 of 18 [27.8%]; $p = 0.017$) and tonsil (CO = 0 of 20 [0%]; FL = 6 of 18 [33.3%]; $p = 0.006$) were statistically different between the two states. Haemoplasma spp. DNA was detected in similar numbers of blood samples (CO = 1 of 20 [5%]; FL = 2 of 18 [11.1%]), salivary glands (CO = 3 of 24 [12.5%]; FL = 2 of 18 [11.1%]), and tonsils (CO = 3 of 24 [12.5%]; FL = 2 of 18 [11.1%]). **Conclusions:** To our knowledge, this is the first report of Bartonella DNA or haemoplasma DNA in salivary glands or tonsils from naturally infected cats. This may merely reflect the presence of infected erythrocytes within the tissues. Alternately, the results may support the hypothesis that the organisms are passed in these tissues as a mode of transmission. In situ PCR is to be performed on the tissues to further localize the organisms.

Correction of Acute Functional Mitral Regurgitation: Development of a Dynamic Epicardial Device

B Gleyzolle, C Orton, S Earley, S James, E Monnet

Purpose: Left ventricular remodeling is the most important factor leading to Functional Mitral Regurgitation (FMR) and is not effectively addressed by annuloplasty or CABG. The purpose of this study was to correct FMR by repositioning of the papillary muscles with an epicardial device. **Materials and Methods:** Aortic, left ventricular and left atrial pressures, left ventricular volume, aortic blood flow, and ECG were recorded on seven sheep. Left ventricular volumes and annulus size were recorded using sonomicrometry. Acute FMR was induced by aortic banding. The hemodynamic data were recorded at baseline, aortic banding baseline and aortic banding with device. Aortic and left ventricular stroke volumes, mitral regurgitant flow, left ventricular end-systolic and end-diastolic pressures and volumes, left atrial pressure and PV-loops were analyzed. **Results:** The aortic banding model induced a left ventricular dilatation associated with a mitral regurgitant flow of 15.2 ± 5.8 mL. The annulus size significantly increased from 74.6 ± 7.8 mm to 75.9 ± 7.8 mm in diastole ($p=0.031$) and from 68.7 ± 7.4 mm to 73.0 ± 7.3 mm in systole ($p<0.001$). The external device significantly reduced acute FMR from 15.2 ± 5.8 to 9.1 ± 5.1 mL ($p=0.001$), however, the annulus size did not decrease (75.9 ± 7.8 mm to 75.5 ± 7.6 mm in diastole ($p=0.075$) and 73.0 ± 7.3 mm to 72.5 ± 7.3 mm in systole; $p=0.080$). Although passive left ventricular stiffness (β) was significantly increased from 0.92 ± 0.5 to 1.18 ± 0.59 ($p=0.044$) after application of the device during aortic banding, there was no interaction between β and the presence of the device for the correction of the FMR ($p=0.453$). **Conclusion:** Acute FMR was significantly reduced with the application of a dynamic epicardial constraint. We were able to decrease the posterior papillary muscle tethering by repositioning the papillary muscles, without modification of the annulus size.

Ultrasound validation for anatomic liver size relative to the coelom in captive Southern stingrays (*Dasyatis americana*)

KR Grant, TW Campbell, TI Silver, FJ Olea-Popelka

Purpose: Southern stingrays (*Dasyatis americana*) are a well-represented elasmobranch species in public aquaria throughout the world. They are often displayed in exhibits that allow public interaction which may contribute to their popularity. This study was conducted at a facility that experienced mortalities in their collection. A common gross finding during past necropsies was an abnormally small liver. The purpose of this study was to assess the reliability of ultrasound imaging in detecting the length of the liver with respect to the coelom.

Materials/Methods: Fourteen adult Southern stingrays were studied. The animals were either deceased or undergoing surgery during examination and data collection. Ultrasound imaging of the liver was performed and the distance from the caudal margin of the liver to the pelvic cartilaginous girdle was measured. The distance measured using the ultrasound was compared to the actual distance from the caudal liver margin to the pelvic cartilaginous girdle during necropsy or surgery.

Results: Due to the small sample size, the Wilcoxon sign rank test was used to statistically compare the ultrasound measurement to the actual measurement. No significant differences were found between the ultrasound technique and actual measurements. The mean difference between these measurements was 0.06 cm (p -value = 0.945).

Conclusion: In conclusion, ultrasound imaging is a valid technique for indication of liver length relative to the coelom based on this method. This technique may be used during routine physical examinations to further assess the health status of these animals.

Evaluation of Interlaboratory Variance in Paired Serum Bile Acid Assays

KC Kennedy, MR Nanfelt, CM MacPhail

Purpose: Paired serum bile acid assays are commonly used in veterinary medicine for the diagnosis of hepatobiliary dysfunction and portovascular anomalies. When combined with routine diagnostic tests, pre- and post-prandial bile acid serum concentrations have been shown to be an indicator of hepatic insufficiency. Serum bile acid concentrations are also utilized to monitor postoperative gradual attenuation of portosystemic shunts. However, aberrant values in serum bile acids are common and can occur for a variety of reasons, including interlaboratory variability. The purpose of this study was to determine and compare the variability, sensitivity, specificity, and diagnostic accuracy of the serum bile acid assays performed at 3 laboratories. **Material and methods:** Client-owned dogs weighing greater than 3kg were enrolled in this study. The dog's history, physical exam, clinical signs, and diagnostic results allow classification into one of three groups. Fasted and 2-hr postprandial serum bile acid samples were collected from normal dogs (Group 1) and dogs with hepatobiliary dysfunction (Group 2) or portosystemic shunts (Group 3). These samples were then analyzed by CSU Clinical Pathology, Antech, and Idexx laboratories. Data was assessed using one-way ANOVA to compare all three labs and post-hoc test to evaluate between lab pairs. Differences were considered statistically significant if less than $p=0.05$. **Results:** To date, 33 animals have been fully enrolled in the study (23 in Group 1, 6 in Group 2, and 4 in Group 3). There were no statistically significant differences between the pre- or post-prandial serum bile acid results from the three laboratories ($p=0.71$). Sensitivity was 100% for all laboratories and specificity ranged from 84-90% depending on the laboratory. **Conclusion:** If these results are consistent with increased study enrollment, we will conclude that any suspected aberrancy in serum bile acid values are not likely due to interlaboratory variation.

Cigarette smoking and mammographic density: The Study of Women's Health Across the Nation (SWAN)

LM Butler, SM Conroy, EB Gold, CJ Crandall, GA Greendale, N Oestreich, CP Quesenberry, LA Habel

The opposing carcinogenic and antiestrogenic properties of tobacco smoke may explain why epidemiologic studies have not consistently reported positive associations for active smoking and breast cancer. In support of an antiestrogenic mechanism, mammographic density, a strong risk factor for breast cancer, appears to be lower among current smokers, compared to never smokers. However, few studies have evaluated whether active smoking influences mammographic density after controlling for secondhand smoke (SHS) exposure. We used multivariable linear regression to assess the association between active smoking and SHS exposure, and mammographic density among 799 pre- and early perimenopausal women in SWAN. SHS exposure was defined as at least one hour of exposure in the past seven days at home, work, or other setting. Smoking status was defined as follows: (1) never smokers with and (2) without SHS; (3) former smokers; and (4) current smokers. We observed a trend of lower mean percent density (dense tissue area/breast area) across increasing levels of smoke exposure, from 48.1% among never smokers without SHS to 38.4% among current smokers ($p < 0.001$). Smoking status remained inversely associated with percent density after adjusting for age, race/ethnicity, study site, body mass index, and parity ($\beta = -6.49$, $SE = 2.3$, $p = 0.01$ for current smoking versus never smoking without SHS). SHS exposure was not associated with percent density among never smokers. Inverse associations were observed for starting to smoke before age 18 ($\beta = -5.3$, $SE = 2.4$, $p = 0.03$) and smoking 20 or more cigarettes per day ($\beta = -8.17$, $SE = 3.0$, $p = 0.02$), among ever active smokers. The inverse association with smoking status and percent density was confined to parous women, or those who had at least one full-term birth ($\beta = -7.84$, $SE = 2.5$, $p < 0.01$ for current smoking versus never smoking without SHS). Our data support an antiestrogenic hypothesis for the relation between smoking and breast cancer.

Flow Cytometric Prognostic Factors in Canine B Cell Lymphoma

EC Marcus, SE Lana, AC Avery

Purpose: Recent studies suggest that length of survival in human follicular lymphoma patients can be predicted based on the type of non-neoplastic infiltrating cell populations present. However, these trends have not yet been investigated in canine diffuse large B cell lymphoma. The purpose of this study was to evaluate lymph node aspirates from confirmed cases of canine B cell lymphoma via flow cytometry to determine if correlation exists among the number of macrophages and T cells present, B cells size, survival and disease free interval.

Materials/methods: The study population included all dogs within a two year period admitted to the Veterinary Teaching Hospital with B cell lymphoma that had lymph node aspirates assessed via flow cytometry. Follow up data including disease free interval and survival duration from 43 cases of diffuse large B cell lymphoma was collected and compared to immunophenotype data collected via flow cytometry. Relative size of B cells was determined by measuring geometric mean linear forward scatter.

Results: Preliminary data analysis suggests a negative correlation between B cell size and disease free interval.

Conclusion: B cell size may provide valuable prognostic information to clinicians and clients as they assess treatment plans for canine B cell lymphoma patients.

The Effects of a Predominantly Onion Diet on Pregnant Does

JM Neary, AP Knight, T McBride, G Parsons, F Olea-Popelka

Purpose: Determine if feeding cull onions to pregnant does induces a severity of anemia that would clinically affect the animals, and reduce fertility. Cull onions, as by-products of the onion industry, are commonly fed to goats in major onion-producing areas. Onions contain methyl and propenylcysteine sulfoxides which are converted to thiosulfinates when the plant tissue is damaged. Rumen microorganisms break thiosulfinates down to disulfides, which have strong oxidative activity, and can result in hemolytic anemia. Materials/Methods: Eighty Bohr goats were randomly assigned into 2 equally sized groups. One group was fed predominantly free choice cull onions. The other group was fed free choice grass and grass hay. Fertility tested bucks were introduced to the groups after the does had been eating onions for 30 days. Body Condition Scores (BCS), pregnancy rates and fetal numbers of the does were assessed 15, 36, 57, 89 and 123 days after the trial was started. Packed cell volume (PCV) and Heinz bodies indicative of oxidative damage of 23 of the 40 onion-fed does were also measured. Results: The PCV of the onion group decreased from an average of 29% (range 25-36) to 21% (range 14-30) at day 57. On average 30% of erythrocytes had Heinz bodies. On day 89 the PCV had returned to 25% and only 9% of erythrocytes had Heinz bodies. Ultrasound examination on day 89 showed a similar pregnancy rate between the groups. Body mass also remained comparable. Conclusions: Pregnant does adapt to a predominantly onion based diet. Although the does developed significant anemia due to the oxidative injury from the sulfides in the onions, the anemia was transitory. BCS, body mass and pregnancy rates were comparable to controls. As previously shown in sheep on an exclusive onion diet, goats can adapt to an onion diet without detriment to the pregnancy rates. Adaptation is likely similar to sheep that evolve a rumen microflora that is able to metabolize the onion sulfides.

Comparison of temperature readings from a percutaneous thermal sensing microchip with temperature readings from a digital rectal thermometer in equids.

TR Robinson, SB Hussey, AE Hill, CC Heckendorf, JL Traub-Dargatz.

Body temperature measurement can assist in early detection of contagious equine diseases. However, using rectal thermometers increases the risk of personnel injury with unruly horses, bacterial contamination, and time required for measurement. A safer means of obtaining body temperature would be valuable in biosecurity programs. Our objectives were to compare body temperature measured using NAIS ISO compliant percutaneously placed thermal sensing microchips to rectal temperature. Temperatures were compared in two groups of ponies (Groups 1 and 2) enrolled in vaccine challenge studies and one group of 2 year old Quarter Horses (Group 3) enrolled in a colt training class, Group 1 in July-August (average ambient temperature 84.2°F, observed 17 d), Group 2 in January-February (average ambient temperature 27.1°F, observed 23d), and Group 3 in September-November (average ambient temperature 50.8°F, observed 19d). Ambient temperature and equine coat color were also recorded. Data were analyzed using PROC GENMOD with sensor temperature as a dependent variable, controlling for clustering within each horse. Sensitivity and specificity of thermal sensing microchip at detection of fever (rectal temperature = 102°F) was estimated separately at temperatures = 60°F and > 60°F. Rectal temperature readings ranged from 97.2 to 107°F, whereas biothermal sensor readings ranged from 75 to 108°F. Thermal sensor readings varied with ambient temperature and rectal temperature. Sensitivity for fever detection was 87.4%, 53.3%, and 58.3% in Groups 1 to 3 respectively. The thermal sensing microchip appears to have potential utility for initial screening in a biosecurity program, however performance of the chip in the individual animal and ambient temperature would need to be taken into consideration.

Serotonin Transporter Expression Is Locally Down-regulated In Canine Degenerative Mitral Valves

SM Scruggs, S Disatian, EC Orton

Purpose: Tryptophan hydroxylase 1 (THP1) is the rate limiting enzyme necessary for peripheral serotonin synthesis and the serotonin transporter (SERT) is a key component of serotonin metabolism. SERT transports serotonin across the cell membrane for intracellular metabolism and competes with serotonin receptors for interaction with serotonin. We have recently reported an autocrine serotonin signaling mechanism in canine degenerative mitral valves based on up-regulation of THP1 and down-regulation of SERT in late-stage disease. It is unknown whether SERT down-regulation occurs early or late in degenerative mitral valve disease (DMVD) or whether its down-regulation is a local or systemic phenomenon. **Materials/methods:** SERT expression was determined in canine normal (n=4), early-(n=4), and late-stage (n=4) degenerative mitral valves by immunohistochemical (IHC) and immunoblot (IB) analyses. SERT expression was also evaluated in circulating platelets from normal dogs and dogs with DMVD. **Results:** SERT was expressed in all layers of normal and early-stage mitral valves based on IHC. SERT was markedly down-regulated in valve interstitial cells, but not valve endothelial cells, of late-stage mitral valves. SERT expression was significantly decreased ($p < 0.05$) in late-stage, but not early-stage mitral valves on IB. Up-regulation of TPH1 in late-stage degenerative mitral valves was confirmed. No difference in SERT expression was apparent in circulating platelets from normal and DMVD dogs. **Conclusions:** SERT down-regulation is a local and late-stage phenomenon in canine DMVD. SERT down-regulation likely enhances autocrine serotonin signaling in late-stage DMVD by decreasing local serotonin metabolism and increasing interaction of serotonin with its receptor.

Prevalence of environmental Salmonella in Colorado animal shelters

K Steneroden, AE Hill

Purpose: Animal shelter animals and workers are a potentially vulnerable population whose exposure to zoonotic diseases may be greater than the general population. *Salmonella enterica* is an important zoonotic disease and nosocomial infections and epidemics have occurred in animal facilities. The objective of this project is to estimate the prevalence of environmental *Salmonella* in animal shelters in Colorado.

Methods: Environmental samples will be collected by electrostatic wipe from select locations throughout the animal shelters. Samples will be tested for *Salmonella* and compared within shelter to evaluate high and low risk areas, as well as between shelters to evaluate differences in environmental contamination by geographic location, shelter size, shelter type and species.

Results: Twenty eight percent (9/32) of shelters statewide were positive for environmental contamination with salmonella including forty four percent (8/18) of shelters located on Colorado's Front Range. Six different salmonella serogroups were identified. Thirty one percent (31%) of the samples were resistant to six or more antibiotics. Prevalence within shelter samples ranged from 0-100%. Positive locations within shelter were associated with areas that house reptiles, canines and mixed companion animals.

Conclusion: Environmental contamination with salmonella exists statewide in animal shelters in Colorado with particularly high prevalence in the eastern 1/3 of the state. This is one of three studies focusing on animal shelters in Colorado and surrounding states. The results of these studies will help focus education policy on issues of infection control and zoonotic disease awareness in regional animal shelters.

Clinical experience with stereotactic radiosurgery for extremity osteosarcoma

J Tuohy, S Ryan, J Harmon, S LaRue

Purpose: Osteosarcoma (OSA) is the most common primary bone tumor in dogs. The standard of care therapy for canine extremity OSA is removal of the primary tumor either by amputation or limb-sparing surgery plus adjuvant chemotherapy. Some patients are poor candidates for amputation, and limb-sparing surgery is limited to the distal radius anatomic site and can be associated with a high complication rate. Stereotactic radiosurgery (SRS) delivers high dose conformal radiation to a tumor volume with a sharp gradient in dose to adjacent normal tissues. The purpose of this study is to report the initial clinical experience with a curative intent SRS and chemotherapy protocol in canine extremity OSA patients. **Methods:** 13 client-owned dogs received SRS treatment of extremity OSA. A hypofractionated radiation protocol with carboplatin chemotherapy was used. A frame-based immobilization system using bone anchored circular ring fixator components provided reproducible positioning between the planning CT and SRS fractions. Response to therapy was assessed by clinical evaluation, lesion radiographs, measurement of bone turnover biomarkers, whole body nuclear scintigraphy, and in some cases force plate gait analysis. **Results:** The mean and median radiation doses to 95% of the patient tumor volume (PTV) were 42 and 40Gy. The dogs tolerated the fixator apparatus well during therapy. Complications included acute radiation skin effects in the first 3 cases. The dose prescription was modified so that no more than 0.5% of the skin received more than 35Gy and no further skin complications were observed. A decrease in lameness and significant pain palliation were observed in all cases. 3 pathologic fractures occurred and 1 case developed tumor recurrence outside the radiation field. **Conclusions:** Current results demonstrate that SRS is potentially a viable non-surgical limb-sparing option for OSA. Longer follow up is required before conclusions about long term outcome can be made.

Efficacy of nitazoxanide as an antiviral agent for the treatment of EHV-1 infection

S Wilsterman, RJ Callan, LS Goehring, L Ashton

Objectives: To determine whether or not treating horses with nitazoxanide (Navigator) paste prior to and during infection with EHV-1 was efficacious in protecting the treated horses against clinical disease, and whether or not this treatment diminished the nasal shed of virus or decreased the extent of viremia. **Methods:** 16 yearling horses were randomly assigned to a treatment (n=8) or control group (n=8). Horses were verified EHV-1 seronegative prior to the experiment. The treatment group was treated with 25 mg/kg of nitazoxanide by mouth twice per day starting two days prior to EHV-1 infection for a total of 25 days. The control group received a placebo. All horses were challenged with a 5x 10⁷ PFU of EHV-1 (Ohio 03). Horses were evaluated daily by a veterinarian who did not have knowledge of the treatment groups and a clinical score was determined (0= no abnormalities). Viremia and the nasal shed of virus were determined using quantitative PCR for the viral glycoprotein B gene. Clinical score data was analyzed using a Wilcoxon non-parametric test. Physical exam parameters, viremia, and nasal shedding were analyzed by linear regression. Duration of nasal shed of virus and viremia were analyzed using Poisson regression. **Results:** There were no significant differences in the clinical scores or physical exam parameters between the treatment and control groups following EHV-1 infection. The log peak titer of viremia was lower in the treatment group but not significantly different. There were no significant differences noted between the treatment and control groups in regard to the peak nasal titer, the duration of nasal shed of virus or the duration of viremia. **Conclusion:** The treatment of horses with nitazoxinide does not significantly decrease viremia, nasal viral shed or ameliorate the clinical signs associated with EHV-1 infection.

Sodium valproate to enhance doxorubicin sensitivity: Phase I evaluation

LA Wittenburg, DH Thamm

Purpose: Osteosarcoma (OS) remains an incurable and ultimately fatal disease in many patients, and novel forms of therapy are needed. The enzyme histone deacetylase (HDAC) has recently emerged as a promising target in cancer therapy. We previously demonstrated that pre-treatment with the histone deacetylase inhibitor sodium valproate (VPA) enhanced the antitumor effects of doxorubicin (DOX) in canine OS cells in vitro and in vivo. There are currently no published reports investigating the safety, pharmacokinetics or efficacy of HDAC inhibitors in canine cancer. The purpose of this study was to evaluate the safety, pharmacokinetics, and biological activity of VPA administered in combination with DOX in tumor-bearing dogs.

Methods: Tumor-bearing dogs scheduled to receive DOX were pre-treated for 48 hours with escalating doses of sustained-release VPA (Depakote, Abbott), according to an accelerated dose escalation protocol. Hematologic and serum biochemical parameters were monitored regularly. All dogs were observed for at least two weeks before escalation to the next dose.

Pharmacokinetic studies and fluorescence cytochemical assessment of histone acetylation in peripheral blood mononuclear cells (PBMC) were performed. Results: Twenty one patients met entry criteria. VPA dosing began at 30 mg/kg loading followed by 15 mg/kg twice, daily and doses were escalated in 15 mg/kg increments. The highest evaluated dose was 240 mg/kg loading followed by 120 mg/kg twice, daily. No dose-limiting toxicities were encountered. DOX dose reductions were required in 2 of 21 patients. There was a linear and dose-dependent increase in trough serum VPA concentrations. Post-treatment accumulation of acetylated histones was detected in PBMCs from dogs in the highest dose cohort. **Conclusions:** VPA can be safely administered in combination with DOX, is well tolerated, and inhibits its intended biological target in vivo.

The effects of joint geometry on fracture in Thoroughbred racehorses

CA Zimmerman, CE Kawcak, K Easton

Purpose: Catastrophic injuries in the racehorse industry remain to be one of the major issues within the sport. It has been shown that abnormalities in joint geometry predispose a horse to injury. The goal of this study was to assess the association between joint geometry and fracture in Thoroughbred racehorses. Developing diagnostics to assess joint geometry in vivo may help to decrease the frequency of injuries. **Materials/Methods:** Computed Tomography (CT) scans of paired cadaveric limbs were obtained from a large epidemiological study in the UK. This included metacarpal condyles from catastrophic condylar fractures (n=51,FX) the contralateral condyles from FX horses (n=61,NFX), and control group (n=80,CTL) consisting of horses that were euthanized at UK racetracks for non-orthopaedic reasons. OsteoApp was used to render the CT images into 3-D as well as measure the condylar width at 9 sites and radius of curvature (ROC) at 7 sites. Analysis of Variance and least squares means were performed using SAS to compare groups. The geometry data will be used in conjunction with finite element (FE) modeling work to determine how the stress distribution patterns in the joint change with differing geometries.

Results: ROC varies significantly between the FX and CTL groups at 5 sites, as well as between the CTL and NFX groups at 4 sites. Likewise, the ratio of the lateral-to-medial condylar width was significantly different between FX and CTL groups at 8 of 9 sites and between CTL and NFX groups at two sites. **Conclusions:** Abnormalities in width and ROC can predispose a horse to condylar fracture. Use of this data to develop a FE model will allow clinicians to evaluate MCP joint surface geometry and aid in the prevention of catastrophic injuries. The project was supported by Grant F31AR056192 from NIAMS. The content is solely the responsibility of the authors and doesn't necessarily represent the official views of NIAMS or NIH.